SALSA

Swift Aerobatic Light Sport Aircraft

2015-2016 AIAA Undergraduate Aircraft Design Competition

Design Synthesis Exercise Fall 2015 Final report - Group 04

Name: Student #: R. Boerma 4146506 4226844 S.A. van Empelen R.F.J.P. Heijmans 4235231 4155394 K.N. Huijsing T.P. de Jong 4172930 L. Kaur 4174984 B. Koops 4209885 J. Mussini 4204875 P. van Pelt 4168712 S.J. van Rooijen 4135091

Tutors and coaches:

Dr.ir. R. Vos Dr.ir. H.G. Visser Dr. D. Zarouchas

Date:

January 26, 2016





Change Record

Issue	Date	Pages affected	Brief description of change
1	January 21, 2016	all	Initial issue
2	January 26, 2016	all	Error correction and content rearrangement

Preface

This report is the final deliverable of the Design Synthesis Exercise "Aerobatic Light-Sport Aircraft Family" by group 04 as part of the Bachelor Aerospace Engineering curriculum at Delft University of Technology. We were given the task to design a two-member family of light sport aircraft, that meets the requirements and objectives as stated in the request for proposal issued by the American Institute of Aeronautics and Astronautics (AIAA). This report contains the conceptual design of the two-member aircraft family, as a part of the design process performed to achieve the following mission:

To design a competitive and FAA-certifiable two-member family of aerobatic light-sport aircraft with 75% commonality by weight between the one and two-seat variants for entry into service in 2020.

This report is submitted to Dr.ir. R. Vos, Dr.ir. H.G. Visser, Dr. D. Zarouchas and Dr.ir. E. Mooij. We would like to express our gratitude towards the aforementioned, the faculty of Aerospace Engineering and its staff for the guidance and for providing us with workspace, software and other facilities.

Contents

Ch	nange Record	i		7.5 Control Forces	52
Pr	eface	ii	8	Structural Design	53
	st of Symbols st of Abbreviations	iv v		8.1 Materials	53 54 58
	mmary	vi	l .	8.4 Structural Design of the Empennage8.5 Loads on the Landing Gear	59 61
1	Introduction	1		Subsystem Design	62
2	Mission Specification 2.1 Market Analysis	2 6 8 9		9.1 Fuel and Oil Systems	62 63 65 65 66
3	Configuration Choice 3.1 Design Approach	11 11 11 13	10	Performance Analysis10.1 Aerodynamic Analysis	67 67 70
	3.4 Concept Design	15 17 20 21	11	Verification and Validation 11.1 Requirements Validation	75 75 75 75
4	Aircraft Layout 4.1 Overview	23 23 24 26 29 31 32	12	 11.4 Control and Stability Verification 11.5 Structural Analysis Verification 11.6 Control Surface Design Verification 11.7 Performance Analysis Verification 11.8 Financial Analysis Verification Realization 12.1 Operations and Logistics 	77 78 78 78 78 79
5	Propulsion 5.1 Engine Selection	34 34 35 36 37		12.2Production Plan12.3Maintenance12.4Reliability12.5Availability12.6Safety12.7Sustainability	80 84 85 85 86
6	Weight and Balance 6.1 Approach to Weight Estimations 6.2 Approach to Commonality 6.3 Weight Estimations Methods 6.4 Component Weight Estimations 6.5 Centre of Gravity	38 38 38 39 39		12.8 Risk Assessment	87 90 92
7	Stability and Control	42		12.14 Requirement Compliance	96
	7.1 Horizontal Tail Sizing7.2 Control Surface Design	42 43	13	Conclusion	100
	7.3 Eigenmotions	45 45	14	Recommendations	101
	7.4 Control System	50	Bib	oliography	102

List of Symbols

Symbol	Description	Unit	Symbol	Description	Unit
\overline{A}	Aspect ratio	[-]	P_{bl}	Power loading per blade	[hp/ft ²]
b	Wing span	[m]	P_{t}	Load tail wheel strut	[N]
c	Climb rate	[m/s]	$P_{ m m}$	Load main gear strut	[N]
$ar{c}$	Mean aerodynamic chord	[m]	q	Dynamic pressure	[Pa]
$C_{ m D}$	Drag coefficient (3D)	[-]	$r_{ m h}$	Horizontal tail root thick-	[m]
$C_{ m d}$	Drag coefficient (2D)	[-]		ness	
$C_{ m L}$	Wing lift coefficient (3D)	[-]	$r_{ m v}$	Vertical tail root thickness	[m]
$C_{ m l}$	Wing lift coefficient (2D)	[-]	s_{s}	Stroke distance shock ab-	[ft]
$C_{ m M}$	Moment coefficient	[-]		sorber	
$c_{ m p}$	Specific fuel consumption	[kg/J]	V	Velocity	[m/s]
$c_{ m r}$	Root chord	[m]	$V_{ m A}$	Design maneuvering speed	[kts]
c_{t}	Tip chord	[m]	$V_{ m C}$	Cruise speed	[kts]
D	Drag	[N]	$V_{ m D}$	Dive speed	[kts]
D_{p}	Propeller diameter	[m]	$V_{ m S}$	Stall speed	[kts]
$d_{ m f}$	Diameter fuselage	[m]	$V_{ m h}$	Horizontal tail volume co-	[-]
e	Oswald factor	[-]		efficient	
g	Gravitational acceleration	$[m/s^2]$	$V_{ m v}$	Vertical tail volume coeffi-	[-]
L	Lift	[N]		cient	
$L_{ m f}$	Fuselage length	[m]	W	Weight	[N]
$l_{ m fc}$	Length tail cone	[m]	W_{A}	Aerobatic weight	[N]
$l_{ m m}$	Length main gear to CG	[m]	$W_{ m e}$	Engine weight	[N]
l_{t}	Length tail wheel to CG	[m]	W_{emp}	Empenage weight	[N]
M	Mach number	[-]	$W_{ m f}$	Fuselage weight	[N]
$N_{ m g}$	Ratio max load/ max static	[-]	$W_{ m fs}$	Fuel system weight	[N]
O	load per leg		W_{g}	Landing gear weight	[N]
n	Load factor	[-]	$W_{\rm n}$	Engine cowling weight	[N]
$n_{ m p}$	Number of propeller blades	[-]	W_{prop}	Propeller weight	[N]
$n_{ m s}$	Number of struts	[-]	$W_{ m pwr}$	Powerplant weight	[N]
P	Power	[N]	$W_{ m Wr}$	Wing weight	[N]

Greek Symbols	Description	Unit
α	Angle of attack	[deg]
$\eta_{ m p}$	Propeller efficiency	[-]
$\eta_{ m s}$	Shock absorber efficiency	[-]
η_{t}	Tire absorbing efficiency	[-]
δ	Induced drag factor	[-]

Subscripts

Symbol	Description	Symbol	Description		
Е	Empty	p	Propeller		
emp	Empenage	PL	Payload		
F	Fuel	r	Root		
f	fuselage	TO	Take-off		
h	Horizontal	ult	Ultimate		
L	Landing	V	Vertical		

List of Abbreviations

Abbreviation	Full description
AIAA	American Institute of Aeronautics and Astronautics
ASTM	American Society for Testing and Materials
ATC	Air traffic control
ALSA	Aerobatic light-sport aircraft
CG	Center of gravity
DOC	Direct Operating Cost
FAA	Federal Aviation Authority
FAR	Federal Aviation Regulations
FH	Flight Hour
FBS	Functional breakdown structure
FFD	Functional flow diagram
GA	General Aviation
GHG	Green house gasses
HLD	High lift device
IAC	International Aerobatic Club
IOC	Indirect operating costs
IFR	Instrument flight rules
LEMAC	Leading edge mean aerodynamic chord
LSA	Light sport aircraft
MAC	Mean aerodynamic chord
MMOI	Mass moment of inertia
MNS	Mission need statement
MTOW	Maximum take-off weight
NACA	National Advisory Committee for Aeronautics
nmi	Nautical miles
OEW	Operational empty weight
RAMS	Reliability, Availability, Maintainability & Safety
RFP	Request for Proposal
rpm	Revolutions per minute
SFC	Specific fuel consumption
SLSA	Special light sport aircraft
SSR	Secondary Surveillance Radar
USAF	United States Air Force
VFR	Visual flight rules
VHF	Very high frequency

Summary

The American Institute of Aeronautics and Astronautics (AIAA) issued a Request For Proposal (RFP) to design an aerobatic light sport aircraft family containing a one-seat and a two-seat variant. The one seat aircraft should be aimed at competition aerobatics, while the two-seater should fulfill the role of aerobatic training aircraft.

The report describes details regarding the design methods and philosophies behind the design, and the resulting performance, of the proposed aircraft family of aerobatic light sport aircraft named SALSA.

The final concept has a standard taildragger mono-wing configuration, mainly favored over a biplane design for its higher visibility. This is appreciated in aerobatic competitions, since it gives the pilot a better feeling for his position with respect to the judges.

The one seat aircraft has a wingspan of 7.8 meters and the two seat aircraft has a wingspan of 9.8 meters. Both aircraft feature no dihedral and no wing twist to keep aircraft performance similar when flying inverted.

The final concept features detachable wings to offer more flexibility to aircraft owners and reduce operational costs. The extra required wing area of the two-seater aircraft is using with root extensions. The aircraft is mainly produced out of a glass fibre composite and foam sandwich structure. Additionally, the main spar of the wing is constructed out of carbon fibre to meet the weight budget for this component. Both aircraft feature the same Rotax 915 engine, providing 135 hp of power.

The one seat aircraft has a maximum takeoff weight of 465 kg, a maximum limit load factor of +8 g and a maximum negative limit load factor of -6 g. The two seat aircraft has a maximum takeoff weight of 595 kg, a maximum load factor of +6 g and a maximum negative load factor of -5 g.

Furthermore, what makes these aircraft special compared to other LSA are their straightforward detachment of the wing and horizontal tail, low maintenance cost, strong aerobatic performance capability, a full aircraft parachute, high commonality and a full glass cockpit. The results presented in this report indicate that this SALSA family meets all requirements as imposed by the request for proposal.

Introduction

The number of certified aerobatic light sport aircraft on the market is relatively small. Therefore, the American Institute of Aeronautics and Astronautics (AIAA) issued a Request For Proposal (RFP)¹ to design an aerobatic light sport aircraft family containing a one-seat and a two-seat variant. The purpose of this report is to present the conceptual design of the proposed family of the Swift Aerobatic Light Sport Aircraft (SALSA).

The Federal Aviation Authority has issued the LSA class in July 2004 [1]. The significantly lower certification costs involved in certifying SLSA (Special LSA)², compared to a type certified aircraft, mean that more pilots can afford to fly and the accessibility to general aviation is increased. However, only few of the available LSA are capable of aerobatic flight. An aerobatic LSA, certified according to the ASTM F2245-15 standards [2], provides a means for pilots with a sport pilot license to compete in intermediate category aerobatic competitions.

This report includes the design philosophies and methods used to arrive at the resulting SALSA family. Additionally, the feasibility and performance of the family is investigated in depth and its position within the LSA market is investigated.

The report begins by specifying the purpose of this design (Chapter 2). The mission that the design must fulfill is clearly defined by generating a list of requirements. This is followed by a design concepts study in Chapter 3 and a trade-off to select the most suitable concept. The chosen concept is then further elaborated upon, starting with an aircraft layout and wing design in Chapter 4, an engine selection (including a noise and emissions analysis) in Chapter 5 and a component weight and balance estimation in Chapter 6. At this point the location of subsystems is fixed and the stability and control of the design along with its performance are elaborated upon in Chapters 7 and 10. Chapter 8 details the structural design of the SALSA family. This is followed by an in-depth analysis of subsystems in Chapter 9. Chapter 11 discusses the verification and validation performed throughout the design methodology. Finally, the realization of the aircraft including operations and logistics, a production plan, a financial analysis and a RAMS analysis are discussed in Chapter 12. The report is concluded with recommendations for future work on the SALSA family.

¹www.aiaa.org/UndergradTeamAircraftDesignComp/ [cited 8 December 2015]

²www.generalaviationnews.com/2012/09/09/the-cost-of-certification [cited 8 December 2015]

Mission Specification

Before any design process can begin, an analysis of the requirements and specifications has to be made. In section 2.1 the current and future market will be analyzed to determine what is needed to competitive in the LSA market. The functional analysis and requirements will be described in Section 2.2 and 2.4, followed by the mission description in Section 2.3.

2.1. Market Analysis

The events and developments in the LSA market's short existence are analyzed to identify opportunities and pitfalls, to learn from the missteps made by other manufacturers. In this section, the main competitors are identified, the size of the current US market is estimated, other potential markets are evaluated and the size of future markets is predicted.

2.1.1. Industry Background

In 2004, a new category of aircraft was created by the FAA: the Light Sport Aircraft category. [1] There are two general types of LSAs: Special LSAs (SLSA) that are built in factories and Experimental LSAs (ELSA) that are kit builds. These aircraft are certified under ASTM consensus standards and are estimated to be over 100 times cheaper to certify than Part 23 aircraft, allowing manufacturers to build less expensive aircraft.¹

The leisure aircraft market is dominated by venerable designs and most new models entering the market are based on new technological developments such as heavy use of composites or electric/hybrid engines ². Their selling point is based on the new features of their aircraft and the SALSA aircraft family fits well into this business model, because of its emphasis on aerobatics, low production and maintenance costs, and high part commonality. Currently, there are few dedicated aerobatic LSAs on the market, although this is expected to change in the coming years.

The largest manufacturer of general aviation (GA) aircraft (in annual unit sales), is the Cessna Aircraft Company. Cessna's decision to withdraw its Skycatcher from the LSA market caused an uproar in the sector and was viewed by many as a sign that there was no future for the LSA category. The future of the LSA market was much debated, both

 $^{^1}www.general aviation news.com/2012/09/09/the-cost-of-certification\ [cited\ 6\ January\ 2016]$

 $^{^2}www.flyingmag.com/aircraft/lsasport \ [{\it cited 6 January 2016}]$

2.1. Market Analysis 3

negatively ^{3 4 5} and positively ^{6 7}.

Based on the literature study, it becomes evident that the LSA designs that have failed did so because of the following three reasons: the costs were too high, the performance was not sufficient compared to competitors and the useful load was too low.

The two aircraft of the SALSA family will be certified as SLSAs. Selling the aircraft as a kit would decrease production costs and allows anyone to perform servicing, repair and alterations. However, ELSA cannot be used for rental or paid instruction which would rule out flight schools as potential customers. [3] Therefore only SLSAs will be considered in the following sections.

2.1.2. Market Research

In 2013 the special light-sport aircraft (SLSA) category in the USA consisted of 2,056 registered aircraft. The predicted average annual market growth is 4.1% per year from 2013 to 2034. At the entry-into-service (EIS) of the first SALSA variant, in 2020, the volume of the market is expected to be 3,080 SLSAs. The number of registered SLSAs is predicted to be 4,880 in 2034 [4], that is an increase of 1,800 aircraft, which are assumed to all be resulting from new aircraft sales. This is deemed to be a realistic assumption considering the young age of the LSA category and its aircraft, established in 2004, compared to the average age of general aviation (GA) aircraft of 40.7 years. [4]

To increase potential sales, foreign markets are assessed. Potential markets are suitable if they meet the following requirements: their respective countries must have (or plan to have) a regulatory framework similar to that of the USA and they must be large enough to justify the additional certification costs. The following markets are selected for future expansion: Australia, Brazil, Canada, China, Europe, New Zealand and South Africa. [4]

Table 2.1 shows the predicted amount of registered LSA at EIS, in 2034, the average annual growth, the expected market share and the number of aircraft sold in this time period. Predictions regarding the number of registered LSA-compatible aircraft are based on the current amount of aircraft on each market and statistics derived from growth of the US GA market. [4] The average annual growth percentage of each market is based on the predicted 4.1% for the US, as well as the maturity and size of its current SLSA market.

³ www.avweb.com/blogs/insider/AVwebInsiderBlog_USSportAviationExpo_LSAFailureToLaunch_208077-1.html [cited 6 January 2016]

 $^{^4}www.flyingmag.com/blogs/going-direct/light-sport-aircraft-segment-critical-condition\ [cited 6 January 2016]$

 $^{^5}www.airfactsjournal.com/2014/04/skycatchers-death-proves-lsa-rule-failure/\ [cited 6\ January\ 2016]$

 $^{^6}blog.aopa.org/opinion leaders/2014/02/27/in-support-of-light-sport-aircraft-lsa/~[cited~6~January~2016]$

 $^{^{7}}$ www.avweb.com/blogs/insider/Skycatchers – Demise – Barely – a – Ripple – 221074 – 1.html [cited 6 January 2016]

2.1. Market Analysis 4

Table 2.1: Registered special light-sport aircraft (SLSA) in 2020, 2034, the average annual growth, the market share and the number of one- and two-seaters sold. [4]

Market	Registered SLSAs in		Average annual	Market share	One- seaters	Two- seaters
	2020 [-]	2034 [-]	growth [%]	[%]	sold [-]	sold [-]
USA	3,080	4,880	4.1	10	60	129
Australia	2,450	4,290	4.1	15	83	194
Brazil	320	740	6.2	15	19	44
Canada	1,500	2,640	4.1	15	34	136
China	70	210	8.2	15	6	15
Europe	1,430	3,290	6.2	10	37	149
New Zealand	290	660	6.2	15	17	39
South Africa	1,550	2,710	4.1	15	53	123
Total	10,680	19,410			309	828

2.1.3. Competitor Analysis

Five manufacturers (Flight Design (13.4%), CubCrafters (11.7%), Cessna (9.7%), Czech Sport Aircraft (7.5%) and American Legend (7.1%) represented almost half of the total amount of registered SLSA in the USA at the end of 2014. Moreover, three manufacturers (CubCrafters (25.1%), Van's (13.1%) and Progressive Aerodyne (9.5%)) were responsible for almost half of the newly registered SLSA in 2014. With over 90 manufacturers offering more than 100 models the market can be considered somewhat saturated. To attain a market share the SALSA family must clearly differentiate itself from the competition (in terms of price, performance or technology). From a long list of competitors the ones with comparable performance (planned or currently in production) are selected and listed in Table 2.2.

Table 2.2 shows that only two one-seater LSA have been identified as competitors for the SALSA one-seater. Both are dedicated aerobatic aircraft, with the Tecnam Snap designed to compete in the IAC Intermediate category. However, neither of these LSAs would comply with the limit load requirements (+6 G, -5 G) stated in the RFP [5]. From the IAC Intermediate category three aircraft are listed here, to compare them to the requirements in the RFP. All three of them exceed the climb rate requirement (7.62 m/s (1500 fpm)), while two of them meet the limit load requirements. Their price, however, is at least \$64,500 higher than both the LSA one-seaters. The one-seater presented in this report is therefore believed to fill a gap in the current market, as it combines the advantages of an LSA (low-cost license and certification) with the aerobatic capabilities of larger aircraft.

For the two-seater there are more direct competitors. The Harmony, Falcon LS 2 and FK12 Comet meet the requirements on both the limit load (+6 G, -3 G) and climb rate (4.1 m/s (800 fpm)). However, with the installed engines, they are incapable of performing inverted and negative-g flight. The performance requirements for the two-seat aircraft are not as critical as those for the one-seater as it is primarily intended as an aerobatic training and leisure aircraft. Additionally, there are noteworthy competitors with large (future) market shares in the leisure category: the

2.1. Market Analysis 5

Table 2.2: LSA market competitors. (M)/(B): monoplane/biplane. (*) indicates a kit aircraft. For the engine: L (Lycoming), R (Rotax) and J (Jabiru).

Manu- facturer	Model	Base price [\$]	Engine	P [kW] ([hp])	Pos. / neg. limit load [g]	Climb rate [m/s] ([fpm])		
One-seater LSA								
Renegade LS	Lil Rascal LS 1 (B)	125,000	L IO-233-LSA	87 (116)	6 / -3	N/A		
Tecnam	Snap (M)	158,500	R 912 iS Sport	75 (100)	6 / -3	10.2 (2000)		
	Two-seater LSA							
Evektor	Harmony (M)	102,000	R 912 ULS	75 (100)	6 / -3	5.2 (1,020)		
Van's Aircraft	RV-12 (M)	115,000	R 912 ULS	75 (100)	N/A	4.6 (900)		
SAM Aircraft	SAM* (M)	117,900	R 912 ULS	75 (100)	5.2 / -5.2	4.1 (800)		
Renegade LS	Falcon LS 2 (M)	125,000	L IO-233-LSA	86 (115)	6 / -3	7.6 (1,500)		
Prog. Aerodyne	Searey Elite (M)	125,000	R 914 UL	86 (115)	N/A	4.2 (825)		
Arion Aircraft	Lightning LS-1 (M)	130,000	J 3300	89 (120)	4 / -2	6.1 (1,200)		
BRM Aero	Bristell NG 5 LSA (M)	133,500	R 912 iS Sport	75 (100)	4 / -2	5.1 (1,000)		
FK Lightplanes	FK12 Comet (B)	140,000	R 912 ULS	75 (100)	6 / -3	7.0 (1,378)		
Flight Design	CTLSi (M)	167,700	R 912 iS	75 (100)	4 / -2	4.1 (800)		
Tecnam	Astore (M)	171,900	R 914 UL	86 (115)	4 / -2	5.6 (1,100)		
CubCrafters	Carbon Cub SS (M)	189,990	ECi TITAN 340	134 (180)	4 / -2	9.6 (1,890)		
Icon	A5 (M)	247,000	R 912 ULS	75 (100)	N/A	N/A		
	IAC Intermediate competitors							
Pitts	S-1S (B)	158,000	L IO-360-B4A	134 (180)	6 / -3	13.2 (2,600)		
Pitts	S-2C (B)	223,000	L AEIO-540	194 (260)	6 / -5	14.7 (2,900)		
Extra	EA-300L (M)	230,000	L AEIO-540 L1B5	224 (300)	10 / -10	16.3 (3,200)		

Flight Design CTLS(i), the Icon A5 and the Searey Elite. To compete with these in terms of price and, for example, cabin layout are more important than aerobatic performance. As shown before, the available options for a customer interested in the aerobatic LSA market are very limited. Keeping in mind the three attention criteria – price, performance and useful load – the intended design of this family of aircraft has great opportunities in the current market. The SWOT analysis in Figure 2.1) summarizes the factors that have a correlation with the current and future market.

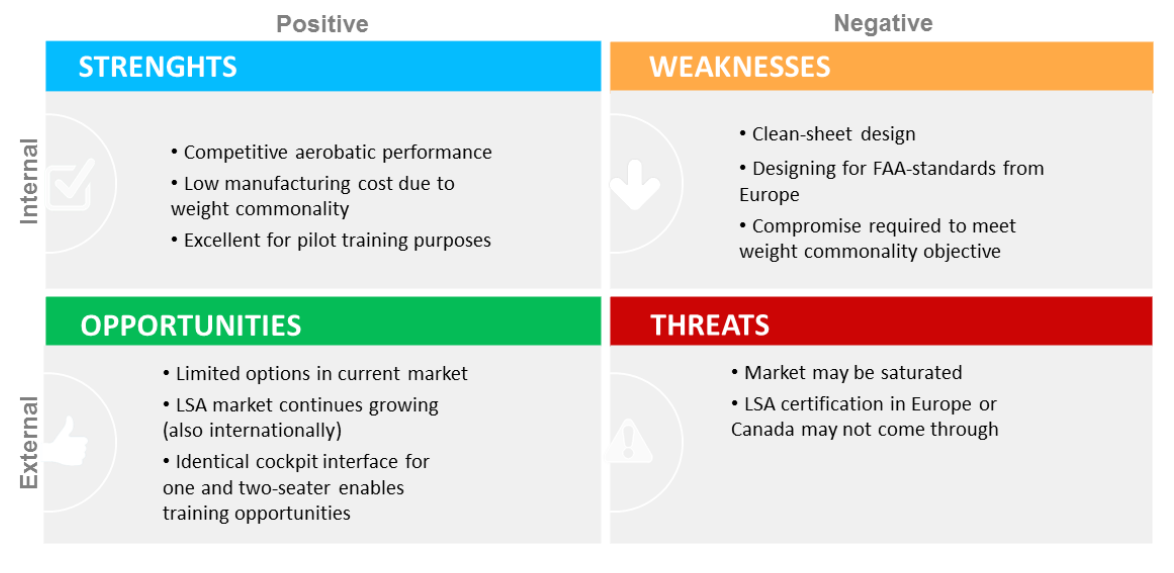


Figure 2.1: SWOT Analysis of the SALSA project.

2.2. Functional Analysis

This section contains the functional flow diagram, which represents all functions that may occur during a mission in a logical time dependent order, and the functional breakdown structure of the SALSA.

2.2.1. Functional Flow Diagram

The functional flow diagram (FFD) represents the logical order of functions that the aircraft has to perform in order to fulfill the mission. The functional flow diagram for the aircraft can be found in Figure 2.2. All essential functions to be performed during a typical mission are included in this diagram, starting from pre-flight operations, followed by the take-off, flight and landing phases. Optional functional paths are represented using an OR junction. The highest level functions are numbered one to five and lower level functions are denoted using lower level numerals. The function of maintaining the aircraft is optional and will not occur during every mission. However, it has been included for completeness.

2.2.2. Functional Breakdown Structure

The time independent functionalities that the aircraft has to provide are grouped in related disciplines, which form the functional breakdown structure (FBS). Together these groups form the functionality of the aircraft and provide a useful overview of what the product needs to do in order to perform its mission. The functional breakdown structure can be found in Figure 2.3.

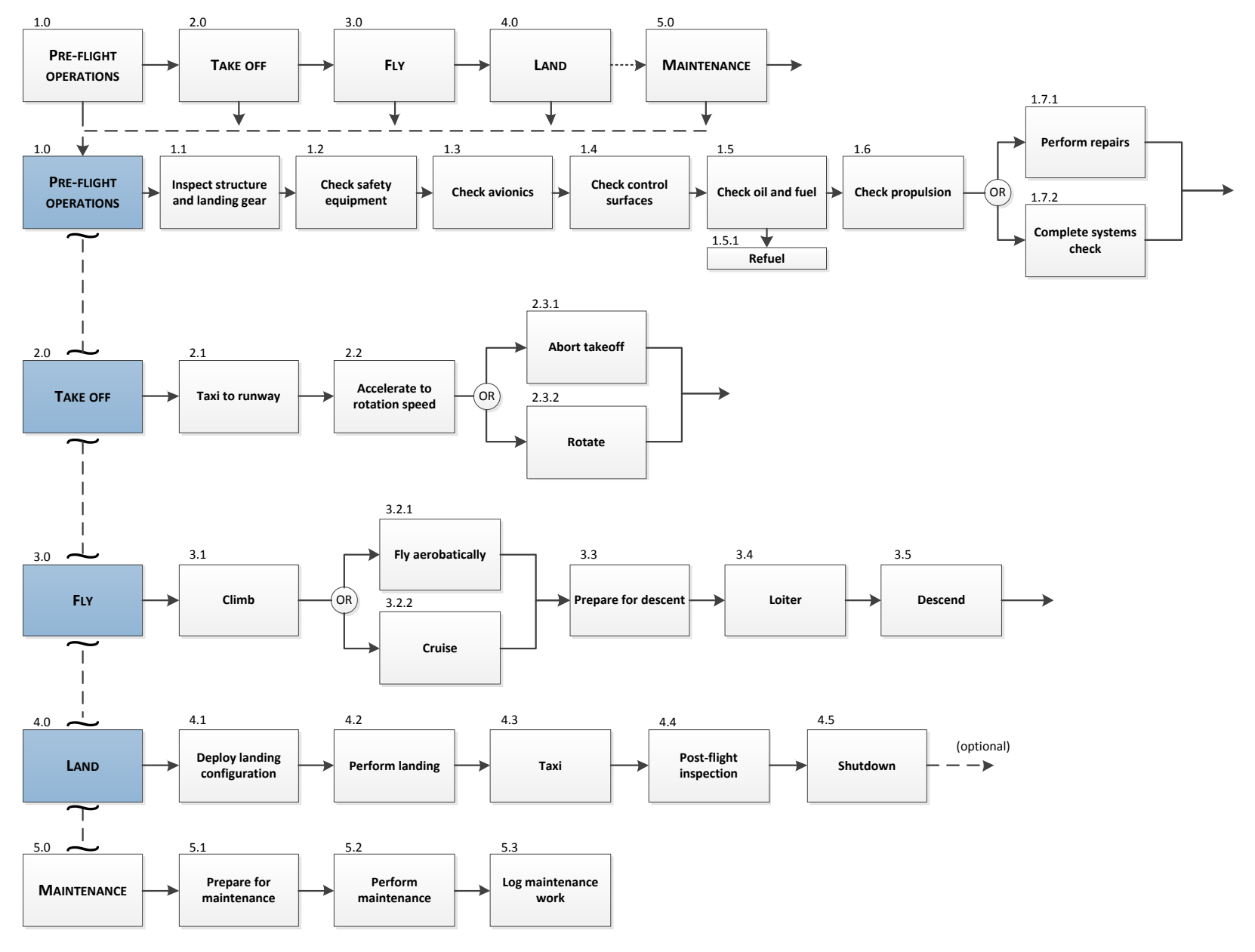


Figure 2.2: Functional Flow Diagram

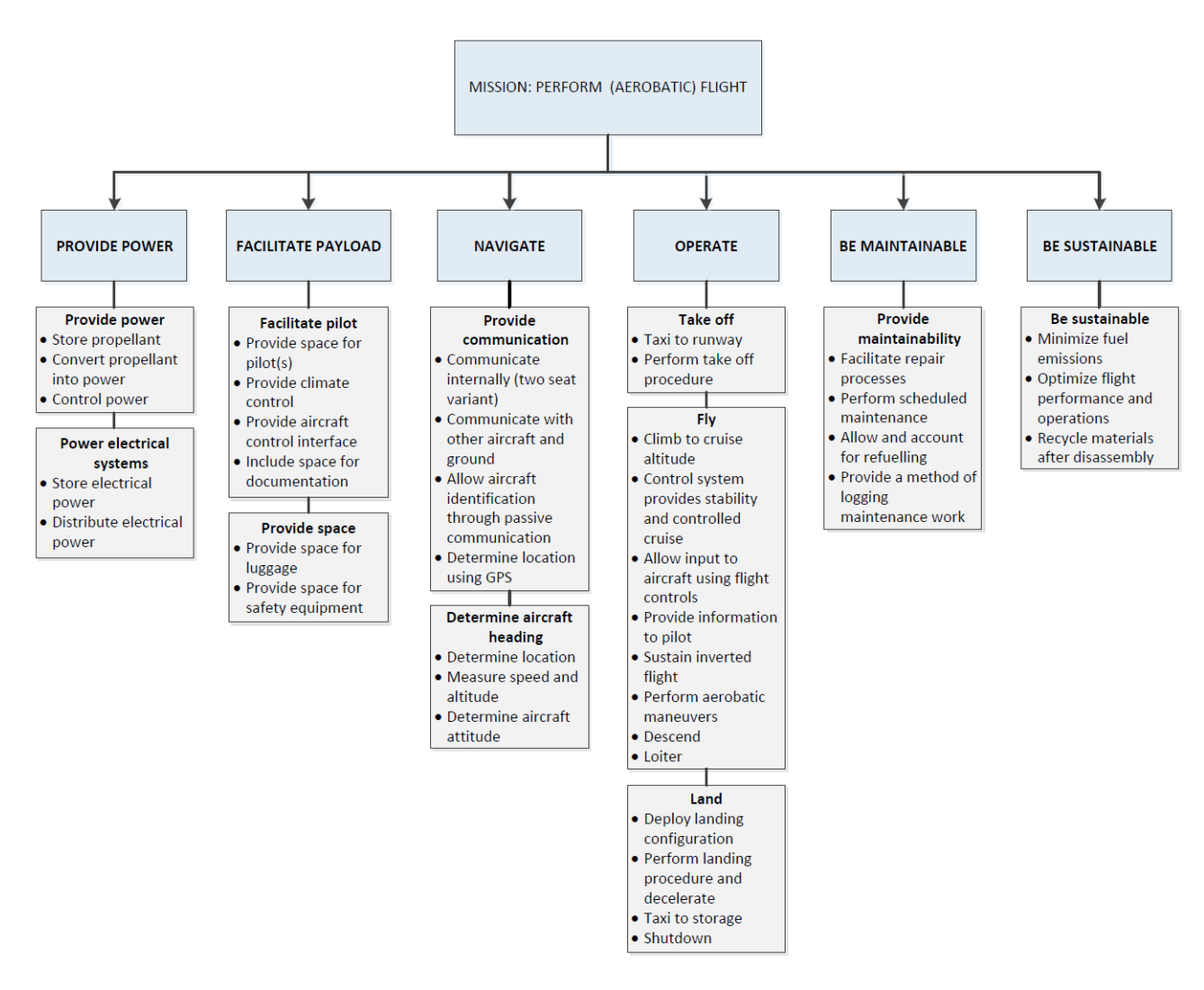


Figure 2.3: Functional Breakdown Structure

2.3. Mission Description

The one-seat aircraft needs to perform an aerobatic and a ferry mission and The two-seat aircraft needs to perform a ferry mission. Figure 2.4 shows each important phase of the aerobatic mission, from engine start-up until shutdown. Figure 2.5 shows the ferry mission profile. The latter loiter phase in both mission profiles can be used to divert to other airports when necessary.

2.4. Requirements 9

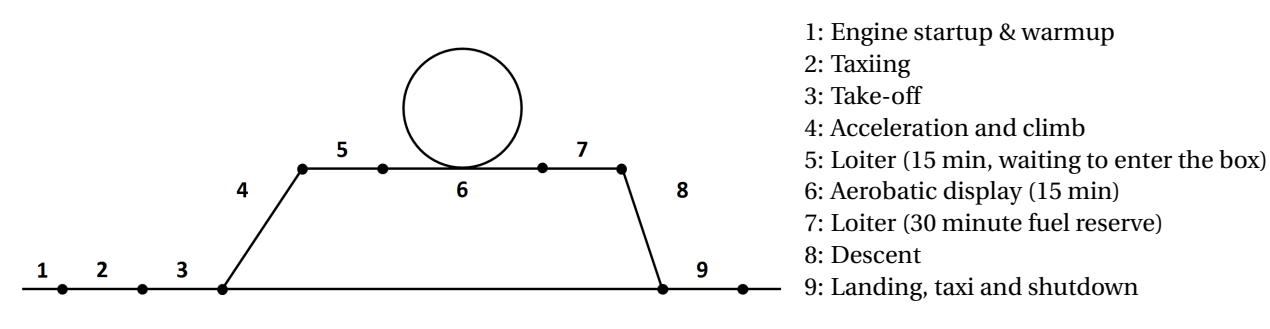


Figure 2.4: Aerobatic display mission profile

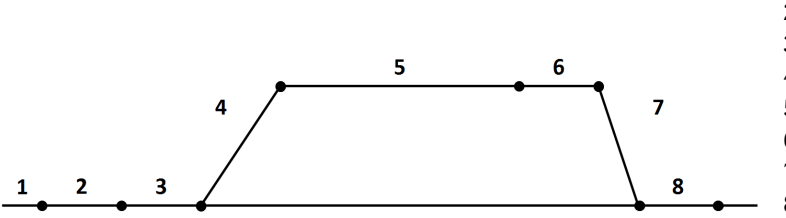


Figure 2.5: Ferry mission profile

- 1: Engine startup & warmup
- 2: Taxiing
- 3: Take-off
- 4: Acceleration and climb
- 5: Cruise flight
- 6: Loiter (30 minute fuel reserve)
- 7: Descent
- 8: Landing, taxi and shutdown

2.4. Requirements

The design phase is started with identification of all requirements. A large number of requirements originate from the Request for Proposal. [5] Additional requirements followed from the market analysis. This section will only mention the most important requirements that are imposed on the project. The complete list of requirements can be found in Section 12.14. The following abbreviations are used in the requirement identifiers: TEC (technical), CON (constraint), OPS (operations), DES (design), OS (one-seater), TS (two-seater), FP (flight performance).

2.4.1. Primary User Requirements

The following requirements are of primary importance to the user:

- SALSA-CON-OPS.2 The aircraft shall be able to operate in controlled airspace.
- SALSA-CON-OPS.3 The aircraft shall be able to operate in uncontrolled airspace.
- SALSA-CON-DES.4 The aircraft shall accommodate 95% of human pilot sizes.
- SALSA-CON-DES.17-OS/TS The aircraft shall provide space for 30 / 30 pounds and 4 / 6 cubic feet of baggage for ferry missions.

2.4.2. Driving Requirements

The following requirements drive the design substantially more than average:

- SALSA-TEC-FP.2 The aircraft shall have control feedback characteristics that are characterized as level 1 handling qualities.
- SALSA-TEC-FP.3-OS The aircraft shall be competitive in the IAC intermediate category.

2.4. Requirements

- SALSA-CON-DES.1 The gross take-off weight shall be at most 1320 lbs.
- SALSA-CON-DES.8 The stall speed shall be at most 45 knots CAS in clean configuration.
- SALSA-CON-DES.9-OS The climb rate of the one-seat variant shall be at least 1500 fpm at sea level, at International Standard Atmosphere (ISA) + 10° C.
- SALSA-CON-DES.10-OS/TS The negative limit load of the one-seat variant shall be at most -5G / -3G (for the two-seater), with 230 lbs / two 200 lbs pilot(s), 15 lbs / two 15 lbs parachute(s) and 1.5 hours / 1.5 hours of fuel.
- SALSA-CON-DES.11-OS/TS The positive limit load of the one-seat variant shall be at least 6G / 6G, with 230 lbs / two 200 lbs pilot(s), 15 lbs / two 15 lbs parachute(s) and 1.5 hours / 1.5 hours of fuel.
- SALSA-CON-DES.15-OS The roll rate of the one-seat variant shall be at least 180 degrees per second at the maximum cruise speed or 120 knots CAS, whichever of the two is lowest.

2.4.3. Killer Requirements

Killer requirements are requirements that can not be accomplished without driving the design of the product to an unacceptable extent. None of the requirements were deemed to be of this kind.

2.4.4. Targets

A number of targets are set to make sure that the aircraft does not only meet the requirements, but is competitive in aerobatic competitions as well. Targets for the one- and two-seat variants are presented in the following.

The following aspects are considered most important for the one-seat variant. They are obtained from a discussion with Dr. Alexander in 't Veld, who regularly competes as an aerobatic pilot in the IAC intermediate category [6].

- The aircraft should have "crisp" stall characteristics: The wing should stall completely within a small angle-of-attack range and reattach readily.
- Good visibility. The pilot should be able to see the judges and be aware of his position in the "box".
- The aircraft should have straight lines and sharp edges, such that the judges can accurately see the orientation of the aircraft during maneuvers. This enables the pilot to show his accuracy in performing maneuvers.
- The aircraft should be able to achieve large roll rates.
- The aircraft should be able to withstand large maximum load factors, such that also more "heavy" maneuvers can be flown than is required in the IAC intermediate category.

The following targets were set for the two-seat variant:

- The aircraft should have complete controls in the front and rear seats.
- The aircraft should have relatively good aerobatics characteristics compared to other two-seat training aircraft.
- The aircraft should be one of the cheapest on the market.

Configuration Choice

This chapter presents how the task of producing a design for the RFP was approached, in Section 3.1, as well as how the aircraft configuration was determined, in Sections 3.2 to 3.5. The approach to achieving commonality between the aircraft variants is discussed in Section 3.6. Finally, the initial sizing of the aircraft family is discussed in Section 3.3.

3.1. Design Approach

Making an unconventional design requires much testing, in order to verify that the concept actually works and to make it reliable. The authors had no opportunity to do such testing, which means that choosing an unconventional configuration would come with large risk. For that reason, selecting a conventional configuration is preferred. For the same reason, the conventional solutions for fulfilling functions like propulsion, stability, control, etc., are preferred over ideas that might be innovative, but whose successful application cannot be guaranteed.

3.2. Configuration Options

The design space is bounded by multiple requirements, such as: using an unpressurized cabin, a single engine, fixed landing gear, max. two seats, propeller-driven, and a fixed-pitch propeller see [5]. Five main configuration options appeared to determine the aircraft layout mostly are investigated in this section.

Engine position. Since only one engine is available, the mounting positions considered are the front (tractor) and the back (pusher) of the fuselage, as can be seen in Figure 3.1a. According to Anderson [7] the following factors have most influence on the choice between these options. Tractor configurations aid stability and the propeller operates in undisturbed flow. Additionally, the proposals of a tractor configuration can be used in low speed aerobatic maneuvers. This gives the tractor configuration a decisive advantage. However, a tractor configuration produces more skin friction drag, and airflow around fuselage, wings and tail-planes is degraded. For pusher configurations the noise and pilot view are improved w.r.t. a tractor configuration, but ground clearance and engine cooling pose a challenge.

Tail type. In order to achieve longitudinal stability, either a canard or horizontal tail is required, see figure 3.1b. A canard is discarded as a viable option, because performing an snap roll (as required by the IAC) with this configuration is impossible. This maneuver requires the main wing to stall, which will not happen with a canard configuration. The reason for this is that the design will be such that the canard will always stall before the wing stalls, otherwise the aircraft will become uncontrollable during stall. A T-tail is aerodynamically more efficient, but has the risk of being in the wake of the main wing during stall [8]. For this reason this option is also discarded. The V-tail and inverted V-tail configurations are also discarded, because they would require a more complex and thus heavier control system. The conventional tail configuration, which consists of a horizontal tailplane mounted on the fuselage (or just above it, on the vertical tailplane), is most easy to design and has good stall characteristics. For these reasons, a conventional tail configuration is selected

Seating arrangement. In the two-seater aircraft of the family, the pilots can be seated side-by-side or in a tandem configuration. Side-by-side seating is advantageous for communication and training, and saves costs and weight on double controls and avionics. The tandem configuration has less frontal area and produces much less drag. The tandem configuration also results in a more symmetric aircraft, which is important in aerobatics, as discussed in the Section 3.1. For these reasons the tandem configuration is selected.

Landing gear arrangement. The landing gear needs to be a fixed landing gear by requirement. A conventional landing gear has a two-wheel main gear and a third wheel at either the front or the rear of the aircraft. Therefor the following two options are considered: the nose wheel and the tail wheel configuration. Aircraft equipped with tail wheels are less stable on the ground (see Figure 3.1c), and have inferior visibility during take-off and landing because the aircraft's nose is raised higher when all wheels are on the ground. However, these drawbacks can be easily coped with by aerobatic pilots, because they are experienced pilots, according to [6].

Nose wheel landing gears are more stable when braking and more often used, but have a larger mass because a nose wheel needs to stronger than a tail wheel. Additionally, a nose wheel has a longer strut and produces much more drag than a tail wheel because of that. The tail wheel configuration is selected for its advantages in weight and drag.

Wing configuration. The most significant configuration option is the wing configuration. The possible choice can be made between biplane and monoplane, as can be seen in Figure 3.1d. The bi-plane can achieve shorter wingspan for the same surface area and has more structural efficiency, while the mono-plane is aerodynamically more efficient, according to [8]. Since there is no clear indication that one concept is better than the other, the choice is made to analyze both options in more detail.

3.3. Conceptual Sizing 13

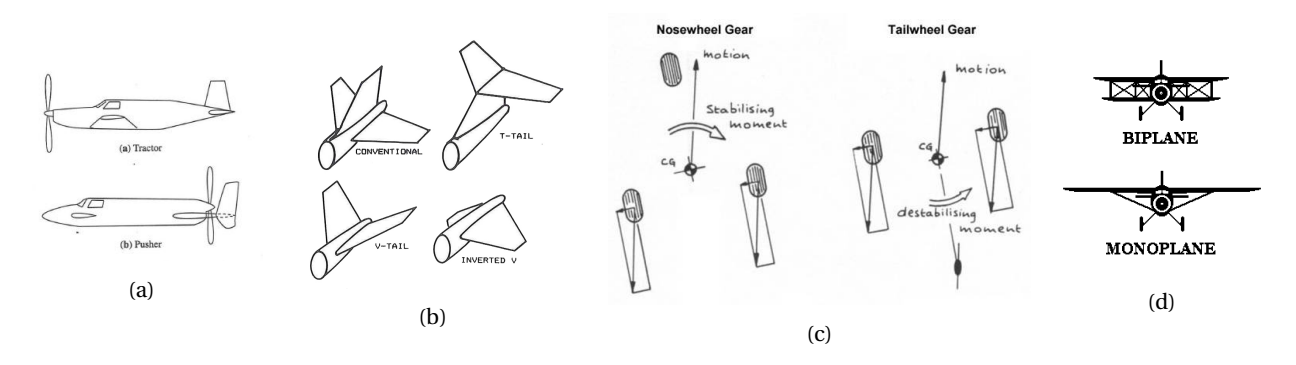


Figure 3.1: Options for four main configuration choices.

Combination of configuration options. Table 3.1 summarizes the configuration choices and shows which two combinations will be investigated further.

Table 3.1: Configuration summary of the two chosen concepts

	Wing type	Landing gear type	Propulsion	Tail	Seating arrangement
Concept 1	Biplane	Tail	Tractor	Conventional	Single/tandem
Concept 2	Monoplane	Tail	Tractor	Conventional	Single/tandem

3.3. Conceptual Sizing

Initial values for the take-off W_{TO} , payload W_{PL} , fuel W_F , empty weight W_E and minimal required power, are calculated using the Class I design methods as specified by the Roskam [9]. The payload weight is determined by the components specified in the Request for Proposal, resulting in a payload weights of 275 lbs and 460 lbs for the one-seat and two-seat variants, respectively.

In the later design stages it is determined that the Class I estimation for specific fuel consumption is too optimistic, which is then corrected for. Hence, the Class I fuel weights are updated to $W_F = 46 \text{ kg}$ (100 lbs) and 54 kg (199 lbs) for the aircraft. Parameters used for this calculation are shown in Section 10.2.4.

Table 3.2: Payload weight and components

Aircraft:	One s	seater	Two seater		
$W_{ m PL}$	1220 N	275 lbs	2050 N	460 lbs	
$W_{ m Pilot}$	1020 N	230 lbs	(2x) 890 N	(2x) 200 lbs	
$W_{\mathrm{Parachute}}$	67 N	15 lbs	(2x) 67 N	(2x) 15 lbs	
$W_{ m Baggage}$	130 N	30 lbs	130 N	30 lbs	

Based on the driving requirements a design point in the available design space is chosen. The requirements on the design space are: stall speed, landing and take-off distance, rate of climb and maneuvering requirement. Of which the stall speed, climb rate and maneuvering requirements are the most restrictive.

3.3. Conceptual Sizing 14

The stall speed must be less than 45 knots without the use of lift enhancing devices, as defined in the LSA definitions in [3, Section 6 434.a.4]. The minimum maneuvering performance required for the International Aerobatic Club Intermediate Category is a sustained 60 degree bank turn [10], which corresponds to a 2G sustained load factor.

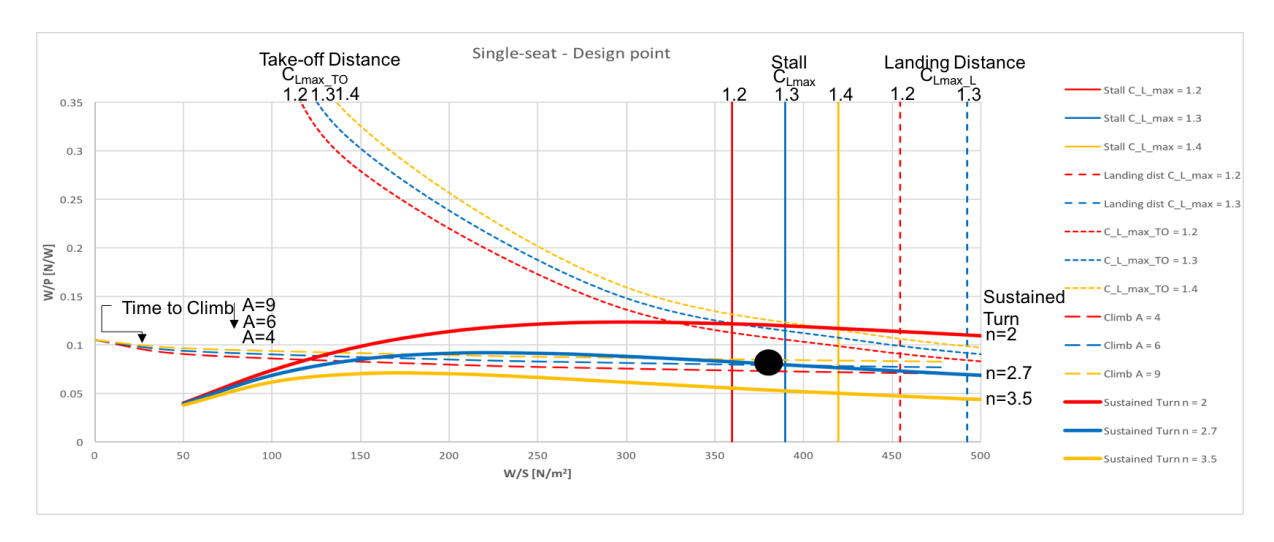


Figure 3.2: W/P-W/S diagram and design point for the single-seat aerobatic LSA.

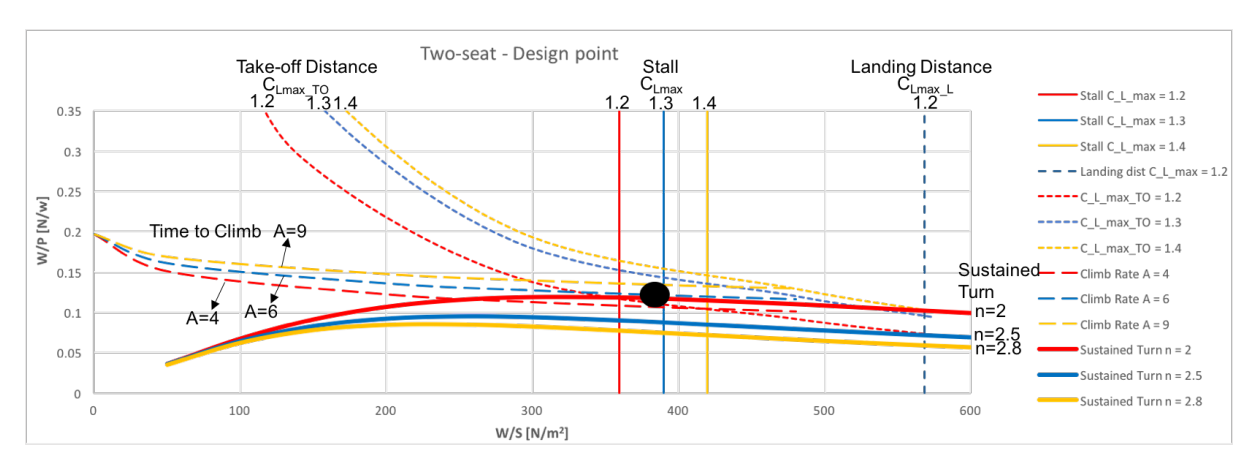


Figure 3.3: W/P-W/S diagram and design point for the two-seat aerobatic LSA.

The selected design points are presented in Table 3.3. From these, a required surface area and power can be obtained. The results are summarized in Table 3.4.

Table 3.3: Design points for the aircraft family including maneuverability

	Power load	ling , W/P	Wing load	ling, W/S
One-seater	0.079 N/W		$390 N/m^2$	8.2 lbs/ft
Two-seater	0.118 N/W	20 lbs/hp	$390 \ N/m^2$	8.2 lbs/ft

3.4. Concept Design

Table 3.4: Class I weights and initial sizing parameters

	MTOW		$W_{\mathbf{E}}$		$W_{\mathbf{F}}$		S		$P_{\mathbf{min}}$	
One-seater										
Two-seater	591 kg	1300 lbs	343 kg	756 lbs	37 kg	81 lbs	$14.9 \ m^2$	$160 f t^2$	49.4 kW	66 hp

3.4. Concept Design

3.4.1. The monoplane concept

The monoplane conceptual design has a conventional layout. The only difference between the one-seat and two-seat variant is in the wing. In order to achieve much part commonality the fuselage, tail-planes, landing gear and propulsion system are identical for both variants. There would be little gain when these components are sized separately to avoid over-design for one of the variants. The wing, however, has a different design, because the wing is the heaviest single component and has much influence on aerodynamic drag.

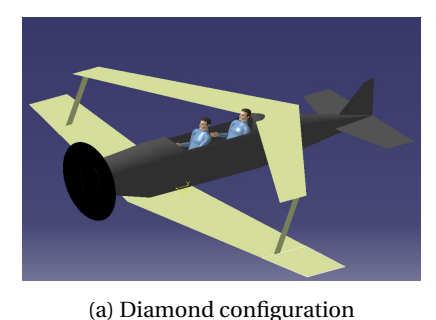
In order to be able to design two different wings and still have common wing parts for both variants, the concept of wing extensions is used. The wing surface can be increased by either adding a wing section at the tip or by inserting a wing section between the wing root and the fuselage. The latter option is used, because the aspect ratio increase due to a root extension is less than due to a tip extension, and weight increases with aspect ratio.

A low-wing configuration is selected instead of a mid-wing or a high-wing configuration. In a high-wing configuration it would be more difficult to attach the wing to the fuselage due to interference with the canopy. Furthermore it would require excessive anhedral to avoid too much lateral stability. In a mid-wing configuration the wing spar would interfere with the pilot position (in the likely case that a spar construction will be used in the wing).

3.4.2. The biplane concept

Like the monoplane concept, the biplane concept has a conventional layout. However, the extra wing introduces more design parameters that need to be determined, including stagger, sweep, and relative wing location. Seven concepts, each with different combinations of these parameters, are generated. These included a diamond configuration (see Figure 3.4a), plain forward stagger, double gull wing, canard landing gear (see Figure 3.4b) and bottom gull wing (see Figure 3.4c). The same wing extension concept as explained in the previous section was used in the in the biplane concepts. All designs feature tip extensions to transform the wing from the one-seat variant to the wing of the two-seat variant. The most potent biplane concept is determined to be (Figure 3.4c), since it is thought to have, amongst others, good structural efficiency and very good potential for high commonality.

3.4. Concept Design







(b) Canard landing gear configuration

(c) Bottom gull wing configuration

Figure 3.4: Selection of biplane configurations

3.4.3. Comparison

All major design parameters and some performance characteristics from the concept design are summarized in Table 3.5. The main difference in the weights is the wing weight for both aircraft: 40 kg (88 lbs) / 47 kg (104 lbs) for the monoplane variants and 102 kg (225 lbs) / 108 kg (238 lbs) for the biplane variants. This large difference can partially be explained by the different methods that were used to estimate component weights. The Cessna method for general aviation airplanes, as published by Roskam [11], was used to estimate component weights for the monoplane, while the method by Torenbeek [12] was used for the biplane.

Furthermore, the literature for biplane wing design is quite limited as opposed to that for a monoplane. The wing planform for the biplane first had to be converted into an equivalent mono-wing planform (as explained by Stinton [13]), before any calculations could be performed. The distribution of loads through the biplane structure was also more complex than for the monoplane, which all led to a rather conservative estimate for the wing weight. This is however not correct: a biplane wing can actually be lighter than a monoplane wing. The structural advantage of biplane wings over mono-wings is investigated in Section 3.7.

3.5. Concept Trade-off

Table 3.5: Summary of concept analysis between biplane and monoplane

		Mono	plane	Biplane		
Parameters	Units	One-seater	Two-seater	One-seater	Two-seater	
Weights						
Engine	[kg] ([lbs])	84 (185)	84 (185)	89 (196)	89 (196)	
Wing	[kg] ([lbs])	40 (88)	47 (104)	102 (225)	108 (238)	
Horizontal tail	[kg] ([lbs])	8.9 (20)	8.9 (20)	10 (22)	10 (22)	
Vertical tail	[kg] ([lbs])	3.4 (7)	3.4 (7)	10 (22)	10 (22)	
Fuselage	[kg] ([lbs])	40 (88)	33 (73)	60 (132)	60 (132)	
Nacelle	[kg] ([lbs])	15 (33)	15 (33)	13 (29)	13 (29)	
Propeller	[kg] ([lbs])	11 (24)	11 (24)	4.8 (11)	4.8 (11)	
Fuel system	[kg] ([lbs])	2.3 (5)	2.3 (5)	3.6 (8)	3.6 (8)	
Flight controls	[kg] ([lbs])	6.5 (14)	8.4 (19)	10 (22)	10 (22)	
Electrical system	[kg] ([lbs])	10 (22)	14 (31)	5 (11)	5 (11)	
Avionics	[kg] ([lbs])	15 (33)	29 (64)	6 (13)	10 (22)	
Landing gear	[kg] ([lbs])	26 (57)	29 (64)	11 (24)	11 (24)	
Other	[kg] ([lbs])	0 (0)	0 (0)	15 (33)	22 (49)	
OEW	[kg] ([lbs])	262 (578)	285 (628)	339 (748)	356 (786)	
Useful load	[kg] ([lbs])	170 (375)	257 (567)	260 (573)	240 (529)	
MTOW	[kg] ([lbs])	422 (930)	523 (1153)	484 (1067)	600 (1320)	
Wing	0					
Wing area	$[m^2]([ft^2])$	10.1 (109)	13.3 (143)	14 (151)	16.6 (179)	
Wingspan	[m] ([ft])	7.8 (26)	9.9 (32)	6 (20)	8 (26)	
Root chord	[m] ([ft])	1.5 (5)	1.6 (5)	1.5 (5)	1.5 (5)	
Tip chord	[m] ([ft])	1.1 (4)	1.1 (4)	0.78(3)	0.52(2)	
Aspect Ratio	[-]	6	7.3	5.2	7.7	
Airfoil	[-]	NACA 632-415	NACA 632-415	NACA 63 ₁ -212	NACA 63 ₁ -212	
MAC	[m] ([ft])	1.31 (4)	1.36 (4)	1.21 (4)	1.12 (4)	
Fuselage						
Width	[m] ([ft])	0.6(2)	0.6(2)	0.7 (2.3)	0.7 (2.3)	
Length	[m] ([ft])	6 (20)	6 (20)	6.1 (20)	6.1 (20)	
Tail		, ,	, ,	, ,	, ,	
$S_{\rm h}$	$[m^2]([ft^2])$	2.5 (27)	2.5 (27)	2.5 (27)	2.5 (27)	
$S_{\rm v}$	$[m^2]([ft^2])$	1.5 (16)	1.5 (16)	1.3 (14)	1.3 (14)	
Horizontal tail arm	[m] ([ft])	3.4 (11)	3.4 (11)	3.5 (11)	3.5 (11)	
Drag		• •	. ,	• •	. ,	
$C_{\rm D}$ (at $C_{\rm L}$ =0.3)	[-]	0.069		0.023		
Drag area	$[m^2]$ (ft ²])	0.25 (2.7)		0.33 (3.6)		
Moment of inertia	1 (1)	- 🕻 🧳		- ()		
Ixx	$[kgm^2]$ ($[lbsft^2]$)	363 (8614)	513 (12174)	411 (9753)	429 (10180)	
Iyy	$[kgm^2]$ ($[lbsft^2]$)	616 (14618)	762 (18083)	766 (18177)	794 (18842)	

3.5. Concept Trade-off

This section presents how the trade-off between the monoplane concept and the biplane concept is done. Trade-off criteria, analysis methods and result of the trade-off are discussed.

3.5. Concept Trade-off

3.5.1. Trade-off criteria

Six criteria are used to evaluate both concepts in order to find the best option. All of these criteria are given a weight factor from 1 until 5, with 5 signifying the most importance. The weights can be found in Table 3.6.

Performance Since the assignment specifies an aerobatic aircraft, performance has to be one of the main priorities. Therefore, this parameter is given the highest weight factor. In Table 3.5 it is shown that the monoplane concept performs better in terms of weight, drag area and moment of inertia around the roll axis. This means that the monoplane will outperform the biplane during aerobatic maneuvers as well as in normal cruise conditions.

Pilot visibility Good visibility is key during aerobatic flight and for safety. An aerobatic pilot requires excellent visibility during a competition routine and prefers to be able to see the aircraft's position with respect to the judges to optimize figure accuracy [6]. For this reason, visibility is graded with maximum weight factor as well. The biplane performs much worse w.r.t. the monoplane due two its two wings, of which the top wing blocks a considerable part of the upward and forward view. Furthermore, struts and brace wires between the biplane wings further limit the pilot's field of vision.

Useful load An important criterion for the customer is the amount of payload he/she can take along on a normal, non-aerobatic flight. Contrary to the other trade-off criteria, a requirement for payload is posed in the RFP [5]. Looking at the values in table 3.5 it is clear the biplane has much more payload capability in terms of weight than the monoplane.

Risk of concept The risk of a concept mainly depends on how much the feasibility of the concept has already been proven. Both the monoplane and the biplane concepts are proven concepts. However, very little design information is available about biplane aircraft, because the concept is considered to be outdated and is rarely applied. This means that the design of a biplane concept will be much harder, and the risk of making an incorrect or sub-optimal design is larger. This was already experienced during the initial planform design and weight estimation of the biplane wing.

Versatility The versatility aspect comes down to the different functions that the aircraft can perform. If both concepts are similar but one of the designs is capable of performing more functions and more diverse missions it has a significant advantage in the market and is therefore awarded a weight factor 3. The tip extensions make the biplane

3.5. Concept Trade-off

more versatile since one plane could, in theory, perform both of the mission profiles.

Cost A lower production cost will tend to result in lower unit price, which would make the design more competitive in the LSA market. Additionally, low operational costs will increase market competitiveness even further. To make the aircraft competitive, this criteria is marked with a weight factor of 4. The spar and skin of a biplane wing are stressed less than in a mono-wing, which makes production of the biplane wing easier. The major design difference between two concepts is the fact that the biplane one-seat variant can be converted into the two-seat variant. This means basically only one aircraft has to be produced and only minor changes are needed to convert one variant into the other.

3.5.2. Analysis methods for trade-off

Both concepts are designed mainly using methods from Roskam [9], [14], [15], [16], [11]. However, different methods are used during analysis of the performance of the concepts. For example, the Cessna method for general aviation airplanes, as published by Roskam [11], is used to estimate component weights for the monoplane, while the method by Torenbeek [12] is used for the biplane. Drag estimation is also done using different methods for both concepts. These differences made it hard to compare the two concepts. The difference occurred since each concept is designed by two teams working separately, without much communication. By the the time is became evident, there was not enough time to redo the analyses with the same methods for both concepts. Still, it is possible to judge that the mono-plane is a better option to continue the design process with.

3.5.3. Trade-off results

All the points and final scores for the concept are summarized in Table 3.6. It can be seen that the monoplane has an advantage over the biplane overall. Furthermore, if the criteria with the highest weight factors are isolated it is clear that the monoplane is the better option to continue the design process with.

Table 3.6: Summary of trade-off table with all parameters, weights and point division

		Poir	ıts	Score		
Parameter	Weights	monoplane	biplane	monoplane	biplane	
Performance	5	5	3	20	15	
Pilot visibility	5	3	2	15	10	
Useful load	2	3	5	6	10	
Risk of concept	4	5	2	20	8	
Versatility	3	2	4	6	12	
Production cost	4	3	5	12	20	
Total				84	75	

3.6. Approach to Commonality

As mentioned in the request for proposal, a high level of part commonality is critical for the success of the SALSA family. The basic idea behind commonality within an aircraft family is that a smaller total number of unique aircraft components results in a reduction in production cost. Therefore, the goal is to achieve maximum commonality between both family members. Additionally, the aim is to reduce the amount of parts in the individual aircraft, to drive down the cost of production even further. The approach to achieve maximum commonality within the SALSA family is discussed in this section.

3.6.1. Family commonality

The difference between the one-seater and two-seater is mostly found in the wings. These differ in size because of the difference in maximum takeoff weight between the aircraft versions. The two-seat aircraft has a larger maximum takeoff weight and as such requires more wing surface area to comply with the stall speed requirement of 45 kts. To achieve the 75% commonality minimum mentioned in Chapter 2, however, the wings definitely have to show commonality between family members.

The choice can be made between root or tip extensions, added to the single seat aircraft wing to give the two seat aircraft its required wing area. The tip extensions impose an extra bending moment into the wing of the single seater which would then require a reinforced structure to cope with the extra loads. The root extension is therefore preferred because this does not force the structure of the one-seater wing to be overdesigned. Moreover, for a tapered single seat wing, adding wing area at the tip would result in a larger wingspan increase than adding wing area at the root. In this respect root extensions are favourable, because a very large wingspan is not desired for aerobatic aircraft (due to an increase in moments of inertia).

The empennage design is identical for both SALSA aircraft for the sake of commonality. It is designed for stability and control of the two-seater, since this drives the size of the surfaces to the largest extent. For the one-seater this results in more controllability.

The fuselage of the family is common in size and shape. This decision followed from the material and construction choice for the fuselage, which is further elaborated upon in Chapter 8.3. Since the fuselage is a semi monocoque structure, the production requires accurate moulds. A common fuselage structure eliminates the production costs of one mould. The largest difference between the two fuselages is the positioning of the pilot and the shape of the canopy. An added benefit of this design is that the landing gear does not have to be redesigned or changed. The length of the fuselage is identical, so the angle between the fuselage and the ground will not change with an identical

main landing gear.

3.6.2. Aircraft commonality considerations

Next to commonality between the SALSA family members, reducing the number of unique components in a single aircraft reduces production costs even further. This is taken into account in the shaping of the SALSA family. The aircraft consists of as many straight parts as possible where structural components have to be placed. Straight components are much cheaper to produce than curved components. The constant diameter section of the fuselage lends itself to reuse a large number of structural components such as fuselage frames.

The position of the wing cannot change between the family members, because that would require a very different fuselage structure and would therefore reduce commonality. The positioning and weight of the pilot greatly influences the weight and balance. The wing is positioned such that stability requirements for both SALSA variants are met for the same attachment position of the wing with respect to the fuselage.

3.7. Mono and Bi-wing Weight Comparison

When struts and brace wires are applied in a biplane wing to connect both wings with each other and with the fuselage, an I-beam is formed, where the wings form the flanges and the connecting parts form the web. When this effect is exploited, the load-carrying structure might weigh appreciably less than a monoplane wing. In order to determine the weight saving that might be obtained by using two wings, the load case and structure are modelled.

The following assumptions are made in general:

- Total lift force is 72 kN (lifting 600 kg mass with a load factor of 12).
- Uniform lift distribution over the span.
- Wing span is 8 m
- · I-beams have equal web and flange thickness.
- I-beams have constant cross-sectional dimensions but with varying thickness along the span.
- Material is Aluminium 7075, with a Youngs modulus of 70 GPa and yield strength of 500 MPa.

The following assumptions are made for the mono-wing:

- · Wing-fuselage connection is clamped.
- Bending moments are carried by thin I-beams.

The following assumptions are made for the bi-wing configuration:

- · Lift force is equally divided over top and bottom wing.
- Vertical separation between top and bottom wing is 1.0 m.

- The vertical strut and attachment point of brace wire to top wing is at 30 % semi-span from the tip. This results in the smallest maximum bending moments.
- Bending moments are carried by thin I-beams.
- The vertical strut consists of a thin-walled hollow circular beam with constant diameter and thickness along its length.
- Wing-fuselage connections are hinged.
- Compressive force in the root part of the top wing is carried by a thin-walled hollow circular beam with constant diameter and thickness along its length.

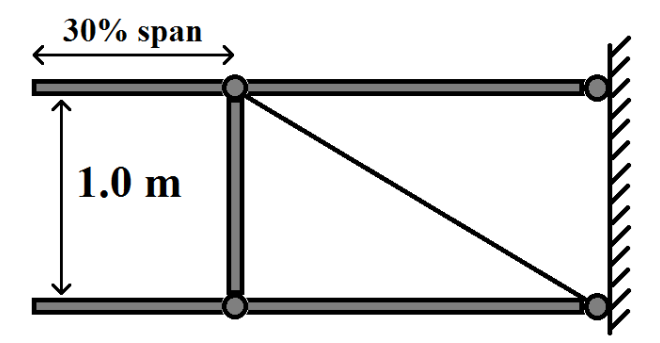


Figure 3.5: Front view of model of biplane wings that was used in the structural analysis.

The following estimations of the required wing structures are obtained. The I-beam required in the mono-wing case would weigh an estimated 6.0 kg. In the bi-wing case, the compression loaded part in the top wing would weigh 3.7 kg. However, the function of this part can also be fulfilled by other constructive parts in the wing, like the spar. The vertical strut would weigh 1.0 kg. The spars in both wings would weigh 0.4 kg. The total structural weight for the bi-wing (neglecting the brace wire) is then 5.6 kg. All of these values are per half of the total wing span.

In conclusion, the weight difference is only 0.5 kg. When no extra compression member is needed in the top wing because its function can be performed by other structures, the weight saving is 4.0 kg per side, or 8 kg in total, which corresponds to about 1% of the MTOW.

4

Aircraft Layout

This chapter presents the general layout of the aircraft and discusses in particular the design of the wing and the fuse-lage, but also the horizontal tail, vertical tail and landing gear. The design of the aircraft is based on the monoplane concept which is presented in Section 3.4.1.

4.1. Overview

This section presents three-views of the aircraft. Figures 4.1a and 4.1b show top views of the one-seat and two-seat variants, respectively. Figures 4.2a and 4.2b show front views of the one-seat and two-seat variants, respectively. A side-view of the two-seater aircraft can be found in Figure 4.3a.

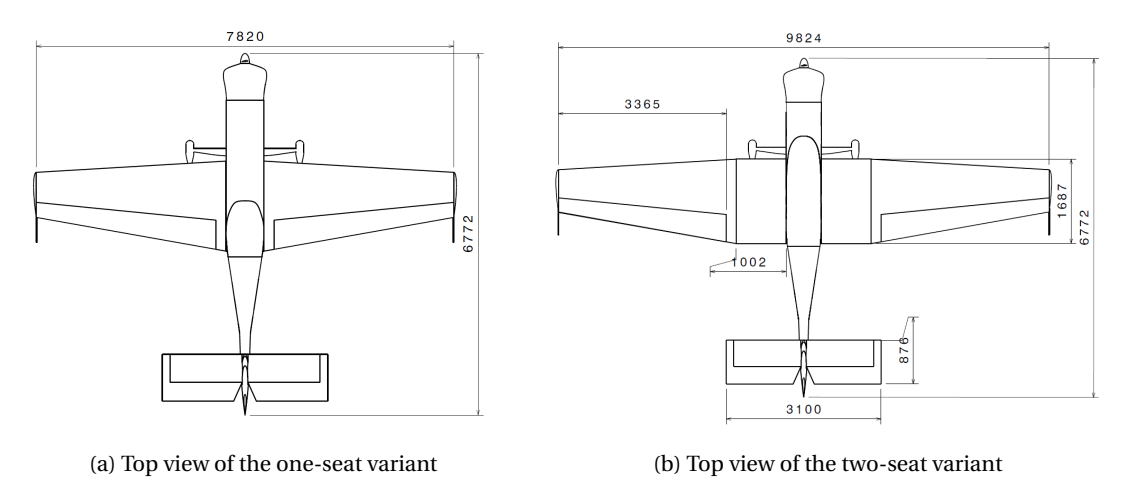


Figure 4.1: Top views of SALSA family members

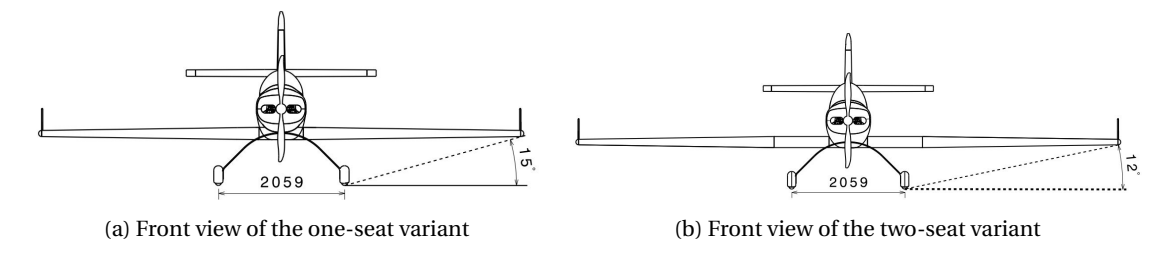


Figure 4.2: Front views of SALSA family members

4.2. Fuselage Design

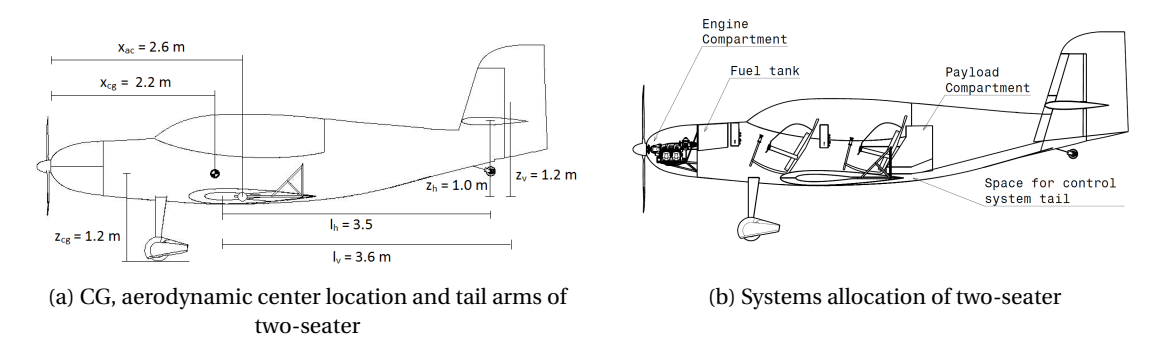


Figure 4.3: Side view of the two-seat variant

4.2. Fuselage Design

The fuselage is characterized by its function of connecting all components of the aircraft. This section presents the design of the fuselage, namely its shape, size and its interface with other components. The cabin layout is discussed in Section 9.3. The structural design of the fuselage is discussed in Section 8.3.

4.2.1. Fuselage layout

Design approach The selected aircraft configuration fixes the relative location of the fuselage, wing, tail planes, cabin, propulsion system and landing gear. However, the exact location of these components can be varied.

The process of determining the location of all systems and components starts with an initial estimate of the positioning of all components and systems. Together with estimations of their weights an estimation of the centre of gravity of the empty aircraft is made. Adding the contributions of payload and fuel results in the centre of gravity of the aircraft in flyable state. Multiple loading situations need to be considered to account for differences in pilot weight, fuel weight and baggage weight. The CG ranges are plotted in a scissor plot, together with functions that define the required horizontal tailplane size, which is required to guarantee static longitudinal stability and longitudinal control (These plots are presented and discussed in section 7). In subsequent iterations, the positions of the pilots and wing are altered in order to size the layout for minimum horizontal tail size. The following targets are kept in mind during this procedure:

- Positioning the front pilot of the two-seater close to CG of the two-seater aircraft. This results in minimum CG range of the two-seater. This is required for minimizing the horizontal tailplane area.
- Positioning the wing such that the aircraft CG at the most likely loading configuration during cruise flight is close to the 25% chord position of the Mean Aerodynamic Chord of the wing. This is beneficial because in that case the lift force does not produce a moment about the aircraft CG.

Longitudinal positioning of systems and components The most forward part of the fuselage is the engine cowling. The engine is mounted to the firewall as well as the fuel tank. The landing gear is attached to the bottom of the

4.2. Fuselage Design 25

fuselage at a longitudinal location between the firewall and the wing. The wing is attached to the bottom of the fuselage, under the pilot(s). The vertical tail is mounted to the end of the fuselage. The horizontal tail is not mounted to the fuselage but attached to the vertical tail. This allows the horizontal tail to be constructed in one piece, while being detachable. The vertical location of the tail and of the aft part of the fuselage is positioned such that a sufficient angle of attack (14°) is reached during ground roll. The canopy smoothly attaches to the aft part of the fuselage in order to prevent flow separation behind the canopy. A side-view of the fuselage is shown in Figure 4.3b. In this Figure 4.3b, aircraft systems, pilot(s) and payload locations can be seen.

4.2.2. Sizing

The length of the fuselage is sized by the required volume of all the systems, like the fuel system, control system, cabin area and payload area. The height of the fuselage is determined by the height of the pilot(s) in sitting position. The seats are slightly inclined backwards. This reduces the required height and is beneficial for comfort during high load factor maneuvers. The maximum height of the fuselage is 1.2 m. The width of the fuselage is determined by the width of the pilot(s). The fuselage is wide enough to accommodate the pilot(s) comfortably. The maximum width of the fuselage is 0.7 m.

4.2.3. Payload Area

The location of the luggage storage volume is located behind the (rear) pilot, measured from the nose. This volume provides sufficient space for 30 pounds and 6 cubic feet of luggage for two-seat variant and 30 pounds and 4 cubic feet for one-seat variant, according to the requirement in the RFP. The internal volume requirements are accommodating 95% of human pilot sizes and required baggage capacity can be seen in Figure 4.4.

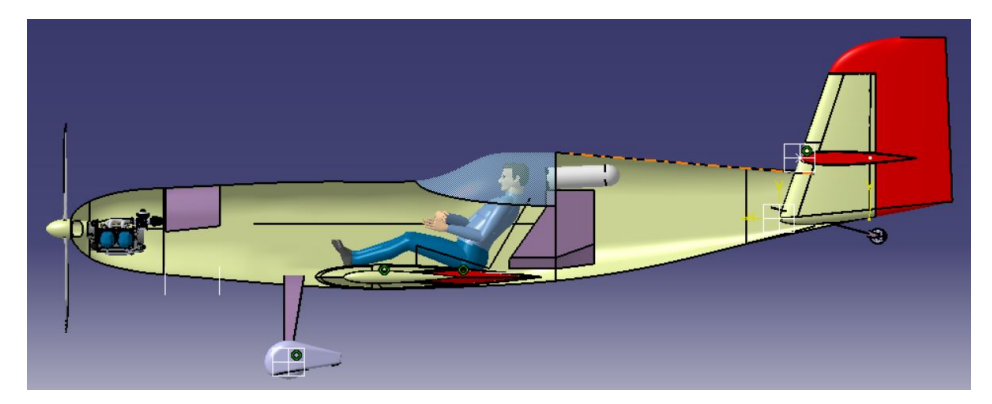
4.2.4. Interfaces

Attachment of tail surfaces The wings and horizontal tail are removable such that the aircraft can be transported on a trailer. Rigging of the wings can be performed easily by two persons, or by one person when using a rigging stand. The attachment of the vertical tail is discussed in more detail in Section 8.4.

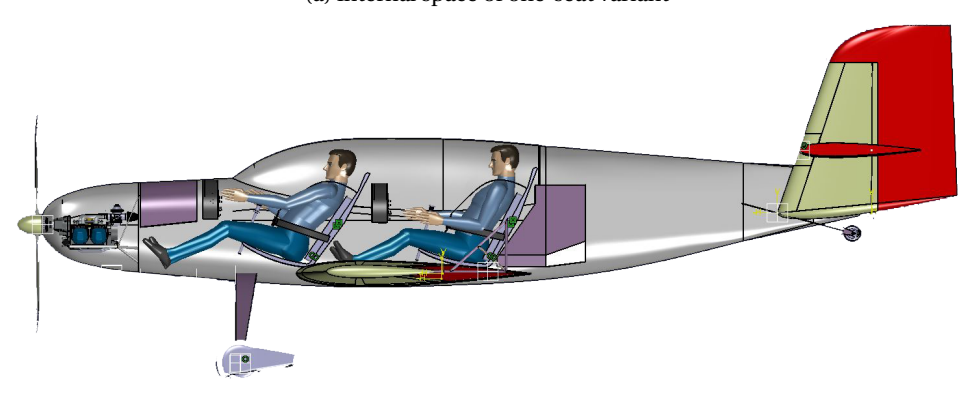
Wing attachment Attachment of the wing to the fuselage is done by a construction that is commonly used in glider aircraft. It is presented in Section 8.2.1.

Engine attachment The engine is located in front of the firewall. The engine is mounted to the firewall by means of a tube structure.

4.3. Wing Design 26



(a) Internal space of one-seat variant



(b) Internal space of two-seat variant

Figure 4.4: Sideview indicating systems allocation

4.2.5. Visibility

The visibility for the pilots are the following: the over-nose angle in horizontal attitude are 6.5 and 4 degrees for the front and rear pilot respectively.

The rearward visibility for the pilots are restricted by the tail. The angles that the pilots can look back from the direction of flight are 170 and 138 degrees for the front and rear pilot respectively.

The pilot can look down with 37 degrees with respect to the horizon.

4.3. Wing Design

This section presents the planform design of the wing, which is defined by the area, aspect ratio, taper ratio, sweep, and twist. In order to determine the wing area, the maximum wing lift coefficient needs to be determined first, by choosing the airfoil.

4.3.1. Airfoil selection criteria

Four criteria for airfoil selection are used, which are explained in the following. The maximum lift coefficient requirement turned out to drive the search for a suitable airfoil the most.

4.3. Wing Design 27

Maximum lift coefficient at low Reynolds numbers An aircraft lift coefficient of 1.3, without the aid of High-Lift Devices (HLDs), is assumed in the Class I design. This implies that the airfoil should have a $c_{l_{max}}$ of at least 1.6, at low Reynolds numbers, which relatively few airfoils can achieve.

Minimum lift coefficient The airfoil has to reach the lift coefficients required to reach load factors of -5G. This requires a relatively large negative lift coefficient, of about -1.0. This drives the selection towards a symmetric airfoil.

Stall characteristics Very "crisp" stall characteristics are favoured by aerobatic pilots. [6] This means that the stall should happen in a small range of angle of attack values, which makes it easier to perform snap rolls.

Symmetry For aerobatic maneuvers a symmetric airfoil is preferred such that there is no difference in lift and drag behaviour between normal flight and inverted flight. A cambered airfoil would produce a great amount of drag when producing negative lift compared to a symmetric airfoil. Furthermore, a different pitch angle would be required to yield the same flight path angle, which is harder to perform correctly.

4.3.2. Airfoil data source and investigated airfoils

Wind tunnel data was strongly preferred over theoretically calculated data because of its reliability. A comprehensive and reliable (published) source of wind tunnel data was found to be "Theory of Wing Sections" [17]. This limited the available airfoils to the NACA series. The following airfoils are found to be potentially suitable, purely based on their maximum lift coefficient:

NACA 0012	NACA 2412	NACA 23015	NACA 63 ₁ -212	NACA 632-215	NACA 64 ₁ -112
NACA 1412	NACA 2415	NACA 63-210	NACA 63 ₁ -412	NACA 632-415	NACA 64 ₁ -A212
NACA 2410	NACA 23012	NACA 631-012	NACA 632-015		

After comparing these airfoils on the additional selection criteria, the NACA 0012 airfoil was selected. This airfoil is fully symmetric and has a maximum (positive and negative) lift coefficient of 1.55 with little variation with Reynolds number. It also shows the most "crisp" stall characteristics of all airfoils that were investigated.

4.3.3. Determining maximum lift coefficient at stall speed

The lift curve shows that the lift coefficient varies slightly with Reynolds number. The maximum lift coefficient drops from 1.6 to approximately 1.5 between Re numbers of 9.0M and 3.0M. The lowest Reynolds number for which measurement data are shown is 3.0M, while the Reynolds numbers at the wing root and tip at stall speed are 2.7M and 1.4M respectively, corresponding to an airspeed of 23 m/s (equal to 45 kts) and chord lengths of 1.69 m (5.5 ft) and 0.85 m (2.8 ft) respectively. It is assumed that the section lift coefficient is at least 1.45 at stall speed.

4.3. Wing Design

However, the airfoil lift coefficient differs from the aircraft lift coefficient. Two properties of general lift distributions were accounted for to determine the aircraft maximum lift coefficient:

- Planform with lower local lift coefficient at the tips than at the root for preventing tip stall. Because of this the wing tip lift coefficient will likely be at least 0.1 smaller than the lift coefficient at the wing root.
- Wing tip vortex-induced decrease of local angle of attack at the wing tips when flying at large aircraft lift coefficients. It was assumed that this effects limits the average wing lift coefficient such that it is at maximum about 0.1 lower than the maximum section lift coefficient.

Accounting for these two effects, the maximum aircraft lift coefficient at stall speed is expected to be 0.2 lower than the average maximum lift coefficient at the wing root and tip at, bringing the maximum aircraft lift coefficient at stall speed to 1.35.

Wing area The wing area follows from the maximum lift coefficient at stall speed when flying at MTOW. The aircraft is required to have a stall speed of at most 23 m/s which corresponds to 45 knots. The required wing surface is then 9.9 m^2 (107 ft²). The wing area was set to 10.2 m^2 (110 ft²) to incorporate a small margin of safety.

Aspect ratio The selection of aspect ratio is mainly a trade-off between aerodynamic efficiency and structural efficiency. The main benefit of a large aspect ratio is greater aerodynamic efficiency, which is represented in the equation for the induced drag coefficient. However, the main benefit of a small aspect ratio is greater structural efficiency. This has two causes: (1) the bending moment in the wing is smaller due to the smaller tailplane span, and (2) the wing is thicker due to larger chords, which increases the bending stiffness of the wing structure.

Low weight was considered to be more important than aerodynamic efficiency, since fuel consumption is not very critical. The method that was used to estimate the wing weight showed a large dependency of wing weight on aspect ratio. In the Class I sizing phase of the design an aspect ratio of 6.0 was assumed for initial calculations. It was decided to keep this aspect ratio for its benefit of low structural weight. If the aspect ratio is increased to 8, it would result in a weight increase of about 20 kg.

Taper ratio The main concerns of taper ratio in this case are the following: (1) Positive taper produces a more elliptical lift distribution, which corresponds to less induced drag. (2) Taper ratio reduces bending moments in the wing because the lift is produced closer to the wing root, hereby reducing the structural weight. (3) Too much taper induces tip stall.

Twist Wing twist can improve stall characteristics, and reduce induced drag when applied correctly. However when flying inverted the effect is adverse. Without twist the aircraft will respond similarly when flying inverted. Therefore the wing has no twist.

Sweep Wing sweep has the following main benefits: (1) Reduced tip stall in case of forward sweep, (2) reduced drag increase at large Mach numbers in case of backward sweep, and (3) moving the aerodynamic centre of the wing. The disadvantage of wing sweep is that it increases torsional moments and reduces structural efficiency because the so-called "structural span" increases. Furthermore, structural divergence may occur in case of forward sweep. Since applying wing sweep has no significant advantage, the wing sweep has been chosen such that the quarter-chord line has zero sweep.

4.4. Horizontal Tailplane Planform

This section presents the aerodynamic design of the horizontal tailplane, defined by the airfoil, aspect ratio, taper ratio, sweep, and twist. Note that the size of the horizontal tailplane is discussed in 7.1. The structural design of the horizontal tailplane is discussed in section 8.4. A picture of the planform is shown in Figure 4.5a.

Airfoil selection The NACA 0012 airfoil is selected for the horizontal tailplane. This airfoil is selected considering following reasons:

- The NACA 0012 airfoil is symmetric. Therefore, the horizontal tailplane has the same lift and drag characteristics during inverted flight as in normal flight. This is beneficial because it makes the airplane more predictable in aerobatic flight.
- The NACA 0012 airfoil has a relatively large maximum lift coefficient, even for low Reynolds numbers, namely 1.6, as can be found in "Theory of Wing Sections" [17]. This high maximum lift coefficient is advantageous since a smaller tailplane will suffice, which lowers the tailplane weight.

Aspect ratio Aspect ratio mainly has effect on weight and aerodynamic efficiency. The weight of the horizontal tailplane has an effect on the balance of the aircraft, making it critical. However, an optimization which takes into account aerodynamic and structural characteristics, to find the most optimal aspect ratio, is beyond the scope of this project. Therefore, the aspect ration is chosen based on aspect ratios of reference aircraft. Table 4.1 shows horizontal tailplane data of aircraft that are designed for similar purpose and have comparable MTOW. The average aspect ratio is 4.0, an aspect ratio of 3.5 is selected as the aspect ratio of the horizontal tail of the SALSA in order to keep the horizontal tail span within limits.

Aircraft	S_h	b_h	r _h	r_h^2/S_h	A _h
	$[m^2]$ ([ft ²])	[m] ([ft])	[m] ([ft])	[-]	[-]
Mudry CAP 10	1.86 (20)	2.9 (9.5)	0.95 (3.1)	0.49	4.5
Extra EA-230	2.0 (22)	2.4 (7.9)	0.91 (3.0)	0.41	2.9
Mylius My-103	1.72 (19)	2.8 (9.2)	0.83 (2.7)	0.41	4.6
XtremeAir Sbach 342	2.7 (29)	3.2 (11)	1.1 (3.6)	0.45	3.8
Corvus Racer 540	2.3 (25)	2.7 (8.9)	1.0 (3.3)	0.44	3.2
Partenavia P.70	1.5 (16)	2.9 (9.5)	0.73 (2.4)	0.36	5.6
Yakovlev Yak-54	3.4 (37)	3.2 (10)	1.3 (4.3)	0.49	3.0
Average	2.2 (24)	2.9 (9.5)	0.97 (3.2)	0.44	4.0

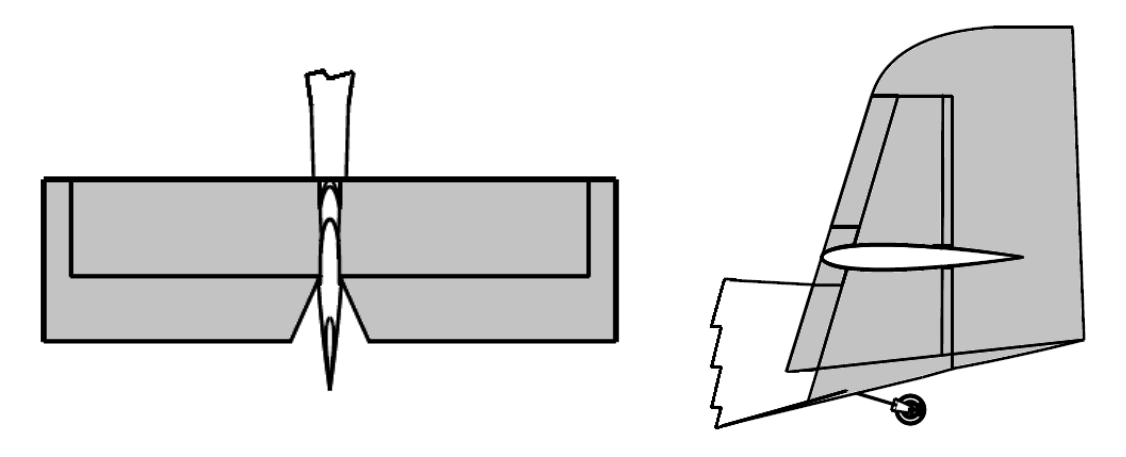
Table 4.1: Reference horizontal tailplane data.

The data are obtained by taking measurements on three-view drawings.

Taper ratio A taper ratio of 1.0 is selected because it will be easier to manufacture than a tapered wing, lowering production cost. This results in a slightly smaller aerodynamic efficiency compared to a wing with taper, but this is considered to be of less importance due to the low penalty.

Sweep The horizontal tailplane has no sweep to allow for easy manufacturing. A small amount of sweep has the benefit of increasing the tail arm by max 0.5 m, such that the tail area can be smaller. However, it is thought that the decrease in manufacturing cost outweighs the benefit of slightly increased tail arm.

Twist The horizontal tailplane produces both positive and negative lift, such that twist is not beneficial in any way. Therefore, the horizontal tailplane has no wing twist.



 $\hbox{(a) Planform of the horizontal tailplane.}\\$

(b) Planform of the vertical tailplane.

Figure 4.5: Planforms of the horizontal and vertical tailplanes.

Incidence angle An incidence angle of zero was selected such that the aircraft would perform equally when flying inverted. This results in an easier aircraft for aerobatic maneuvers.

The downwash of the main wing and the lower aspect ratio ensures that the stall angle is increased compared to wing sections with higher aspect ratio. Therefor the main wing will stall first, this is required for the self stabilization.

4.5. Vertical Tailplane Planform

This section includes the selected vertical tail planform, based on desired aerodynamic and stability characteristics. A picture of the planform is shown in Figure 4.5b.

Airfoil selection A symmetric airfoil is used for the vertical tail. In this case the NACA 0012 is used, because a thickness ratio of 12 percent is common and it has a relative large nose radius to permit a large range of angles of attack.

Size Keeping the design philosophy of maximizing the commonality, it is decided that both aircraft have the same vertical tail. The sizing of the vertical tailplane is dependent upon the directional stability, lateral stability, crosswind landing and spin recovery. First the tail is sized depended the directional stability. After that the vertical tail design is checked if it could recover from a spin. The method described in Torenbeek [12] is used to determine the size for spin recovery. To be able to recover from a spin at least one third of the rudder should be outside the wake region created by the horizontal tail during a spin. Also substantial amount of fixed area beneath the horizontal tail is needed to provide damping of the spinning motion.

Aspect ratio Due to the fact that the horizontal tail is positioned almost in the center of the vertical tail, the aspect ratio is on the low side. This is to provide enough adequate rigidity without any excessive weight penalty.

Taper ratio To reduce the weight of the vertical tail, taper is applied. Due to applied taper, the vertical tail has a sweep angle. Furthermore, an angle of sweep is also appealing factor for the customer.

Table 4.2 shows the design parameters of the vertical tailplane.

Table 4.2: Vertical tailplane parameters

Parameter	Single-seat	Two-seat	Units
Surface area S_{ν}	1.5 (16.1)	1.5 (16.1)	[m ²] ([ft ²])
Aspect ratio A_{ν}	1.5	1.5	[-]
Volume coefficient V_{ν}	0.065	0.039	[-]
Span b_v	1.5 (4.9)	1.5 (4.9)	[m] ([ft])
Sweep angle $\Lambda_{ u}$	15	15	[deg]
Taper ratio λ_{v}	0.6	0.6	[-]

4.6. Landing Gear 32

4.6. Landing Gear

Landing gear supports the entire weight of an aircraft during landing and ground operation, making it an important feature. The designed aircraft should be able to land on a runway with dry pavement as well as on grass field. A fixed non-retractable taildragger configuration is chosen as a tail-wheel undercarriage is lighter than a retractable nose wheel configuration and it makes landing on rough (grass) surfaces much easier. The landing gear sizing has been done according to the Roskam methods. [16]

Landing gear position and minimum required height The disposition of the landing gear struts is decided considering ground clearance and tip-over criteria. Since there are no regulations about propeller clearance in the FAA LightSport Aircraft Certification, the regulation in FAR Part 23 are used. For taildraggers, the clearance between the propeller and the ground needs to be at least 9 inches in the level, normal take-off or taxiing attitude, whichever is most critical. As the landing gears are statically deflected, during normal take-off attitude the aircraft will rotate around its main landing gear bringing propeller closer to the ground and tail touching the ground, thus making it most critical situation. The required propeller ground clearance is calculated to be 1.20 m (3.71 ft) from most forward c.g. location for both variants. In the ideal case, aircraft landing on all three wheels at same time (three-point landing) is desired, allowing for the shortest landing distance. With three-point landing constraints, the required height of the landing gear is determined to be 1.02 m (3.35 ft) from most forward c.g. location. Clearly, the propeller clearance is driving factor for determining the minimum required height of the landing gear. The x-position of landing gear is determined by moving the main gear further forward from the center of gravity to the angle alpha at the tail wheel until three-point criterion are met. This sets the x-position of main landing gear to be at most forward c.g. location. The minimum track width is determined by satisfying the lateral-tip over requirement and setting the lateral tip-over angle to 55°. Constrained by the lateral tip-over criterion, the wheel-track is calculated to be 2.0 m (6.6 ft). With the calculated track width, the roll clearance requirements are checked. For the lateral ground clearance criterion, the minimum angle between the wing tip and the landing gear should be greater than 5°. The angle between landing gear and wing tip is determined to be 15° for one-seat variant and 12° for two seat variant as can be seen in Figures 4.2a and 4.2b. Thus meets the lateral ground clearance criterion.

Tire Selection The tires are sized on the maximum load carried per tire, speed conditions during take-off and landing and pressure criteria for surface compatibility. The maximum allowable tire pressure for wet grassy fields is between 2.1 and 3.2 bar and for small tarmac runways are between 5.0 and 6.3 bar [16]. The aircraft should be able to handle both types of terrains. The selected tire should be designed for low pressure conditions. The calculated load per tire and relative tire dimensions are given in Table 4.3. These tires can carry higher maximum load than required,

4.6. Landing Gear 33

with a safety factor included.

Table 4.3: Tire Data

	Main	Tail	
Load partira	One Seat: 249 kg (549 lbs)	One Seat: 61 kg (133 lbs)	
Load per tire	Two Seat: 319 kg (702 lbs)	Two Seat: 77 kg (170 lbs)	
Tire outer diameter	0.31m (1.00 ft)	0.20 m (0.66 ft)	
Tire width	0.11 m (0.36 ft)	0.05 m (0.17 ft)	
Tire weight	1.30 kg (2.87lbs)	0.5 kg (1.10 lbs)	

For the main landing gear a bending beam without pistons or dampers is selected. The benefit of the bending landing gear strut is that when the tire hits the ground the entire beam starts to bend, taking up the kinetic energy of the impact. This reduces part count, interfaces and weight.

5 Propulsion

In order to select a proper propulsion system for the SALSA family, several parameters have to be taken into account. First of all, the requirements state that the engine should meet the LSA ASTM standards, which implies that the engine has to be certified [5]. Secondly, both aircraft and thus their engines have to be capable of sustaining inverted flight for at least 5 minutes. Furthermore, constraints for the design point have to be implemented, especially the minimum power required of 75 hp / 66 hp. With these parameters taken into account, the engine selection can be performed in Section 5.1. Once an engine has been selected, the propeller can be selected as can be found in Section 5.2. Finally, noise and emission analyses are detailed in Sections 5.3 and 5.4.

5.1. Engine Selection

Considered engine families Since designing and certifying a complete new engine before 2020 is unrealistic, the aircraft will be fitted with an engine from an external manufacturer. Market research into propeller engines produced several families of engines that are suitable for the LSA market. These families included the Lycoming (commonly used in aerobatic aircraft), Rotax (commonly used in LSA's), Sauer S and the D-motor families. The Sauer S engines do not produce enough power and were rejected for that reason. The D-motor family produced very high thrust to weight ratios, but the manufacturer, after contacting them, could not guarantee that their engine would be available for aerobatic flight before 2020. This limits the available options to Lycoming and Rotax engines.

Lycoming vs Rotax engines The Lycoming family is typically used in all aerobatic aircraft throughout the IAC and therefore seems very suitable for the one-seater. However, the engines are built for aircraft of higher mass than the standard LSA class. This means the engines are considerably more powerful than normal LSA engines, starting at 150 hp (112 kW), and also heavier, starting at 120 kg (265 lbs). Furthermore, most engines of the family can not fly inverted and run on Avgas. Avgas is more expensive, more polluting and the engine is not capable to run on a biofuel alternative. The Rotax engines on the other hand, have larger thrust to weight ratios, and have power outputs within the range of what is desired. Additionally, these engines run on Mogas and can also burn biofuel without modification. The Rotax 915 iSc has an installed weight of 84 kg (185 lbs) and a power output of 135 hp (101 kW). It will enter the market and be certified in 2017 and is largely based on the Rotax 912, the most common engine in the LSA market. Additionally, the Rotax engine family is generally more than \$10.000,- cheaper than the Lycoming family. For these reasons the Rotax 915 iSc engine is chosen for both aircraft. Choosing the same engine for both

5.2. Propeller Selection 35

aircraft simplifies production since only one structure for engine-fuselage integration is required.

Engine-fuselage integration The aircraft will be mounted to the firewall in the front of the aircraft. A simple tube structure can be mounted to standardized points in the engine frame making the integration very easy.

Power loading In order to check that the engine choice is capable of competitively performing aerobatics in the IAC Intermediate category, the empty weight of all aircraft competing in this category is compared to their engine power. The results are presented in Figure 5.1. As can be seen from the graph, the current design and engine power are on the regression line. Therefore, it is concluded that the Rotax engine is powerful enough to successfully compete with the one-seater SALSA in the IAC intermediate category competitions.

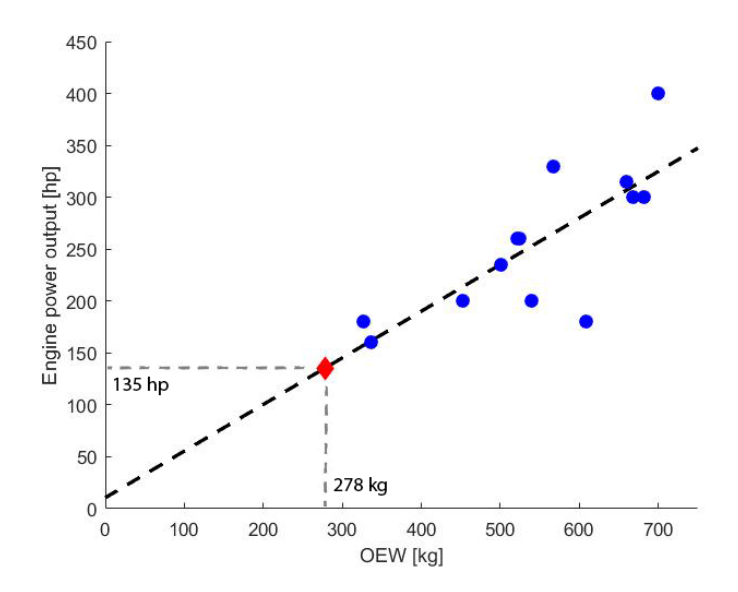


Figure 5.1: Regression between OEW and engine power. Blue circles indicate reference aircraft from Table 5.1, red diamonds indicate the SALSA design one-seater

Aircraft	OEW [kg]	Engine power [hp]	Aircraft	OEW [kg]	Engine power [hp]
Decathlon	608	180	Pitts S1S	326	180
DR107	336	160	Pitts S2A	453	200
Extra 200	540	200	Pitts S2B	521	260
Extra 300	682	300	Pitts S2C	524	260
Extra 300L	668	300	Staudacher S300	567	330
Extra 330 LX	660	315	Sukhoi 31	700	400
Giles G-202	500	235			

Table 5.1: Reference aircraft with corresponding OEW and engine power

5.2. Propeller Selection

Propellers with aerodynamic efficiencies of more than 80 % are available from multiple companies. The propeller will be an off-the-shelf component. For an initial estimation of the size, the method described in Roskam [14] is

5.3. Noise Analysis 36

used. For a power blade loading, P_{bl} , of 2.5 hp/ft², the diameter of the blade becomes 1.79 m (70.3 in). This power loading is consistent with the average blade loading for home-built and single engine propeller aircraft.

A number of propellers were found that are specifically designed for the Rotax family. It was found that certain manufacturers have created blades for all specific engines of the Rotax family. Since the Rotax 915 propeller is not yet available, the chosen design for both aircraft is the "2 Blade Rotax Ground Adjustable Propeller", from Sensenich ¹. This carbon composite blade is 70 inch (1.78 m) in diameter and weighs around 12 lbs (5.4 kg) including spinner. This product is intended for use with the Rotax 912. A similar propeller is expected to be produced by Sensenich once the Rotax 915 is brought on the market. Figure 5.2 shows the propeller and engine including the fuselage integration.

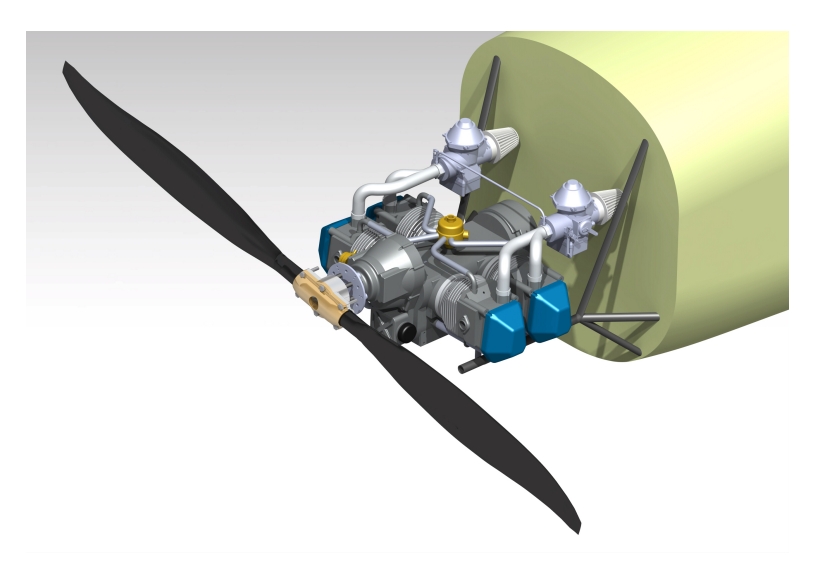


Figure 5.2: Render of the Rotax engine with Sensenich propeller and airframe integration (Note that the spinner has been hidden here)

5.3. Noise Analysis

The project requirements state that both aircraft have to comply with the noise regulations specified in ICAO Annex 16/Volume 1/Chapter 10 [5]. This document specifies that an aircraft certified after 1999 and with a MTOW of 570 kg (1256 lbs) or less, should not produce more than 70 dB, measured at a point 2.500 m (8200 ft) away from the initial ground roll. The method used to estimate the noise level at that point is given in [18, Chp. 7] and is largely based on empirical graphs shown in appendix D of [18]. The inputs for the graphs are shown in Table 5.2, as well as the outputs for the parameters.

$$dB(A) = FL1 + FL2 + FL3 + DI + NC + \Delta PNL - 14$$
(5.1)

Using Equation (5.1), given in Roskam [18], leads to a noise level of 62.5 / 67.5 dB for both aircraft. The difference between these noise levels is due to the shorter ground run and the higher climb gradient of the one-seater. Therefore

¹www.sensenich.com/products/item/44

5.4. Emissions Analysis 37

the one-seater is at a higher altitude above the microphone. These values are below the maximum noise limit. The Effective Perceived Noise level (EPNdB) for take-off is 72.5 / 77.5 dB and for landing 74.5 / 79.5 dB. However, these values are not used for the certification.

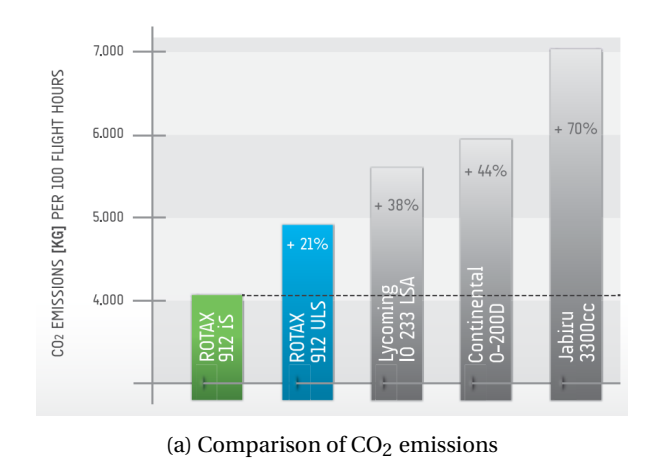
Table 5.2. Inputs and outputs for the noise analysis

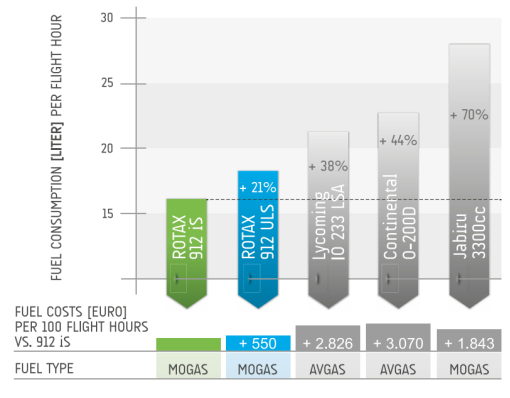
rabic o.z.	mpats and	outputs for	tile moise	arrary

Input	Output [dB]			
Parameter	Value	Parameter	One-seat	Two-seat
D_{prop} [m] ([ft])	1.79 (5.8)	FL1	74	74
$V_{\rm A}$ [m/s] ([ft/s])	340.3 (1116.4)	FL2	12	12
$M_{ m rot}$ [-]	0.62	FL3	-11	-6
$P_{ m output}$ [hp]	135	DI	0.5	0.5
no. of blades [-]	2	NC	0	0
Climb gradient one-seat [-]	0.25	ΔPNL	1	1
Climb gradient two-seat [-]	0.13			
$h_{@2500\mathrm{m}}$ one-seat [m] ([ft])	550 (1800)			
$h_{@2500\mathrm{m}}$ two-seat [m] ([ft])	290 (950)			
<i>M</i> _{tip} [-]	0.65			

5.4. Emissions Analysis

Rotax engines are widely used in the LSA category because they are more fuel efficient and cleaner than most other similarly sized engines as can be seen in Figure 5.3. It can be noted that the Rotax 912iS is almost 40% more fuel efficient than a similar Lycoming engine and up to 70% more efficient than the Jabiru engine. Similar trends are shown for the CO₂ emissions. On average, the fuel consumption of the Rotax 912iS engine is 16 l/hr (4.2 gal/hr) and produces 40 kg (88 lbs) of CO₂ per 100 flight hours. Similar figures are expected for the Rotax 915 version.





(b) Comparison of fuel consumption

Figure 5.3: Emissions and fuel consumption comparison between Rotax 912iS engine and other comparably sized engines².

²www.aviagamma.ru/912is_imagefolder.pdf

Weight and Balance

This chapter presents the Class II weight and balance of both members of the aircraft family. Firstly, the approach to determine the weights of components and of the complete aircraft is presented in section 6.1. The method of taking the commonality between the one- and two-seat variants into account is explained in section 6.2. The methods which are used to determine the weights of components and of the complete aircraft are presented in section 6.3. After that, the inputs for these methods and the corresponding results are presented in section 6.4. Once the component weights and locations are known, the centre of gravity of the aircraft can be determined. The centre of gravity ranges of both aircraft are presented in section 6.5.

6.1. Approach to Weight Estimations

In this section, the Class II weight estimation methods for obtaining component weights, group weights and aircraft weights are presented. The Class I weight estimations are presented in section 3.3, providing the estimation of MTOW and fuel required to fulfil the mission requirements. Based on these first order estimates the wing is sized. When more aircraft parameters, mainly concerning size and shape, are known weight estimates at component level can be made.

It is important to note that a single iteration of this approach does not probably result in a realistic weight estimate. Therefore, the result of the Class II weight estimation should be fed back into the Class I estimation, in which it is checked for consistency. If the Class II estimation does not correspond to the Class I estimation, the Class I estimation W_{TO} has to be tweaked, until the OEW as output of the Class II method is consistent with the OEW that is used as input for the Class I method. Iterations of these steps are performed until both the one-seater and two-seater aircraft have a Class II OEW estimation that is within 1 % from the Class I OEW estimation. At this point the component weight estimation of the aircraft is said to have converged.

6.2. Approach to Commonality

Some of the component weights as mentioned in the first column of Table 6.1 need to be estimated twice, once for the one-seater and once for the two-seater. These components are: the fuel system, the flight controls, the electric system, and the avionics. The remaining components, being the wing, the tailplanes, the fuselage, the landing gear and the nacelle are identical for both variants. For these components, the weight estimations are done using parameters of the two-seat variants, such that the components would be sufficiently sized (actually oversized) for the

one-seater.

6.3. Weight Estimations Methods

This section presents methods used to estimate component weights. For most of the components the Cessna methods for general aviation aircraft as presented in [11] are used to determine respective component weights.

The engine weight is obtained from the manufacturer¹. The propeller weight is 4.5 kg (10 lbs) according to the manufacturer². The wing weight of the one-seater is estimated using the Cessna methods for general aviation aircraft as mention before. Since the wing of the two-seater aircraft consists of the wing of the one-seater and two extensions at the wing roots, it is more logical to estimate the weight of these wing extensions and add this to the weight of the one-seater wing. This is done by assuming a weight distribution as shown in Figure 6.1. The one-seater wing is estimated to weigh 43 kg (95 lbs). When this weight would be distributed uniformly along the span, this would result in a wing weight per unit span of 5.4 kg/m (4 lbs/ft) along the entire span. However, in reality the weight per unit span is larger at the root than at the tip. When the weight is distributed as zero from the tip increasing linearly to a certain maximum at the root as shown by the solid line in Figure 6.1, then the weight per unit span equals 10.8 kg/m at the root. This value is used to estimate the weight of the wing root extensions by multiplying with the span of these extensions. This results in an estimated weight of 12 kg per root extension each.

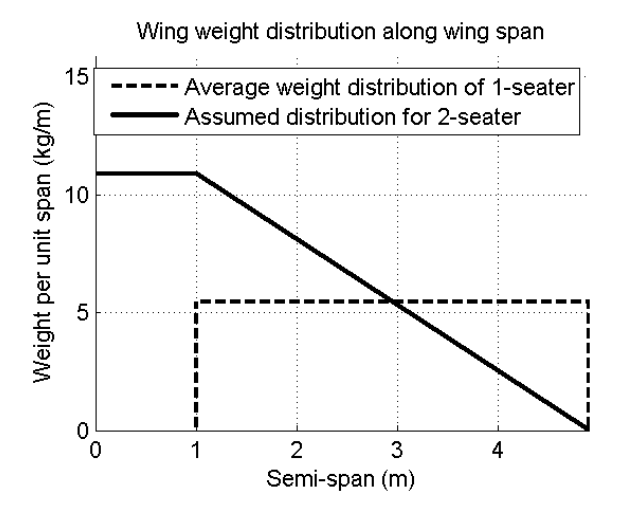


Figure 6.1: Weight distribution used for estimating weight of the root extensions.

6.4. Component Weight Estimations

Parameters Table 6.1 presents the input parameters for the Class II component weight estimations method.

¹www.flyrotax.com/produkte/detail/rotax-915-is-isc.html

²www.sensenich.com/products/item/44

Table 6.1: Parameters used in component weight estimation.

Parameter	Symbol	Value one-seater	Value two-seater
Take-off weight	W _{TO}	461 kg (1016 lbs)	592 kg (1305 lbs)
Ultimate load factor	N_{ult}	12	12
Wing area	S	10.2 m ² (110 ft ²)	13.6 m ² (146 ft ²)
Wing aspect ratio	A	6.0	7.1
Hor. tail area	S _h	$2.7 \text{ m}^2 (29 \text{ ft}^2)$	2.7 m ² (29 ft ²)
Hor. tail aspect ratio	A_h	3.5	3.5
Hor. tail root thickness	$t_{r,h}$	0.10 m (0.33 ft)	0.10 m (0.33 ft)
Ver. tail aspect ratio	A_{v}	1.5	1.5
Ver. tail area	S_v	$1.6 \mathrm{m}^2 (17 \mathrm{ft}^2)$	$1.6 \mathrm{m}^2 (17 \mathrm{ft}^2)$
Ver. tail root thickness	$t_{r,v}$	0.16 m (0.52 ft)	0.16 m (0.52 ft)
Ver. tail sweep (25 % c)	cqs_v	15 deg	15 deg
Fuselage length	$L_{\mathbf{f}}$	5.87 m (19.3 ft)	5.87 m (19.3 ft)
Take-off power	P_{TO}	135 hp	135 hp

Results Table 6.2 presents the results obtained for the component weight estimation for both the one-seater and the two-seater family members.

Table 6.2: Component weight estimations, obtained from the Cessna method for light airplanes as presented in [11].

Component	One-seater weight [kg] ([lbs])	Two-seater weight [kg] ([lbs])
Engine	84 (185)	84 (185)
Propulsion system	10 (22)	10 (22)
Propeller	4.5 (9.9)	4.5 (9.9)
Fuselage	42 (93)	42 (93)
Wing	46 (101)	70 (154)
Horizontal tail	10 (22)	10 (22)
Vertical tail	8.0 (18)	8.0 (18)
Landing gear	31 (68)	31 (68)
Nacelle	6.0 (13)	6.0 (13)
Fuel system	4.0 (8.8)	4.0 (8.8)
Flight controls	7.8 (17)	9.9 (22)
Electrical system	10 (22)	10 (22)
Avionics	6.0 (13)	10 (22)
Aircraft parachute ³	13.2 (29)	13.2 (29)
Empty	278 (633)	316 (697)
Fuel	46 (101)	54 (119)
Pilot(s)	104 (229)	181.4 (400)
Parachute(s)	7.0 (15)	14 (31)
Baggage	14 (31)	14 (31)
MTOW	461 (1016)	592 (1305)

6.5. Centre of Gravity 41

6.5. Centre of Gravity

The longitudinal positioning of systems and components is shown in Figures 4.4a and 4.4b. Together with their weights, the centre of gravity (CG) of the empty aircraft is calculated. The contributions to the CG of additional masses (pilots, parachutes, baggage, and fuel) are added to this in several combinations in order to determine the CG positions for several loading scenarios. The most forward and most aft CG positions determine the required horizontal tail size (which is discussed in section 7.1). Tables 6.3 and 6.4 show the CG positions of both aircraft in multiple loading configurations.

Table 6.3: Estimated CG positions of the one-seater, for different loading situations.

Comment Fuel Pilot Parachute Bagga		Doggogo	one-seater	one-seater		
Comment	ruei	ruei Filot Faraciiute		Baggage	(from nose)	(% MAC from LEMAC)
Empty					2.0 m (78 in)	11 %
Ground most FWD CG	X				1.9 m (75 in)	-1 %
Most FWD CG	X	light			2.1 m (83 in)	13 %
Most AFT CG		heavy	X	X	2.4 m (94 in)	39 %
MTOW	X	normal	X	X	2.1 m (83 in)	20 %

Table 6.4: Estimated CG positions of the two-seater, for different loading situations.

Comment	Fuel	front pilot	front chute	rear pilot	rear chute	Baggage	two-seater (from nose)	two-seater (% MAC from LEMAC)
Empty							2.0 m (78 in)	14 %
Ground most FWD CG	X						1.9 m (75 in)	2 %
Most FWD CG	X			light			2.0 m (78 in)	9 %
Most AFT CG				heavy	X	X	2.4 m (94 in)	42 %
	X	heavy	X	light			2.0 m (78 in)	15 %
MTOW	X	normal	X	normal	X	X	2.1 m (83 in)	18 %

Stability and Control

In this chapter the stability and control characteristics of the SALSA are discussed. Firstly, the horizontal tail sizing method is explained in Section 7.1. The design of the control surfaces is discussed in Section 7.2. The eigenmotion characteristics of both SALSA variants are detailed in Section 7.3. Finally, the flight control system can be found in Section 7.4 and a discussion on control forces is included in Section 7.5.

7.1. Horizontal Tail Sizing

The horizontal tail is designed such that the aircraft can achieve longitudinal static stability. The location of the horizontal tail is set first, after which the required tail size can be determined. A driving factor in horizontal tail design is the aircraft's centre of gravity location. The most aft centre of gravity position corresponds to the most unstable situation and thus determines the required tailplane size for stability. The relationship between the horizontal tail, C.G. and wing is given by Equation (7.1) [19] and is used to create scissor plots as found in Figures 7.1a and 7.1b.

$$\frac{S_h}{S} = \frac{\bar{x_{cg}}}{\frac{C_{L_{\alpha,h}}}{C_{L_{\alpha}}} \cdot \left(1 - \frac{d\epsilon}{d\alpha}\right) \cdot \frac{l_h}{\bar{c}} \left(\frac{V_h}{V}\right)^2} - \frac{\bar{x_{ac}} - S.M.}{\frac{C_{L_{\alpha,h}}}{C_{L_{\alpha}}} \cdot \left(1 - \frac{d\epsilon}{d\alpha}\right) \cdot \frac{l_h}{\bar{c}} \left(\frac{V_h}{V}\right)^2}$$
(7.1)

The most forward centre of gravity requires the largest negative tailplane downforce for moment equilibrium. This situation is most severe during low speeds when the nose-down pitching moment produced by the wing is largest. This is represented by Equation (7.2) [20] and can be seen in Figures 7.1a and 7.1b.

$$\frac{S_h}{S} = \frac{x_{cg}}{\frac{C_{L_h}}{C_{L_{A-h}}} \cdot \frac{l_h}{\bar{c}} \cdot \left(\frac{V_h}{V}\right)^2} + \frac{\frac{C_{mac}}{C_{L_{A-h}}} - x_{ac}}{\frac{C_{L_h}}{\bar{c}} \cdot \left(\frac{V_h}{V}\right)^2}$$
(7.2)

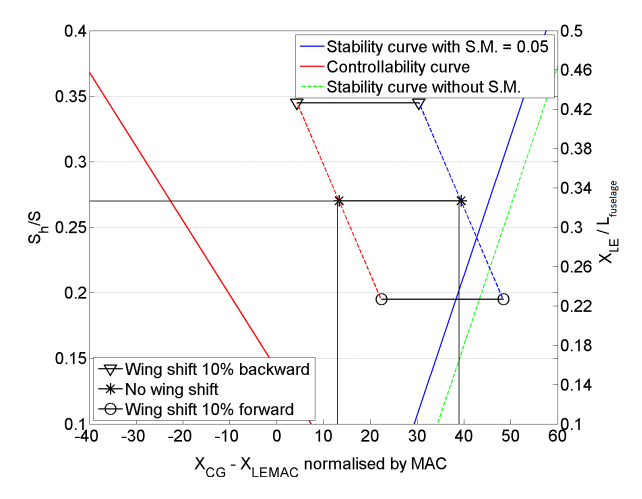
Equations (7.1) and (7.2) are used to obtain Figures 7.1a and 7.1b. The parameters used in this analysis are listed in Table 7.1. They have been determined using methods that can be found in [19], [20], [21], and [13]. The most forward and most aft CG positions have been determined with methods that are discussed in 6.5. Figure 7.1b shows that the one-seater has ample tailplane area for longitudinal stability and control. Its ratio of horizontal tail area to wing area is 0.27. This is due to the fact that its tailplane is actually sized for the two-seater. The ratio of horizontal tail area to wing area of the two-seater is 0.20. Figure 7.1b shows that the aircraft may become unstable (because the CG falls inside the stability margin) when a heavy pilot is seated in the rear of the two-seater. However, pilots can solve this situation by adding mass in front of the CG.

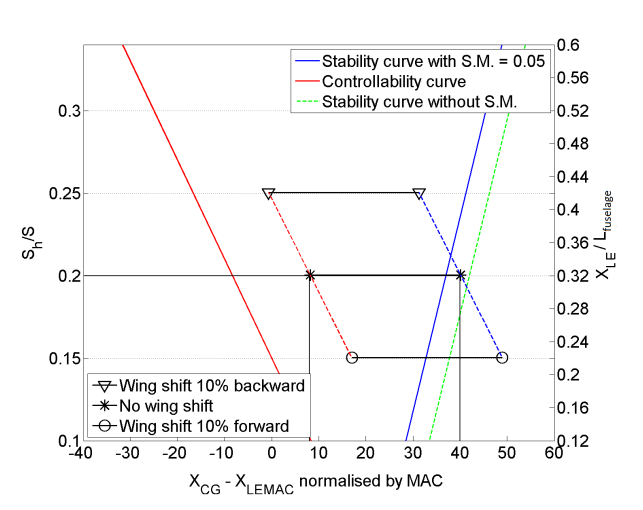
Table 7.1: Parameter values used in Equations (7.1) and (7.2) to produce Figures 7.1a and 7.1b.

* measured from propeller disk and normalized by MAC, as are all longitudinal positions in these equations.

** at location of the horizontal tail.

Parameter	Symbol	One-seater	Two-seater	Unit
Longitudinal pos. of aircraft CG*	$\bar{x}_{ m cg}$	1.5-1.7	1.4-1.7	[m]
Tail lift slope	$C_{L_{lpha,h}}$	3.7	3.7	[1/rad]
Wing lift slope	$C_{L_{lpha}}$	4.7	4.9	[1/rad]
Wing downwash gradient**	$\frac{d\epsilon}{d\alpha}$	0.48	0.48	[-]
Tail arm	$l_{ m h}$	3.4 (139)	3.4 (139)	[m] ([in])
Wing MAC	$ar{c}$	1.4 (55)	1.4 (55)	[m] ([in])
Tail airspeed ratio	$\frac{V_{ m h}}{V}$	0.95	0.95	[-]
Wing aerodynamic centre*	\bar{x}_{ac}	2.2	2.2	[-]
Static Margin	s.m.	0.05	0.05	[-]
Wing moment coefficient about AC	$C_{M_{ m ac}}$	0.0	0.0	[-]
Max. negative tail lift coeff.	$C_{L_{ m h}}$	-1.0	-1.0	[-]
Max. aircraft minus tail lift coeff.	$C_{L_{ ext{A-h}}}$	1.3	1.3	[-]





(a) Scissor plot of the one-seater aircraft. On the vertical axis can be read that the ratio of horizontal tail area to wing area is 0.27. (b) Scissor plot of the two-seater aircraft. On the vertical axis can be read that the ratio of horizontal tail area to wing area is 0.20.

Figure 7.1: Scissor plots of the SALSA aircraft

7.2. Control Surface Design

In this section, the designs of the control surfaces are presented. The one-seater and two-seater use identical control surfaces to reach maximum commonality.

7.2.1. Aileron design

As required, the one-seater should have a roll rate of at least 180 degrees per second at 120 knots CAS. However, a roll rate of 350 deg/s should be achieved in order to be competitive in the IAC Intermediate category. Furthermore, the maximum deflection of the ailerons is set to +/-20 degrees. Since the two-seater has a large moment of inertia compared to the one-seater, it will have a lower roll rate, even though the ailerons are placed more outboard. The method described in Raymer [8] is used to size the ailerons. The resulting aileron design allows the one-seater to achieve a roll rate of 360 deg/s, while the two-seater can roll at 250 deg/s. Table 7.2 shows the resulting parameters of the ailerons.

Parameter	Single-seat	Two-seat	Units
Chord ratio c_a/c	0.33	0.33	[-]
Surface area ratio S_a/S_w	0.38	0.29	[-]
Span ratio b_a/b	0.86	0.68	[-]
Inboard span location	0.55 (1.8)	1.55 (5.1)	[m] ([ft])

Outboard span location 3.9 (13) Maximum deflection angle δ_a 20

Table 7.2: Aileron design parameters for the one-seater and two-seater aircraft

7.2.2. Elevator design

Since the main landing gear is positioned in front of the center of gravity, the elevator design is based on the longitudinal trim requirement. The method described by Sadraey [22] is used to size the elevator. At sea level and at the service ceiling, the aircraft must be able to fly just above its stall speed. Figure 7.2a and 7.2b show the required elevator deflection of the one-seater and two-seater as a function of airspeed, CG location and altitude. It can be concluded that the one-seater and two-seater aircraft need a minimum deflection of -10 and -11 degrees respectively. During aerobatic flight an elevator deflection angle of 25 degrees will be used for both negative and positive elevator deflection. Table 7.3 summarizes the elevator dimensions. It is also possible to change the incidence angle of the horizontal tail in order to decrease the elevator deflection range. This would lower the profile drag but also changes the cleanness of the attitude negatively during inverted flight compares to the upright flying attitude. Since the pilot is judged by how well and strict the manoeuvres are made, having an incidence angle is not beneficial.

7.2.3. Rudder design

The rudder is designed in such a way that the aircraft is able to recover from a spin. This is the most driving requirement in rudder design. Since the two-seater is the most critical of the two aircraft, due to the larger wingspan and larger moment of inertia, the rudder design is done for the two-seat variant. The method to determine the rudder

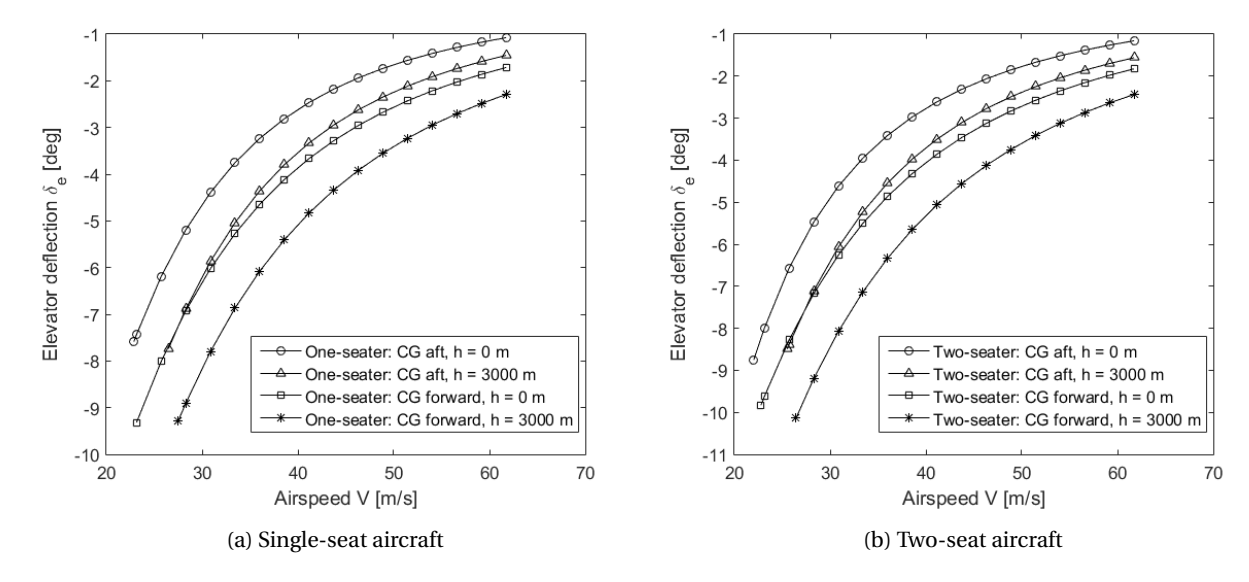


Figure 7.2: Elevator deflection range

Table 7.3: Aileron design parameters for the single-seat and two-seat aircraft

Parameter	Single-seat	Two-seat	Units
Chord ratio c_e/c_h	0.4	0.4	[-]
Surface area ratio S_e/S_h	0.46	0.46	[-]
Span ratio b_e/b_h	1	1	[-]
Maximum deflection angles δ_e	±25	±25	[deg]

size is described in Raymer [8]. Table 7.4 shows the design parameters of the rudder.

Table 7.4: Rudder design parameters for the single-seat and two-seat aircraft

Parameter	Single-seat	Two-seat	Units
Chord ratio c_r/c_v	0.5	0.5	[-]
Surface area ratio S_r/S_v	0.54	0.54	[-]
Span ratio b_r/b_v	1	1	[-]
Maximum deflection angles δ_r	±25	±25	[deg]

7.3. Eigenmotions

In this section the stability and control derivatives of both aircraft are given and the resulting eigenmotions are discussed. The longitudinal stability is described in Section 7.3.2 and the lateral-directional stability is discussed in Section 7.3.3. Moreover, the handling qualities of both aircraft are assessed.

7.3.1. Stability and Control Derivatives

In Table 7.5 the stability and control derivatives of both aircraft are given. They are computed using the method of Roskam[21] and verified against reference aircraft with similar configurations. The flight condition considered here is for sea level atmospheric conditions, an airspeed of 51.4 $\frac{m}{s}$ (100 kts) and an aircraft weight equal to the MTOW. These derivatives are substituted in the symmetric and asymmetric linearized equations of motion[23] in order to assess the longitudinal and lateral-directional stability.

Derivative Two-seater **Derivative** One-seater Two-seater One-seater 0 -0.59 -0.44 C_{x_0} 0 $C_{Y_{\beta}}$ C_{X_u} -0.034-0.030 C_{Y_p} -0.028 -0.018 0.18 0.16 0.41 0.24 $C_{X_{\alpha}}$ C_{Y_r} $C_{Y_{\delta_a}}$ 0 $C_{X\dot{\alpha}}$ 0 0 0 $C_{Y_{\delta_r}}$ C_{X_q} 0 0 0.18 0.14 $C_{X_{\delta_e}}$ 0.12 0.11 -0.0075 -0.012 $C_{l_{\beta}}$ -0.28-0.27-0.45-0.47 C_{Z_0} C_{l_p} -0.55-0.530.068 0.062 C_{Z_u} C_{l_r} $C_{l_{\delta_a}}$ $C_{Z_{\alpha}}$ -5.2 -5.3 0.52 0.46 $C_{l_{\delta_r}}$ $C_{Z_{\dot{\alpha}}}$ -3.4 -2.4 0.0053 0.0035 -9.0 C_{Z_a} -11 $C_{n_{\beta}}$ 0.140.082 $C_{Z_{\delta_e}}$ -0.68 -0.51 -0.038 -0.033 C_{n_p} C_{n_r} -0.088 0.025 0.018 -0.18 C_{m_u} $C_{n_{\delta_a}}$ $C_{m_{\alpha}}$ -1.9-1.6 -0.018-0.018 $C_{m_{\dot{\alpha}}}$ -12 -8.4 -0.082-0.050 $C_{n_{\delta_r}}$ C_{m_q} -28 -21 $C_{m_{\delta_e}}$ -2.5-1.9

Table 7.5: Stability and Control Derivatives

7.3.2. Longitudinal Stability: Short Period and Phugoid

The aircraft's response to the symmetric equations of motion generally consists of two modes. Firstly, the short period describes the aircraft's initial response to an elevator deflection input. This mode is generally highly damped and has a period of only a few seconds. The second mode is the phugoid motion which is lightly damped and has a longer period in the order of 15 to 60 seconds. This mode follows directly after the short period has ceased to act. To get a first indication of the aircraft's response behavior the eigenvalues of the system of symmetric equations can be plotted in a root plot, see Figures 7.3a and 7.3b.

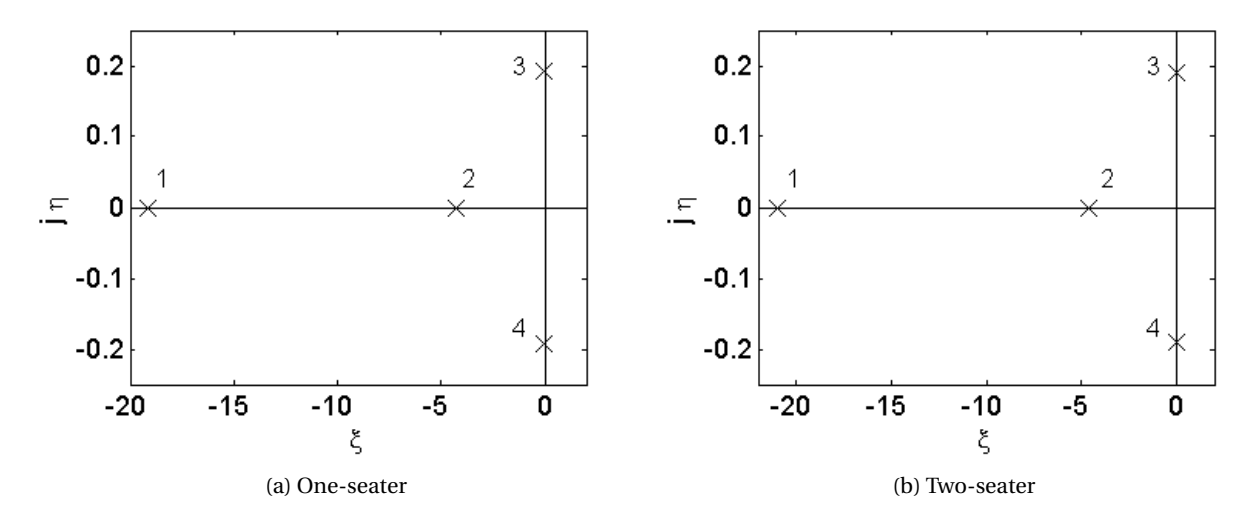


Figure 7.3: Root plots symmetrical equations of motion

All eigenvalues contain a negative real part, implying a motion that decays over time. Moreover, two of these eigenvalues do not contain an imaginary part and are therefore aperiodic. These eigenvalues (indicated 1 and 2) determine the short period mode. Their damping ratio (ζ) of 1.0 meets the level 1 handling quality requirement[22] for the short period mode (0.35< ζ <1.3). The remaining eigenvalues form a complex conjugate pair that determine the phugoid mode. Their damping ratio is 0.069 for the one-seater and 0.062 for the two-seater. This corresponds to a level 1 quality in handling since they exceed the minimum required damping ratio of 0.04. Furthermore, the MAT-LAB command *lsim* is used to simulate the aircraft response to an elevator step input of -1 degree. The resulting short period response is given in Figure 7.4.

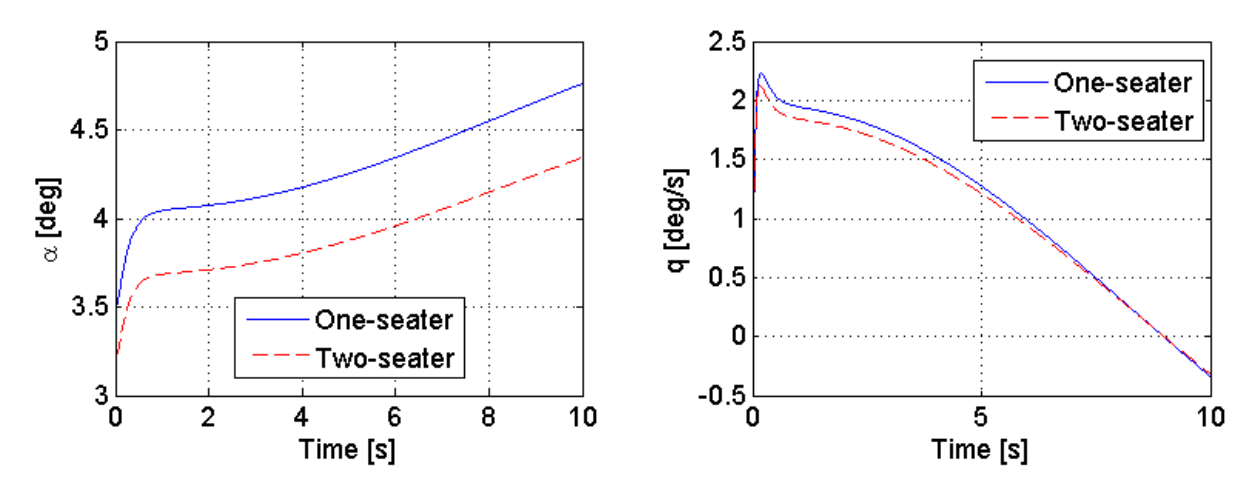


Figure 7.4: Short period response for δ_e = -1 degree

The phugoid is simulated using the same approach and is found in Figure 7.6. Note that there is an offset in the initial angle of attack and pitch angle between the aircraft since they fly at the same speed with differing wing planforms.

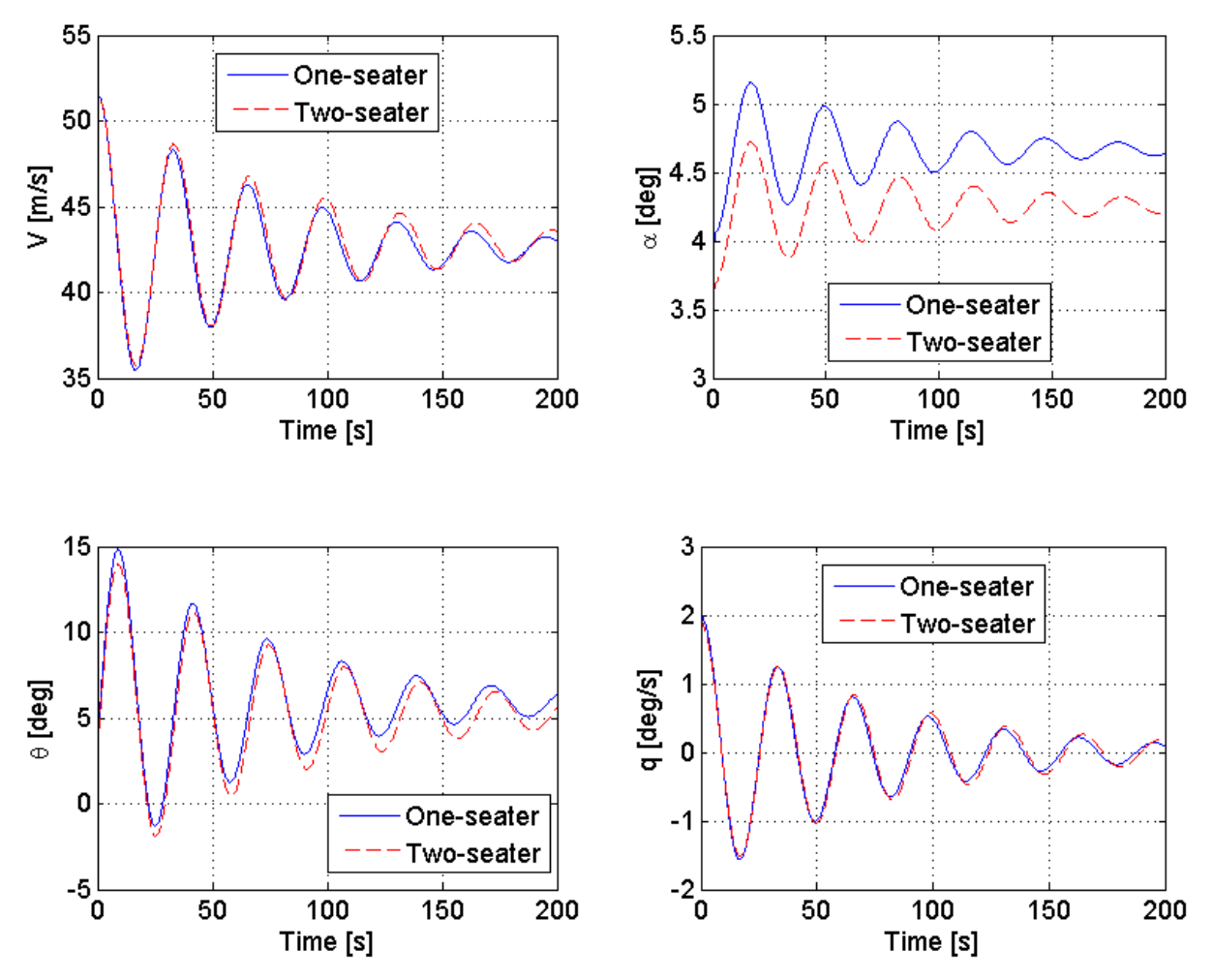


Figure 7.6: Phugoid response for $\delta_e = -1$ degree

A summary of the damping ratios, periods and time to double/half amplitude for these two eigenmotions is given in Table 7.6.

Table 7.6: Longitudinal eigenmotion characteristics

Eigenmotion	Damping Ratio [-]	Period [s]	Time to half/double [s]
Short period one-seater	1.0	N/A	N/A
Phugoid one-seater	0.069	32	52
Short period two-seater	1.0	N/A	N/A
Phugoid two-seater	0.062	33	58

7.3.3. Lateral-directional Stability: Dutch Roll, Aperiodic Roll and Spiral

The right hand side of Table 7.5 contains the lateral stability and control derivatives that have to be substituted in the asymmetric equations of motion. An aircraft's response to these equations generally consists of three eigenmotions: roll damping, the dutch-roll and spiral. Plotting the eigenvalues of the equations of motion once again gives an initial idea of the stability of these eigenmotions.

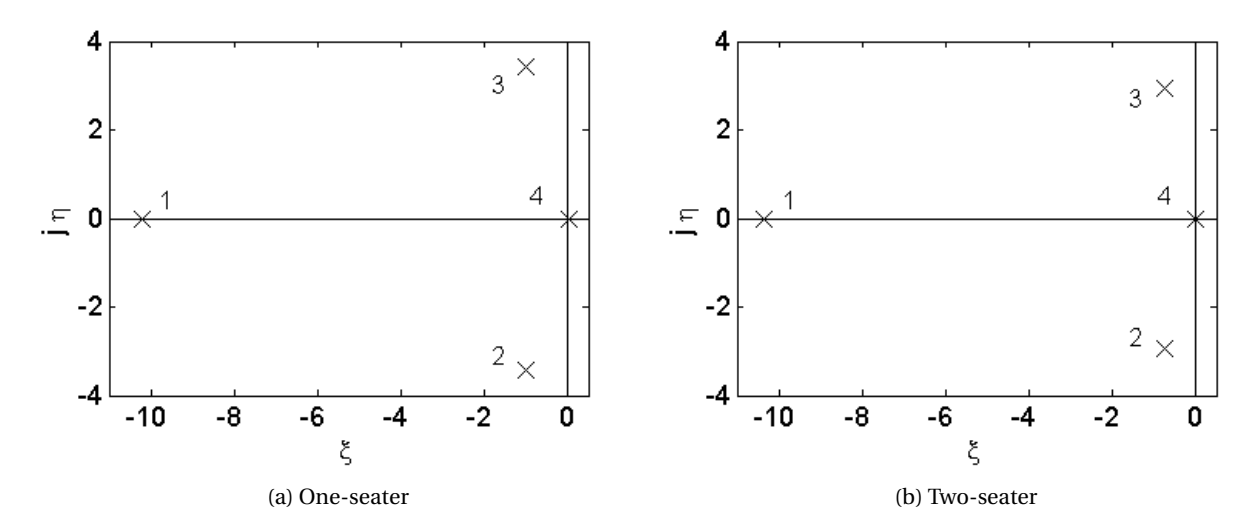


Figure 7.7: Root plots asymmetrical equations of motion

It is found that three of these eigenvalues have negative real parts and are therefore stable eigenmotions. The complex conjugate pair (2,3) corresponds to the dutch-roll eigenmotion. The negative eigenvalue (1) indicates the aperiodic roll damping mode. Eigenvalue 4 is slightly positive and corresponds to the unstable spiral eigenmotion. Once a roll angle is initiated the aircraft will continue to increase its roll angle if no control inputs are applied to counter this motion. This is illustrated in the roll angle over time plot in Figure 7.8. Since the roll rate in this eigenmotion is very low, its response is not included here.

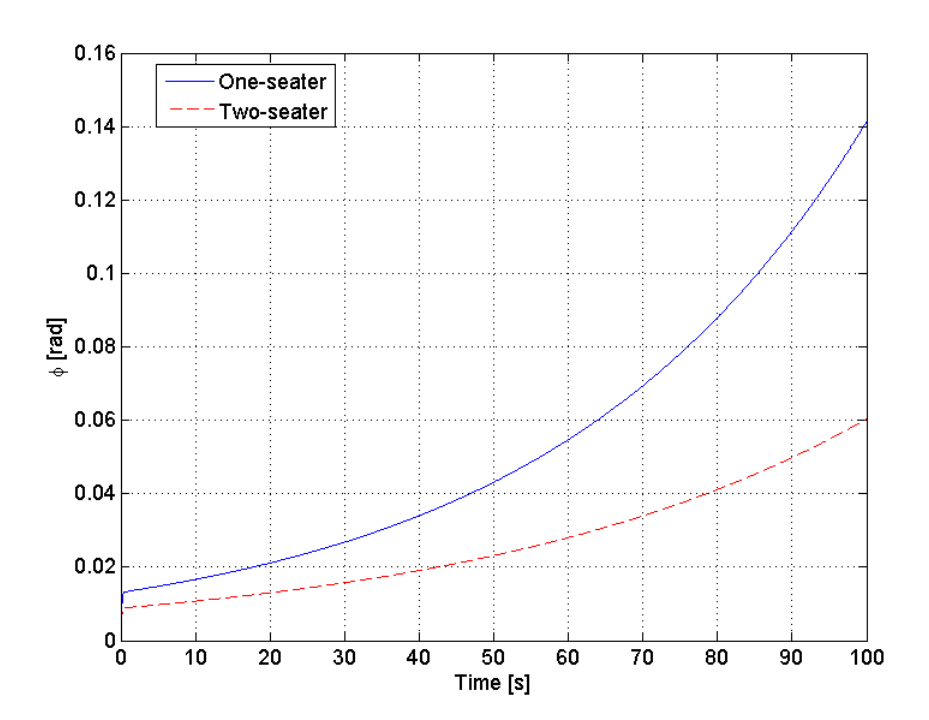


Figure 7.8: Spiral eigenmotion for a pulse shaped -1 degree aileron deflection

To reach a level 1 handling quality the time to double should be at least 20 seconds. It is computed that the time to

7.4. Control System 50

double for the one-seater is 29 seconds and 36 seconds for the two-seater, as can also be concluded from this spiral eigenmotion plot. If the aircraft is being rolling at a high roll rate the aperiodic roll damping mode comes into play. This mode will tend to damp the roll rate of the aircraft until it is constant, mainly caused by the wings that generate an opposing rolling moment. Finally, the dutch-roll eigenmotion response of both aircraft mainly occurs in the yaw and rate of yaw response, as can be seen in Figure 7.9. The roll and rate of roll response is very small compared to the yaw response and is therefore not included in this discussion.

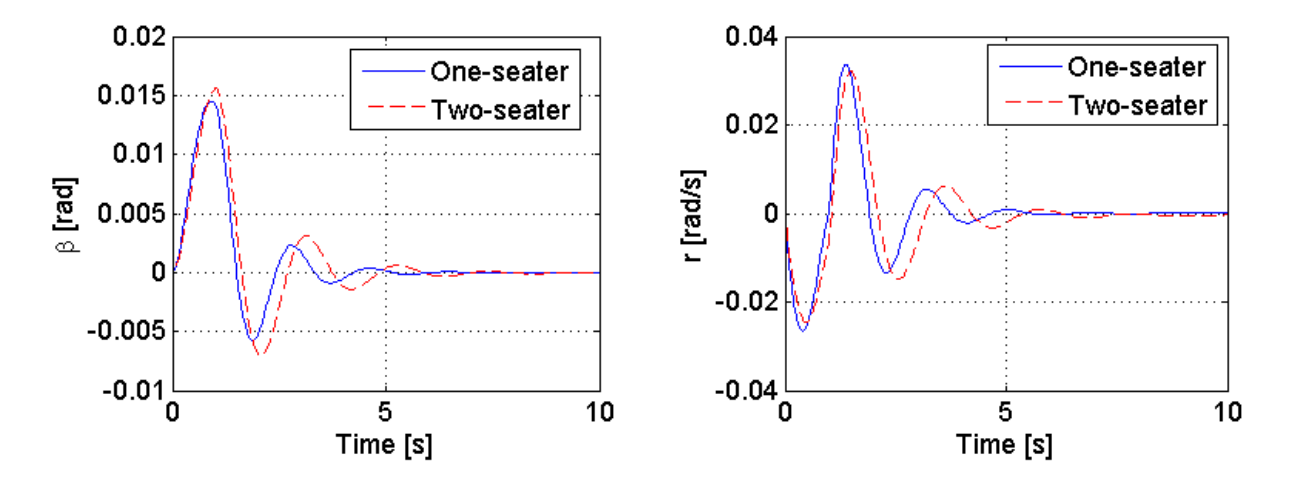


Figure 7.9: Dutch roll response for a rudder deflection of 1 degree

The damping ratio of both aircraft is above the minimum required damping ratio of 0.08. Therefore, it can be concluded that all level 1 handling qualities are achieved. A summary of the characteristics of the lateral-directional eigenmotions can be found in Table 7.7.

Eigenmotion	Damping Ratio [-]	Period [s]	Time to half/double [s]
Spiral one-seater	N/A	N/A	29
Dutch roll one-seater	0.28	1.8	0.69
Aperiodic roll one-seater	N/A	N/A	0.068
Spiral two-seater	N/A	N/A	36
Dutch roll two-seater	0.25	2.1	0.92
Aperiodic roll two-seater	N/A	N/A	0.067

Table 7.7: Lateral-directional eigenmotions characteristics

7.4. Control System

The rudder, ailerons, elevator, brakes and engine have to be controlled from the cockpit. The control systems of the SALSA family consist of a center control stick, rudder pedals including brake control, a throttle lever and an engine control panel. The two seat family member features full dual control for instruction purposes. This includes full dual engine control panel, with manual override function on the rear pilot seat, in which the instructor is seated. This ensures that in case the student makes an error in engine operation procedures, the instructor can take over control

7.4. Control System 51

when desired and make appropriate corrections.

The control inputs of the control stick are transferred to the control surfaces through a series of pushrods and hinges. The pushrod's ball and swivel joint can be connected and disconnected easily during assembly and disassembly of the aircraft. Figure 7.10 shows a detailed drawing of such a joint. The option to implement these joints makes a pushrod control system preferable over a wire connected control system for the aileron and elevator control.

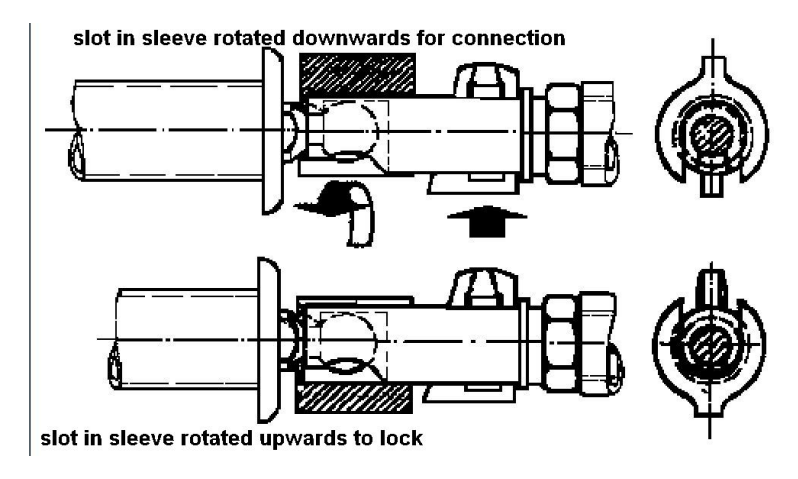


Figure 7.10: Ball and socket quick coupling joint ¹

The rudder pedals are adjustable. Inputs of the rudder pedals are translated to rudder movement through steel cables. The brake pedals can be operated by the pilot with his feet. The brakes are actuated hydraulically and can be operated separately from each other, resulting in differential braking of the two main landing gear wheels. Differential braking combined with a tail wheel that is free to swivel, enables tight and precise ground maneuvers.

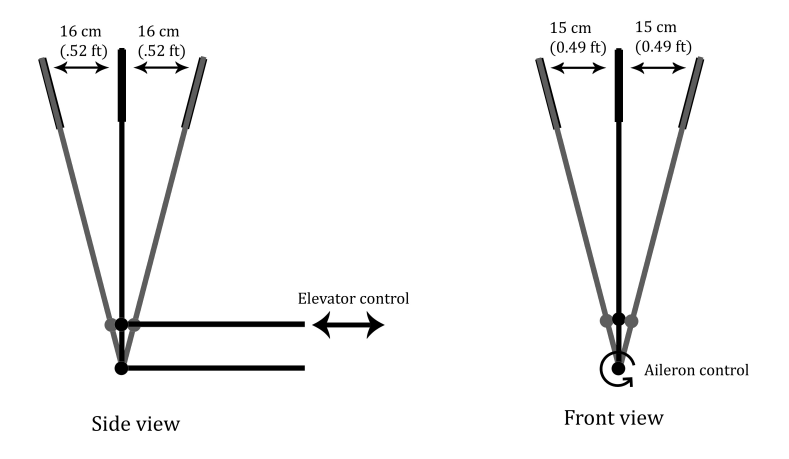


Figure 7.11: Schematic of the control stick, with maximum stick deflections

¹http://aviation.derosaweb.net/wedekind

7.5. Control Forces 52

7.5. Control Forces

The longitudinal control forces in "stick force per G" were estimated with use of the hinge moment derivatives as computed with Roskam's method[21] and relation (7.4). For an aerobatic aircraft it is important that controls are not too heavy, so that the maximum load factor can be achieved without excessively tiring the pilot.² Both aircraft require a minimum control force to obtain maximum load factor of 70 N (16 lbs), for a CG location most aft. [2]

The sizing situation for minimum required stick force per G is that of a wings level pull up, since this results in the least force required for a certain load factor. The aircraft is assumed to be trimmed in steady 1 G flight. From this requirement and from equation (7.4), the required gearing ratio of the longitudinal control system was determined. The results are summarized in Table 7.8. In these estimations, the hinge line of the elevator was moved slightly aft, to decrease the absolute value of $C_{h_{\delta e}}$. In more detailed design the choice could be made to balance the elevator with horn balances.

$$SM_{free} = \bar{x}_{ac_A} - \bar{x}_{cg} + ((C_{m_{\delta e}}C_{h_\alpha})/(C_{L_{\alpha_A}}C_{h_{\delta e}})) *$$

$$(7.3)$$

$$\partial F_s/\partial n = \eta_h q S_e \bar{c}_e G_e * (C_{L1}(C_{h_\delta e}/C_{m_{\delta e}})(SM_{free}) + (gl_h/U_1^2)(C_{h_{\alpha o}} - C_{h_{\delta e}}/\alpha_{\delta e}))$$

$$(7.4)$$

Table 7.8: Longitudinal control system of the ALSA family

	Single seat	Double seat	Unit
Gearing ratio	0.9 (0.27)	1.2 (0.36)	[ft/rad (m/rad)]
Stick force per g	4.3 (19.1)	5.3 (23.6)	[lbs/g (N/g)]
Maximum control force	30 (133) at 8g	27 (120) at 6g	[lbs (N)]

Estimations of lateral and directional control forces have not been included in this report. To reduce lateral control forces in aerobatic aircraft, horn balances or aileron spades are essential. Between these options, the aileron spades are chosen for the SALSA family, because aerobatic pilots often modify these in order to tune the required control forces of the ailerons to their liking. Moreover, aileron spade sizing is outside the scope of this report and should be completed during the detailed design phase.

 $^{^2}$ http://www.flightlab.net/Flightlab.net/Download_Course_Notes_files/6_%20LongitudinalManeu%232BA152.pdf

Structural Design

This chapter describes the structural design of the SALSA family. This includes an explanation of the common structures between the one-seater and two-seater variant, and the design philosophy behind them.

8.1. Materials

For the material selection, different type of aluminium alloys and composites which are widely used in aerospace industry have been considered. Aluminium alloys (AL 7075-T6 or AL 7178-T6) commonly used in aerospace industry display high specific strength and relatively low material cost. However, during the process of material selection, significant importance is given to low structural weight. The main reasons favoring composites over aluminum alloys include high strength-to-weight ratios, resistance to corrosion (resulting in lower maintenance costs) and their strength can be tailored to an extent to meet specific requirements.

In composite laminates, the reinforcement fibers can be oriented in the direction of the load, resulting in anisotropic lay-up with high specific strength and modulus in the direction of the applied load. The other advantage of composites is that better aerodynamic shape of the aircraft can be produced. Composite materials can easily be shaped in double curved surfaces while, metal structures are very limited to the amount of double curvature that can be reached. The major drawbacks of composites are high material cost, more notch sensitivity, impact sensitivity and delamination issues. Among composites, the possible options include glass fiber reinforced plastic or Carbon Fiber Reinforced Polymer (CFRP). Glass fiber has a lower stiffness to weight ratio as compared to carbon fiber, and a high elastic modulus. Moreover, glass fiber is less brittle and its raw materials are much cheaper compared to carbon fiber composites. Considering the fact that glass fiber is relatively cheap compared to carbon fiber and that it requires only little maintenance, glass fiber composite is chosen as the primary airframe structure material. The material properties of S-2 glass fiber chosen as a reinforcement for major structural components and carbon fiber IM are presented in Table 8.1. The selected canopy material is Plexiglas.

Table 8.1: Mechanical properties of S-2 Glass & Carbom IM fiber reinforcement [24].

Material	Relative Density [kg/m^{3}]	Tensile Strength [GPa]	Young's Modulus [GPa]
S-2 Glass	2490	4.0	86
Carbon IM	1740	5.6	295

8.2. Structural Design of the Wing

The load carrying structure in the wing consists of a carbon fibre composite main spar at 25% chord to carry all of the bending loads, and a second spar at 62% to introduce aerodynamic loads of the aileron into the structure and carry shear and torsional loads. See Figure 8.1 for a layout of the wingstructure. The spar material was selected to be with CFRP spar caps and a foam-core CFRP web. In Chapter 12.2 a Figure (12.3) of a wing cut-through is visible. The high specific strength and modulus of the CFRP is desired as spars carry the majority of the loads in the wings.

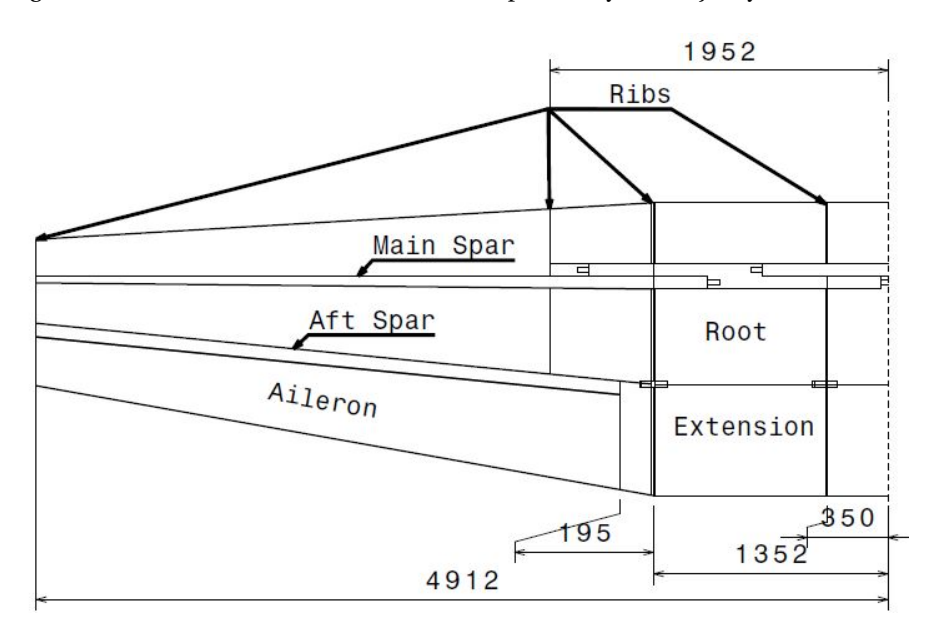


Figure 8.1: Wing structure layout

A comparison has been made between spars made out of a glass fiber layup and a carbon fiber layup. The glass fibers have a tensile failure stress of 520 MPa for a unidirectional layup while the carbon fibers have a failure stress of 1000 MPa. For the failure stresses an additional composite safety factor of 1.5 was applied. The higher failure stress and lower density of the CFRP allows for a main spar that weight about 50% less than a spar made out of fiberglass, saving around 25 kg (54 lbs) of weight. Which is needed to be able comply with the component weight budget of the wing in Chapter 6. However to account for a reduction in strength due to fatigue a fatigue analysis should be made. The S/N curves corresponding to the expected load circles yield a new tensile failure stress. This fatigue analysis is however beyond the scope of this report, for the moment an additional safety factor of 1.5 can be applied.

In combination with the load carrying spar, the sandwich skin allows for a no stringer design, reducing the number of parts in the wing assembly, which in turn makes high part commonality feasible. The wing needs to be optimized such that the skin can carry a part of the bending loads as well. This can decrease the total wing weight.

8.2.1. Wing attachment construction

To improve user convenience, the wings are constructed to be easily detachable. The detachable wings result in less hangar space required for the aircraft and enable the owner to transport the aircraft on a trailer if desired. A drawback is that additional structure is required to accommodate the load transfer. A two spar structure carries the load across the joint, of which the front spar is designed to carry all the bending loads, and the aft spar helps with the shear loads due to lift, and wing torsion. The complete concept is depicted in Figure 8.2 for clarification.

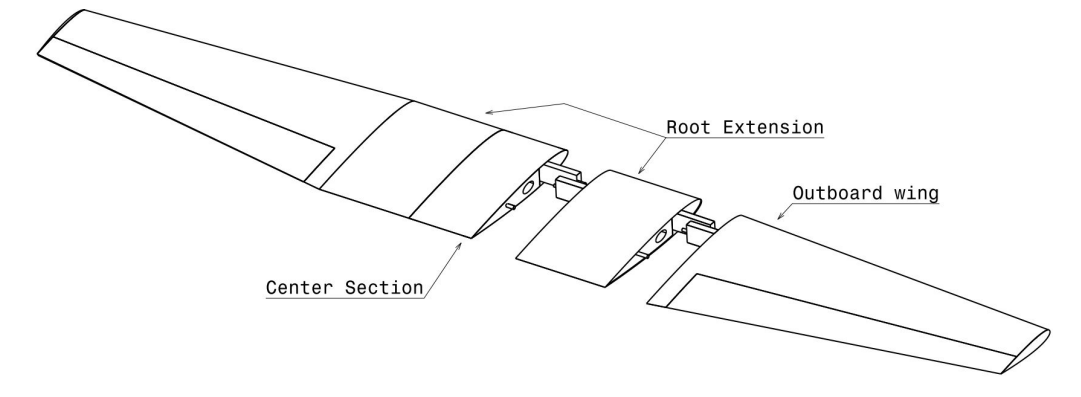


Figure 8.2: Assembly of SALSA wings, depicting root extension elements for the two-seat aircraft

The end of each spar is tapered, to allow the corresponding spar end of the following wing section to easily slide alongside each other into the other wing section. A metal insert is laminated into the end of each spar section, to transfer the loads of the spar cap to the shear pin at the end of the spar stubs. Which transfers the load to a bushing insert on the adjoined wing section. The loads on the pins and bushings are transferred via the insert to the spar caps. This insert reduces the amount of carbon fiber required in the construction and reduces production costs, since a large number of plies would be required if this insert would be made out of composite material. Hence reducing the required labour. With the two inserts joined together, loads can be transferred from spar to spar through the pins and bushings. The connection mechanism is depicted in Figure 8.3. To keep the wing sections together, the wing main bolt is placed through a bushing in the joined spar sections. Due to the construction of the joint, the bolt does not directly carry any loads, though it prevents the joint from coming apart. This bolt is not included in the figures.

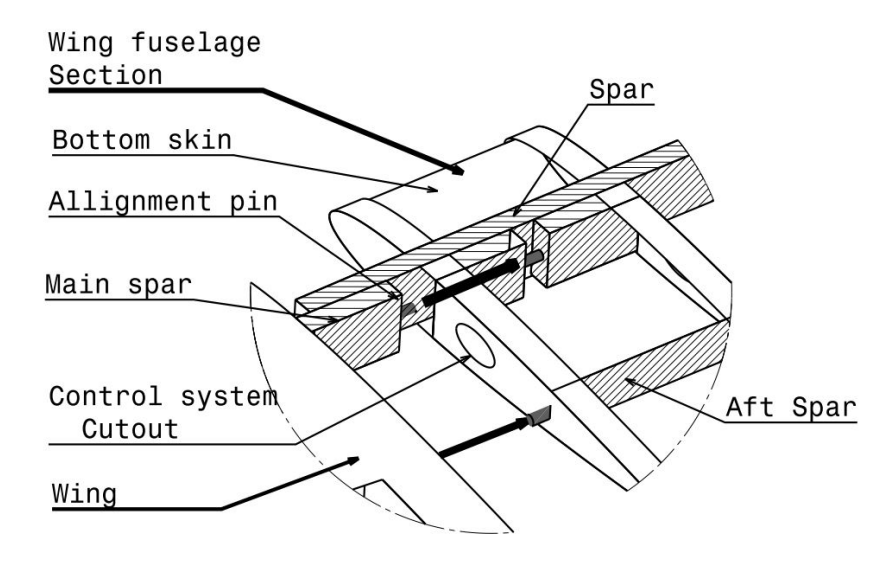


Figure 8.3: Load transfer connection between wing main spar sections

The wing sections and root extensions are constructed such that they can be installed on either side of the aircraft. The wings are fully symmetrical. This is possible since the airfoil and construction is fully symmetrical. The only non symmetrical part would be the aileron control link. But since the deflections up and down remain equal the wing can be installed both on the left and right side of the aircraft. This feature greatly improves commonality within the aircraft and reduces production costs.

8.2.2. Wing Load Diagrams

The bending and torsional loads on the wing are calculated by integrating the lift force along the wing at the worst-case loading scenario. This scenario is flight at the maximum structural load factors (+6/-5 g) for the two-seater, while taking a safety factor of 1.5 into account. The root connection is common for both variants, and because the bending moment at the root of the one-seater is considerably lower, a fractional increase of the load factors is allowed for this variant. This results that the limit loads for the one-seater can be increased to +8 g and -6 g without significantly increasing the weight of the aircraft. Effectively enlarging the flight envelope. The total loads on the section are therefore roughly equal.

The load distributions on the wings are shown in graphs 8.4, 8.5, and 8.6.

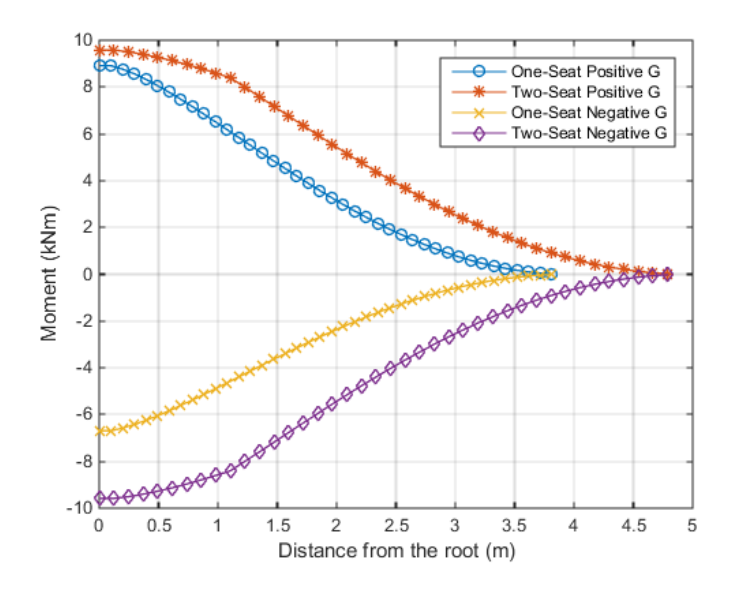


Figure 8.6: Torsional moment as a function of span

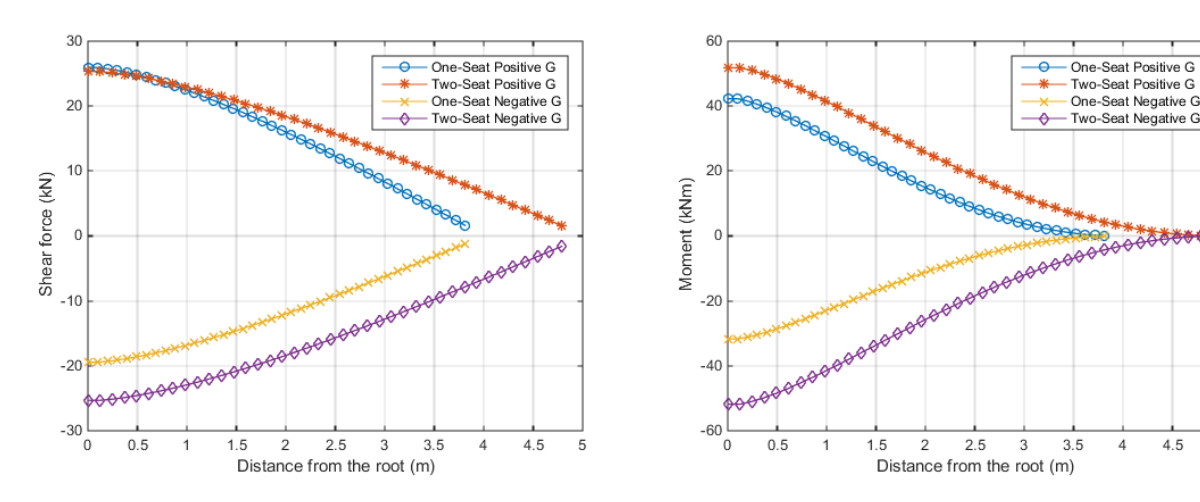


Figure 8.4: Shear force as a function of span

Figure 8.5: Bending moment as a function of span

8.2.3. Flutter

One thing to consider in wing design is its flutter behavior. A quantitative flutter analysis is beyond the scope of this design phase, however some precautions can still be taken. Control surface flutter is dealt with by balancing the hinge moment on the control surfaces as detailed in Chapter 7. Structural flutter is taken into account by recognizing that flutter occurs when flying at high speeds and relatively low stiffness wings. The never exceed speed of both aircraft is 168 kts, and the composite wing structure will be as stiff as or stiffer than a conventional metal wing. Final flutter compliance with the regulations will be proven with test flights of the completed aircraft.

8.3. Structural Design of the Fuselage

The fuselage is designed as a glass fibre composite semi-monocoque structure with a foam filler to achieve the required torsional rigidity. The main bending loads in the fuselage due to tension and compression are carried by the skin and upper and lower longerons. The longerons and skins resist bending loads in both the lateral and vertical directions. The fuselage skins carry the shear and torsional loads, stiffened by glass fiber bulkhead and formers. A semi-monocoque type of structure is preferred over a steel tube frame covered with fabric covering for the SALSA. Although the fabric covered steel frame structure can be made as light as a semi-monocoque structure and is much cheaper to produce, the aerodynamic shape of the aircraft would suffer. Moreover, a steel tube frame covered with glass fibre composite body panels is heavier than a steel tube frame with cloth, the panels do not relieve any structural loading. The canopy is made out of a single piece of Plexiglas. It is produced with a male die, over which the heated Plexiglas is vacuum formed. The method is quite straightforward, though requires experience to guarantee perfect vision without lens effects. ¹ The canopy opens and hinges to the right side of the cockpit.

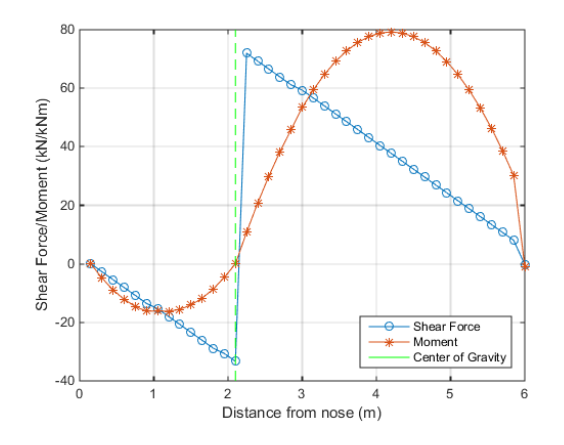
8.3.1. Fuselage load cases

The significant loads acting on the fuselage are identified and their magnitudes are calculated. This leaves the detailed structural design to be done after the conclusion of this report (see chapter 12.13). The sizing load cases considered for the fuselage are:

- Lift from the horizontal tail inducing bending, 15kNm (11,000lbf-ft), and shear, 4kN (900lbf).
- Lift from the vertical tail inducing bending, 5kNm (3,700lbf-ft), and shear,1.3kN (290lbf).
- Lift from the wings inducing bending, 19kNm (14,000lbf-ft), and shear, 54kN (12,000lbs) for each wing.
- Take-off acceleration from the propeller inducing tension.
- Aileron deflections inducing torque.
- Landing gear inducing static and shock loads.

Figures 8.7 and 8.8 show the forces from the flight surfaces on the fuselage in a side and top view. The shear forces come from the lift of the empennage and wing, and the internal moments come as a result of those shear forces.

 $^{^{}m l}$ http://www.professionalplastics.com/MakrolonUC_Polycarbonate



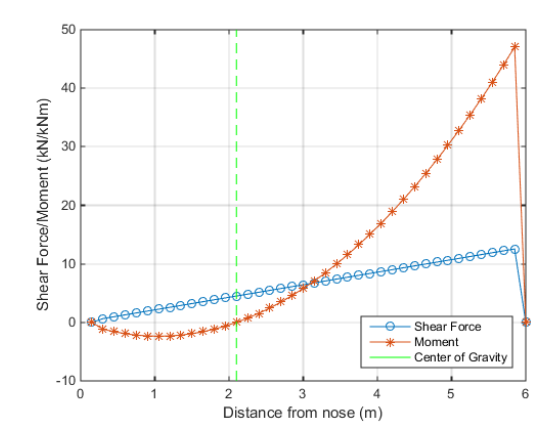


Figure 8.7: Side view of stresses on the fuselage

Figure 8.8: Top view of stresses on the fuselage

8.4. Structural Design of the Empennage

The bending moments and shear of the empennage surfaces are carried by a two spars. The rear spar also introduces the loads of the control surfaces. The horizontal tailplane is detachable for the owner's convenience. This enables storage and transport on a trailer if desired. Average maximum trailer width across the United States is 102 inches, so without a detachable horizontal tail, this would not be possible.

Figure 8.9 depicts the connection mechanism of the horizontal tail to the vertical tail. Loads are transferred through the two pins connecting the rear spars of the surfaces and the four bolts connecting the main spars of the horizontal tail to the vertical tail. Finally, a panel is added to the leading edge to complete the tail surfaces, and the elevator is connected to its control system.

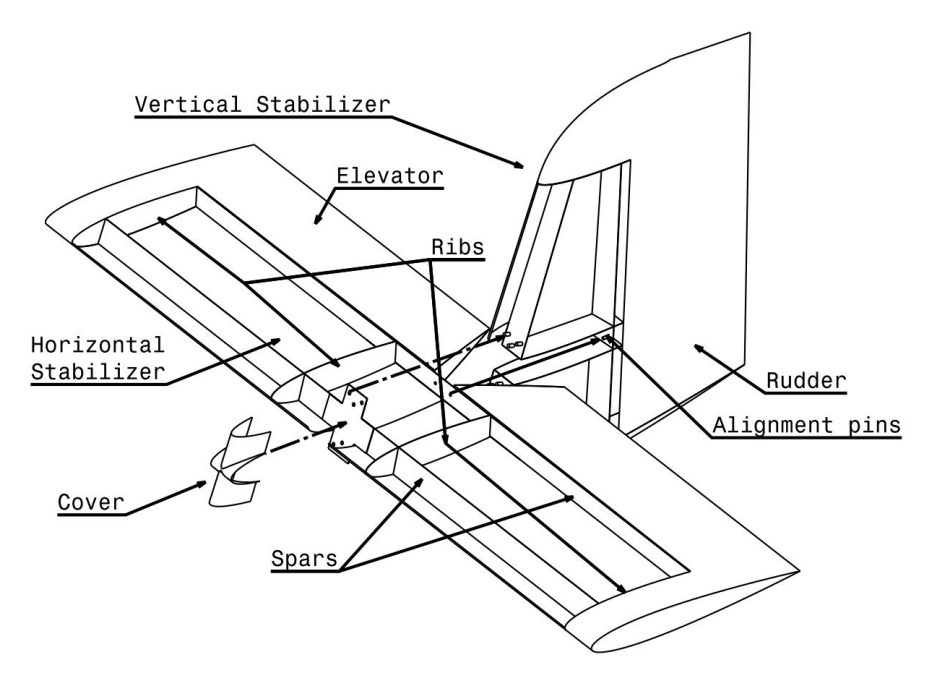


Figure 8.9: The connection mechanism of the horizontal tail to the vertical tail

8.4.1. Empennage Load Cases

The sizing load case on the empennage is at the $C_{L_{max}}$ of the vertical and horizontal tails at the maximum speed V_{NE} in the flight envelope.

8.4.2. Empennage Loading Diagrams

The bending and torsional loads on the empennage are calculated in the same way as for the wing. The load distributions are shown in graphs 8.10 to 8.15. It should be noted that the empennage is identical for the one and two-seater, and so their curves coincide.

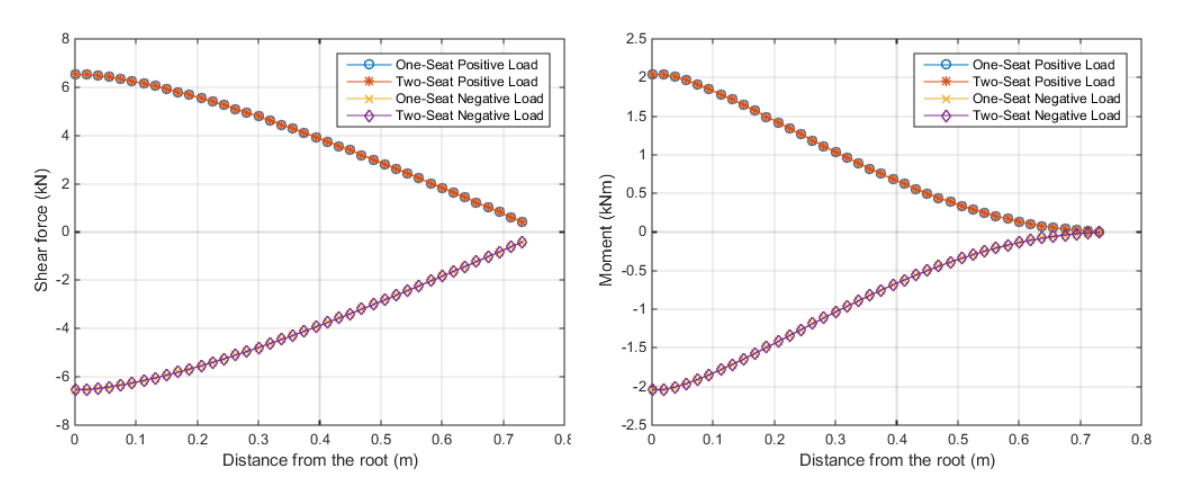


Figure 8.10: Shear force as a function of span. The curves of both Figure 8.11: Bending moment as a function of span. The curves aircraft coincide.

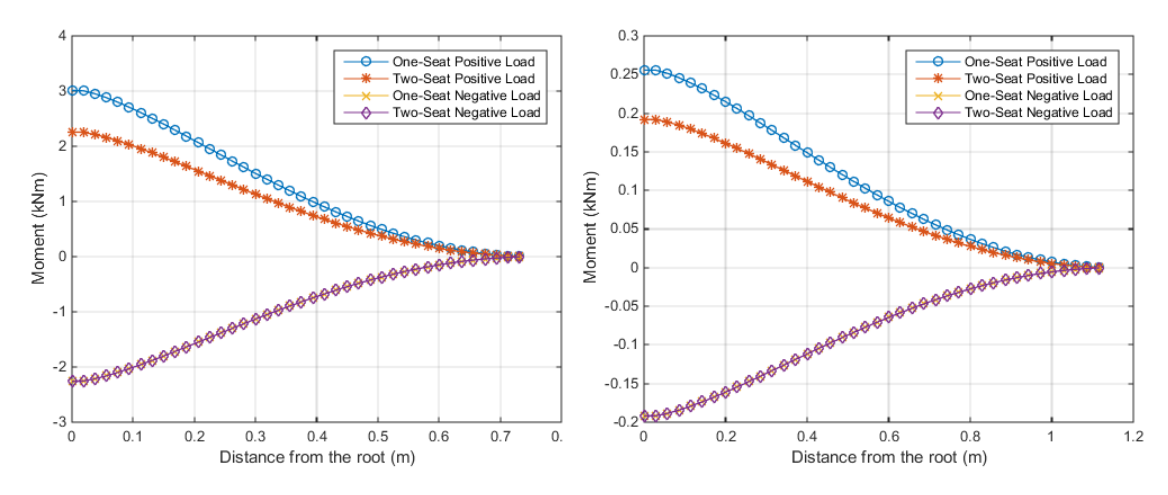


Figure 8.12: Torsional moment as a function of span. The curves Figure 8.13: Torsional moment as a function of span. The curves of both aircraft coincide.

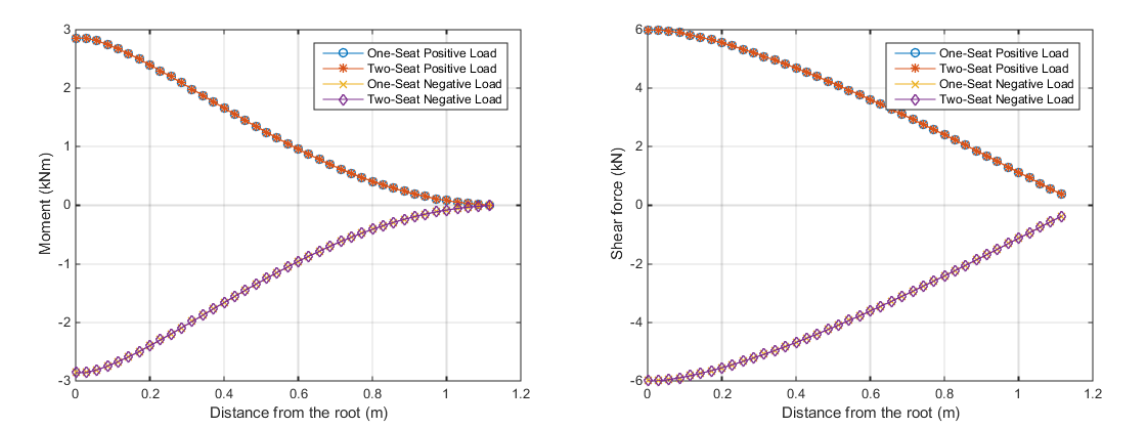


Figure 8.14: Bending moment as a function of span. The curves Figure 8.15: Shear force as a function of span. The curves of both of both aircraft coincide.

8.5. Loads on the Landing Gear

For the main landing gear a curved bending beam without pistons or dampers is selected. The benefit of the bending beam landing gear strut is that when the tire hits the ground the entire beam starts to bend, taking up the kinetic energy of the impact. This reduces part count, interfaces and weight.

Analysis of the loads on the landing gear for LSA's can be performed with the ASTM F2245-15 standard [2], 5.8.1.1 to 5.8.1.3.

The load factor on the wheels, n_j is computed to be 3.3. The reference weight used is the MTOW of the two-seater. The load on the main gear therefore is 19 kN (4270 lbs) in level landing conditions and 15 kN (3320 lbs) in tail-down conditions.

Subsystem Design

This chapter contains the design of subsystems for the SALSA family members. The major subsystems required for the operation of the aircraft are included.

9.1. Fuel and Oil Systems

This section calculates the fuel tank volume and describes the mechanisms used to guarantee the supply of fuel and oil to the engine.

Fuel type and fuel tank volume In Section 3.3 it is found that the fuel weight necessary to comply with the ferry range requirements is 46 kg (100 lbs) for the one-seater, respectively 54 kg (199 lbs) for the two-seater. Consequently, a tank volume of 64 L (17 gal) and 75 L (19.8 gal) is required for the one- and two-seater. This required volume is calculated for AKI 91/RON 95 fuel [25] with a conservative, low density of 720 kg/m³ (6.0 lbs/gal). Both aircraft will use the same fuel tank to increase part commonality. This will increase the maximum range of the one-seater. To account for expansion space the volume is increased by 2%, as required by the FAA. [26] This results in a tank volume of 76.5 L (20.2 gal). The location of the fuel tank is shown in Figure 4.3a and 4.3b.

Mechanism for inverted flight For inverted flight two mechanisms are generally used for inverted flight: A floptube mechanism and a Christen Inverted Oil System. The Christen Inverted Oil System is only installed with wet-sump engines and the Rotax 915 iSc has a dry-sump oil system. Therefore not an option. Therefore, a flop tube mechanism is used to ensure that the aircraft have the capability to fly inverted for a minimum of five minutes. Consequently, the required tank volume can be provided for by one fuel tank, to minimize weight and cost of the fuel system. [16] Additionally, in this configuration the fuel system does not pose a time limit on the inverted flight. For these reasons this method is chosen instead of a header tank or an inner tank with flapper valves. [16] Similar to the fuel system, the dry-sump oil system of the Rotax 915 iSc will be equipped with a flop tube, making it capable of aerobatic maneuvers and inverted flight [25].

Fuel distribution The fuel pump and fuel lines must be able to supply 39.3 L/h (10.4 gal/h) to the engine. [16, 25] The sizing of those will be done at a later stage. Furthermore, an auxiliary fuel pump, a fuel venting system to prevent

 $^{^{1}} http://www.gulf.nl/fileadmin/user_upload/sheets_EN/fuel/PDSEN\%202301\%20Gulf\%20Euro\%2095.pdf [cited 15 January 2016] \\$

9.2. Avionics 63

excessive pressures building up in the tank, drains to eliminate dirt or condensed water, fuel quantity and pressure gauges and a refueling valve are included in the fuel system. A jettison system is not required as both aircraft are able to land at their respective MTOW within requirements, as shown in Section 10.2.

9.2. Avionics

The trend in avionics is moving more and more towards a "Technically Enhanced Cockpit" or glass-cockpit, instead of the standard mechanical gauges. Generally, glass cockpit screens are more detailed and accurate, whilst mechanical gauges improve the pilot's skills [27]. As LSA certified aircraft are not required to have any certified avionics. This significantly lowers the cost.

Since many pilots have their own preference on avionics it is decided to keep the instrument panel customizable. The buyer can choose from a selection of options provided by the manufacturer. For the glass cockpit the SkyView system from Dynon Avionics ² is selected as the main system, since it is the most common non-certified system on the market. The mechanical instrument-panel mainly consist of gauges from manufacturers UMA ³, Falcon ⁴ and Skysports ⁵. Of course, any other instruments are optional when desired.

One additional option that could potentially be bought is the Aero Glass ⁶. This is a wearing virtual reality glass which can display numerous option on the screen. This way a pilot would be able to see real-time his current flight plan, potential obstacles or possible aerobatic maneuvers. However, it is still unknown how much this system will cost, or when it will become available on the market.

The catalog for avionics provided for this aircraft is given in Table 9.1. It should be taken into account that the exact prices and amount of instruments could be changed during more detailed design phase of the project. Furthermore, the analogue system is likely to be more expensive, since it is not a completely integrated system.

These figures give an initial cost estimate for the glass cockpit of between \$11500,-/\$ 15000,- and \$15250,-/\$ 22250,- . Similarly, the cost for the analogue system are around \$8750,-/\$11100. Furthermore, the weight of the complete SkyView system is estimated between 4.2/8.2 kg (9.3/18.1 lbs) and 5.5/9.5 kg (12.1/20.9 lbs). The mechanical system is estimated to weight around 5.7/10.0 kg (12.6/22.0 lbs)

 $^{^2} http://www.dynonavionics.com/downloads/Literature/Dynon-SkyView-WorkSheet-HiRes.pdf$

³http://www.aircraftspruce.com/menus/in/uma.html

⁴http://www.aircraftspruce.com/menus/in/falcon.html

⁵http://www.aircraftspruce.com/menus/in/skysports.html

⁶https://glass.aero/

9.2. Avionics 64

Table 9.1: Catalogue for custom instrument panel for ALSA project

Mechanical cockpit Glass cockpit					
System	Price \$	System	Price \$		
	Disp	lay			
		SkyView 7" display SkyView 10" display	2700,- 3600,-		
	ADAI	HRS			
Skysports altimeter Skysports airspeed indicator Skysports attitude indicator Skysports vertical speed indicator	150,- 175,- 470,- 215,-	Skyview ADAHRS module	1200,-		
	EM	IS			
UMA manifold pressure gauge UMA oil pressure gauge UMA oil temperature gauge UMA Rotax tachometer Falcon fuel gauge	150,- 150,- 150,- 140,- 55,-	Skyview EMS module	1240,-		
	Commur	nication			
iFlyGPS 520 ⁷ Mode-S transponder SkyGuardTWX ADS-B Transceiver ⁸ Radio Intercom system Yaesu FTA-550 AA VHF Transceiver ⁹	399,- 2500,- 1499,- 2100,- 200,- 190,-	Skyview GPS antenna + software Skyview Mode-S transponder Skyview ADS-B reciever Skyview VHF COM Radio, 8.33 kHz Skyview 2-Place Stereo Intercom	700,- 2200,- 995,- 2195,- 295,-		
	Sens	ors			
Pitot tube Static port Pressure sensor Temperature sensor	200,- 20,- 50,- 100,-	Skyview Pitot probe	200,-		
	Cables				
Cables	200,-	Skyview Network cables	250,-		
	Tot	al			
Estimate one-seater price Estimate two-seater price	9000,- 11000,-	Estimate one-seater price Estimate two-seater price	12000,- 15000,-		

9.3. Cabin Lay-out 65

9.3. Cabin Lay-out

This section briefly discusses the cabin layout. Figure 9.1 shows the preliminary cabin lay-out.



Figure 9.1: Graphical render of the initial cabin lay-out with glass cockpit avionics and communication system

Pilot size The cabin is required to accommodate a 95 percentile of pilots. The cabin was designed in CATIA using a digital manikin with the size of a 99 percentile of pilot sizes of European pilots. Since American people are statistically smaller than European people, this guarantees that the requirement concerning pilot size is met.

Instrument panel An instrument panel is located approximately 60 cm in front of the pilot. This panel features either analog instruments or digital screens. The choice of instruments is discussed in Section 9.2.

Seating Note that the seats are inclined backwards by about 25 deg. This reduces the required height and is beneficial for comfort during maneuvering with large load factors.

Control system The flight controls of the aircraft consist of a control stick to control elevator and ailerons, rudder pedals to control rudder and brakes, and a throttle lever to control engine power. As specified before, the pilots are seated in tandem configuration in the two-seat variant. In the two-seat variant the flight control system is built in twice, once for each pilot. The control system of the front and rear pilots are connected to each other. The control system is discussed in more detail in Section 7.4.

9.4. Electric System

The electrical block diagram of the aircraft is shown in Figure 9.2. A lithium-ion battery is used to power the engine starter generator, which in turn starts the engines. On the ground, the battery can also be used to supply power to the electrical system. A power distribution unit distributes available power over all the subsystems at their specific voltages. If required, it can also recharge the battery. In case of insufficient available energy, power will only be supplied to the most essential systems.

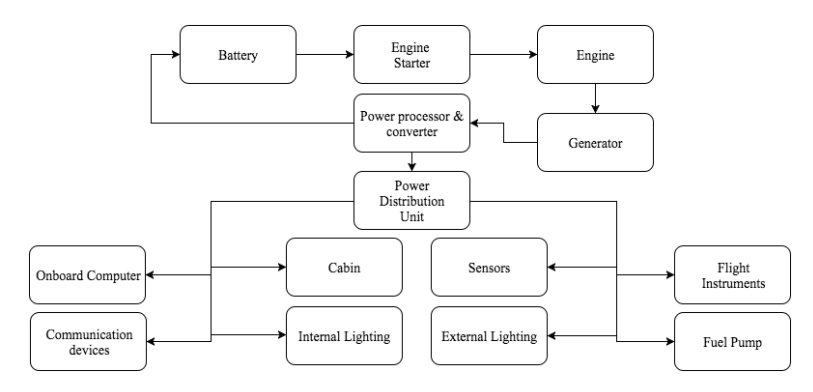


Figure 9.2: Electric Block Diagram

9.5. Communication and Data Handling

The design requirements include that the aircraft shall be able to operate in both controlled and uncontrolled airspace. Airspace consists of several classes ranging from class A to class G, of which classes F and G are uncontrolled airspace. Looking at the mission of the aircraft it is unlikely that the aircraft will be classified in class A. To fly in the other airspace classes only a two-way radio and a transponder with altitude reporting capability are required [28]. The communication flow diagram illustrating the flow of data through the aircraft system, and to and from its environment can be seen in Figure 9.3. The communication flow diagram for both variants is similar, except that in the two-seat variant, a second pilot is present. The data handling and hardware block diagram is also incorporated along with the communication flow diagram.

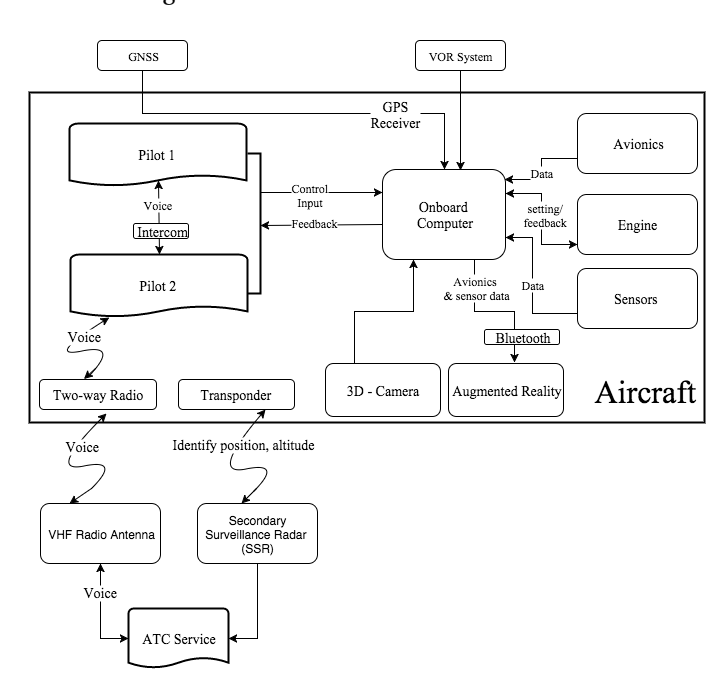


Figure 9.3: Communication flow diagram and Data handling

Performance Analysis

This chapter covers the performance analysis of the current design including aerodynamic characteristics, maneuverability parameters and the flight envelope.

10.1. Aerodynamic Analysis

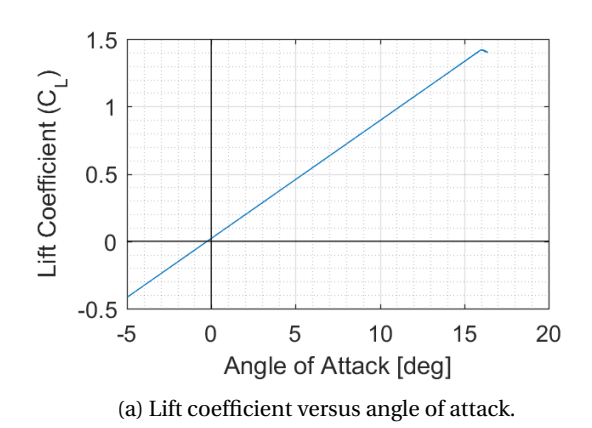
This section covers the aerodynamic analysis of the SALSA family.

10.1.1. Lift analysis

Lift characteristics of the aircraft are shown in Figure 10.1. The aircraft lift curve slope is computed to be $4.8 \ rad^{-1}$. The following assumptions and estimations are made in order to obtain the lift curve:

- The airfoil windtunnel data is obtained from Abbot [17]. Including $\alpha_{\text{CL}_{\text{max}}} = 16^{\circ}$ and the angle of attack of stall.
- · No gap between the aileron and the wing is assumed.
- Calculations are performed for sea-level flight.
- Horizontal tail dynamic pressure ratio is 1.0.

Figure 10.1a shows the trimmed aircraft lift coefficient (C_L) versus angle of attack at MTOW. The curve passes almost through (0,0) due to the wing's symmetric airfoil and the positive contribution of the fuselage to the lift coefficient. The wing features sharp stall characteristics which are favorable for aerobatics, according to [6].



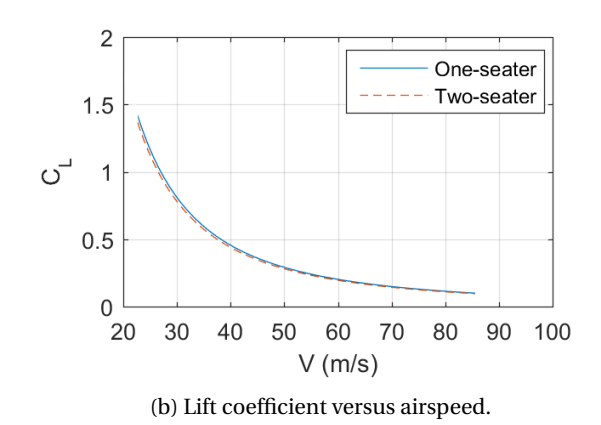


Figure 10.1: Aircraft lift characteristics.

10.1.2. Drag analysis

A drag estimation is performed using methods given in Hoerner [29] and Roskam [21]. For each aircraft component, its drag coefficient is presented. All drag components are summed in order to obtain the zero-lift drag of the complete aircraft. Next to this, interference drag between wing and fuselage and between tail surfaces and fuselage is estimated. All required geometric values are obtained from a 3D CAD-model that is used during the design process. Other important parameters and assumptions are shown below.

Fuselage drag Input parameters include 25 m^2 of fuselage wetted area, 0.7 m^2 of frontal area, $0.51 \cdot 10^{-6}$ equivalent sand roughness [21], flow transition at 20% of fuselage length (Figure 4.78 in Roskam VI [21]) and 8% extra drag due to installations (inlets, outlets, antennas, lights and the sighting devices on the wing tips) [21]. The drag component of the canopy is 0.009 with 0.14 m^2 frontal area and a forebody shape factor of 0.95.

Wing drag The zero-lift drag is obtained from wind-tunnel measurements of the wing section [17]. Its value is 0.006 at zero angle of attack. The induced drag is determined by using the wing drag model as presented in Roskam VI [21]. The efficiency factor $e_{\rm W}$ is computed to be 0.83.

Interference drag Interference drag occurs at the junction of the wings and fuselage and at the junction of tailplanes and fuselage. According to Figure 28 of section 8-12 of Hoerner [29], the interference drag of a conventional tail configuration amounts to approximately 4% of the tailplane drag. The wing-fuselage interference drag is determined to be 7% using Figure 4.1 in Roskam VI [21] and is based on Reynolds number, fuselage length, and Mach number.

Landing gear drag The drag coefficient of the main tires is determined to be 0.25 from Figure 33 of section 13-14 of Hoerner [29]. This is the drag coefficient of a tire with fairing. The drag coefficient of the landing gear is determined to be 0.25 from Figure 35 of section 13-14 of Hoerner [29]. In this case, the landing gear consists of one single beam (with streamlined cross-section) per wheel. The drag coefficient of the tail gear (without streamlined fairing) is determined to be 0.58 from Figure 39 of section 13-14 of Hoerner [29]. The reference areas are 0.10 m² and 0.02 m² for the main gear (including struts) and tail gear respectively.

Horizontal and vertical tailplane drag Transition point of the flow is deducted to be at 20% chord for both surfaces. [30] An increase of drag is caused by the gap between the wing surface and the elevator when in trimmed condition.

Trim drag With a 2 degree elevator deflection and the average elevator chord to horizontal tail chord ratio (aft of hinge line) at 32%, the trim drag was calculated to be 0.008.

Component	One-seater $C_{\rm D0}$	Two-seater $C_{\rm D0}$
Wing	0.0084	0.0077
Fuselage	0.0077	0.0057
Gear	0.0036	0.0026
Horizontal tail	0.0022	0.0016
Vertical tail	0.0012	0.0009
Trim	0.0008	0.0006
Total C_{D0}	0.024	0.019

Table 10.1: Zero-lift drag coefficients of the aircraft components.

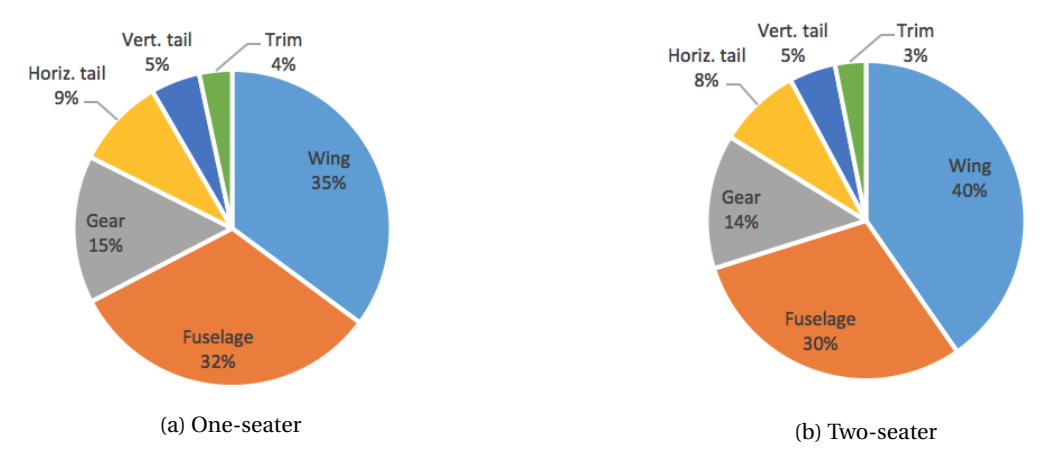


Figure 10.2: Composition of zero-lift drag components.

Summation of Drag Components Table 10.1 presents the drag coefficients of all aircraft components for which the drag is calculated. Both the wing and the horizontal tail drag include their respective interference drags with the fuselage. The coefficients are normalized with respect to wing surface $S_{\rm w}$ (10.2 m² / 13.6 m²) using Equation 10.1. The reference area $S_{\rm i}$ is the frontal area corresponding to the method of determining $C_{\rm D_i}$.

$$C_{D_0} = \sum_{i} \left(C_{D_0}(i) \frac{S_i}{S_w} \right) \tag{10.1}$$

Figure 10.2 shows the contribution of aircraft components to the total zero-lift drag in percentages.

Aircraft Drag As can be seen from Figure 10.3b, the largest difference in aerodynamic characteristics between the one and two-seater is drag. The family flies with the least amount of drag at L/D values around 14 at airspeeds of 32 m/s (62 kts) and 36 m/s (70 kts), as can be seen in Figure 10.4a. This corresponds to C_L values between 0.6 and 0.7. L/D values at cruise speed (62 m/s (120 kts)) are 9 and 7 respectively. Figure 10.4b shows the pitching moment for the linear part of the lift curve (up to 15 degree angle of attack) around the c.g. of the aircraft at MTOW. Near stall, maximum negative pitching moment are reached (one-seater -0.5 and two-seater -0.45).

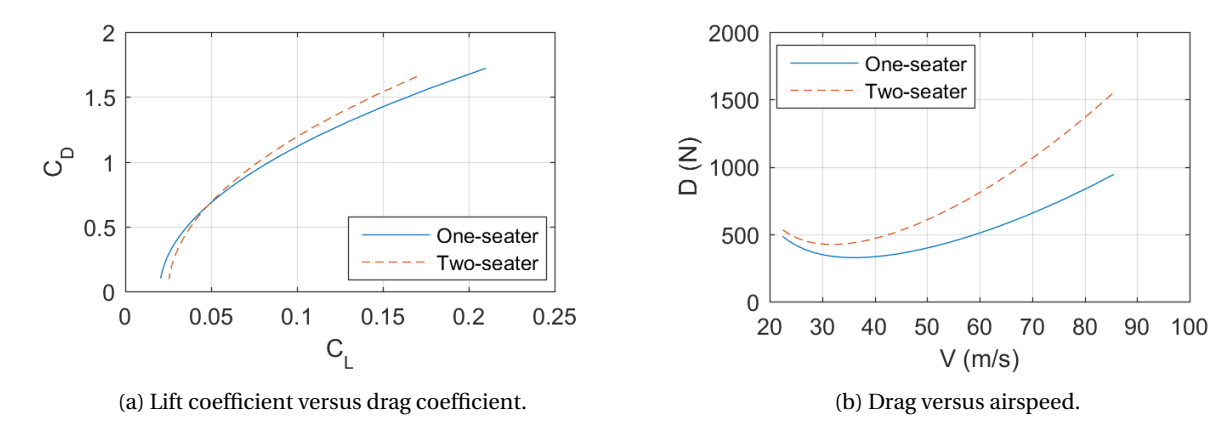


Figure 10.3: Aircraft drag characteristics compared to lift and airspeed.

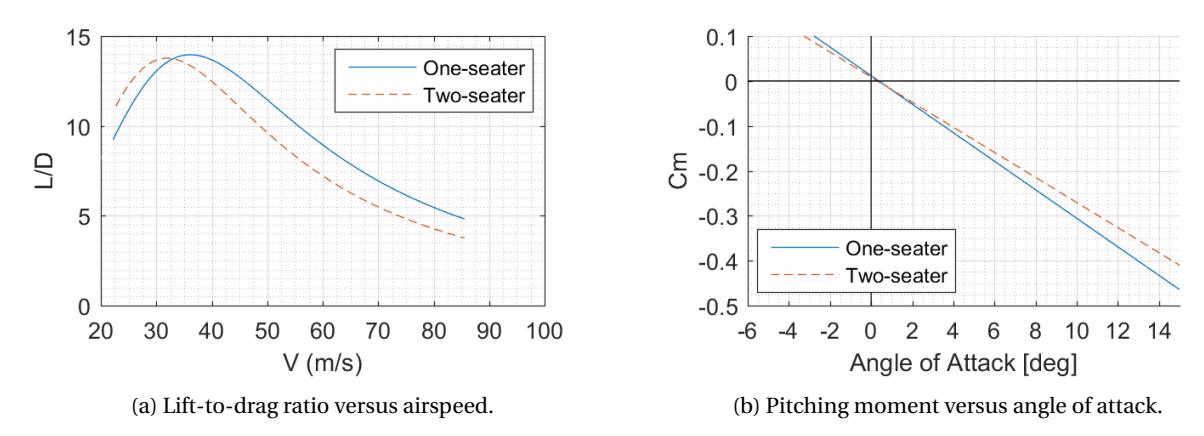


Figure 10.4: Aircraft lift-to-drag ratio and pitching moment characteristics.

10.2. Flight Performance

This section analyzes the cruise, the take-off, the landing and the climb performance of the SALSA family aircraft. Furthermore this section describes the payload range and the V-n diagram for the aircraft.

10.2.1. Cruise Performance

At each flight level, both aircraft have an optimum cruise speed. This is the optimum velocity for achieving maximum range per unit of fuel; it depends on the drag polar of the aircraft (Subsection 10.1.2). Table 10.2 shows the optimum cruise speed for each altitude.

Table 10.2: Optimum cruise speed for each altitude

Altitude [m] ([ft])	One-seat aircraft V _C [m/s] ([ft/s])	Two-seat aircraft $V_{\rm C}$ [m/s] ([ft/s])
0 (0)	48 (157)	44 (144)
500 (1640)	49 (161)	45 (148)
1000 (3281)	50 (164)	46 (151)
1500 (4921)	51 (167)	47 (154)
2000 (6562)	52 (171)	48 (157)
2500 (8202)	54 (177)	49 (161)
3000 (9843)	56 (184)	50 (164)
3500 (11483)	57 (187)	51 (167)

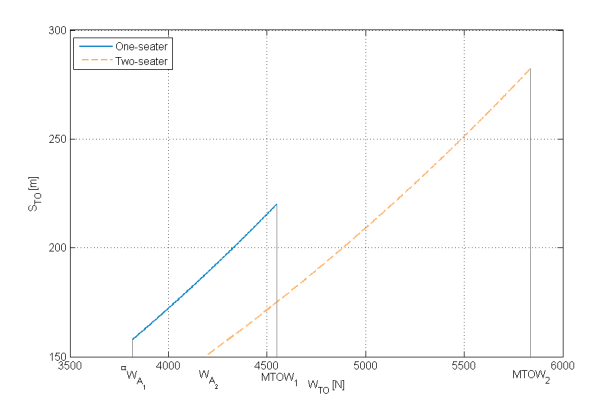
10.2.2. Take-off and Landing Performance

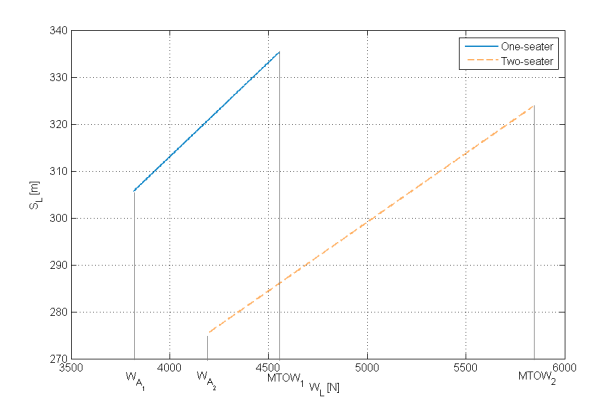
The take-off and landing performance of the two-member family is analyzed using Roskam [31] to verify whether the associated requirements as listed in Section 2.4 are met. Table 10.3 states the required and the corresponding calculated performance. It is shown that when taking off and landing in most critical conditions, at MTOW, the requirements are satisfied.

Table 10.3: Take-off and landing performance requirements and capabilities of the SALSA family. [5]

	Asphalt, sea	level, ISA+10°C	Asphalt, 500	00 ft, ISA+10°C	Grass, sea le	evel, ISA+0°C
		Take-off f	ìeld length [m] ([ft])		
Requirement Performance	370 (1200) 220 (720)	460 (1500) 280 (930)	N/A 260 (850)	N/A 330 (1090)	N/A 240 (790)	N/A 325 (1070)
Landing field length [m] ([ft])						
Requirement Performance	370 (1200) 335 (1100)	460 (1500) 325 (1060)	N/A 365 (1200)	N/A 350 (1150)	N/A 395 (1300)	N/A 380 (1250)

Figure 10.5a shows the take-off field length for the take-off weight ranging from the aircraft loaded for an aerobatic flight (W_A), to MTOW. This weight range is chosen to analyze the performance in aerobatic sequences, when the aircraft will not fly at MTOW. The aerobatic weight is defined as the operating empty weight, a 104 kg (230 lbs) pilot, a 7 kg (15 lbs) parachute and no fuel included yet. This yields a weight of 389 kg (858 lbs) for the one-seater, respectively 427 kg (942 lbs) for the two-seater. Similarly, Figure 10.5b displays the landing field length within this weight range.





(a) The take-off field length of the one- and two-seat variants. (b) The landing field length of the one- and two-seat variants.

Figure 10.5: The take-off and landing performance at sea level (ISA + 10° K) in the weight range from W_A to MTOW.

10.2.3. Climb Performance

The climb performance of the SALSA is of great importance to its ability in performing aerobatic maneuvers. For time-limited aerobatic sequences, a high climb rate is essential to complete maneuvers within a short time, or to rapidly gain altitude for the next one. Because of this reason, other aerobatic LSA, such as the Tecnam Snap discussed in Section 2.1 (climb rate of 10.2 m/s (2000 fpm)), and aircraft competing in the IAC Intermediate category, such as the Extra 300L (climb rate of 16.3 m/s (3200 fpm)), are capable of high climb rates.

The maximum climb rates of the one-seat and two-seat variant are calculated to be $11.0 \,\mathrm{m/s}$ (2,180 fpm), respectively 8.4 m/s (1,660 fpm), at sea level (ISA+ 10° C) with full take-off power. Therefore, both aircraft meet their corresponding requirements. This maximum climb rate is flown at 27 m/s (52 kts) for the one-seater, respectively 26 m/s (50 kts) for the two-seater.

Figure 10.6 demonstrates the effect of altitude on the maximum, steady climb rate of the two variants. The critical altitude of the turbocharged Rotax 915 iSc is at 4,570 m (15,000 ft), causing a decrease in power and consequently climb rate. As can be seen from Figure 10.6, the one-seat variant has a maximum rate of climb of 13.9 m/s (2,740 fpm) at sea level (ISA+10°C) at the aerobatic weight. This maximum climb rate is reached an airspeed of 25 m/s (49 kts).

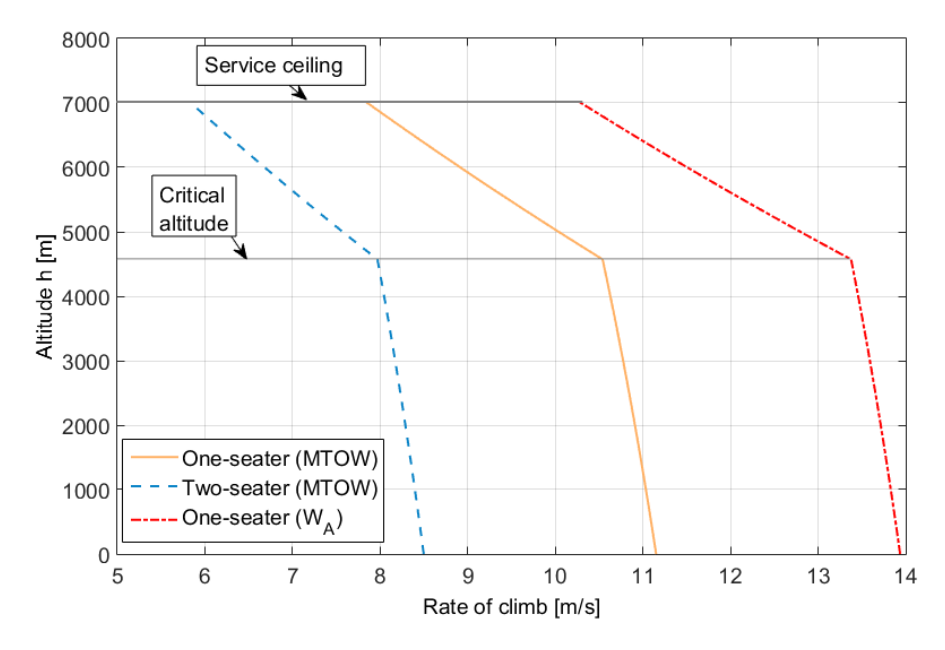
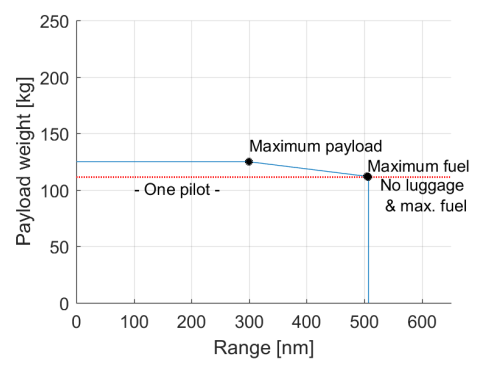


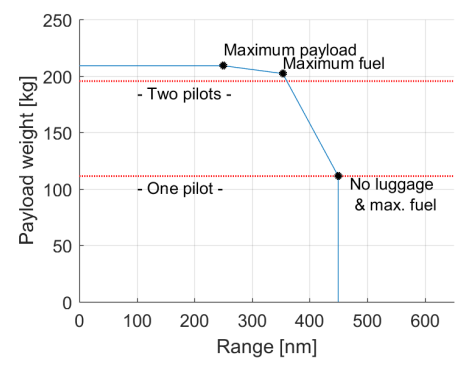
Figure 10.6: Rate of climb at full takeoff power of the one- and two-seater from sea level up to the service ceiling of the Rotax 915 iSc, 7,010 m (23,000 ft) (ISA+0°C). [32]

10.2.4. Payload Range

Figure 10.7 shows the payload-range diagrams of the aircraft family. It appears that the two-seater operated with only one pilot is able to approach the range of the one-seater. It should be noted that the one-seater allows for more payload to be carried than shown, if a compromise in range is accepted. The range and fuel required have been determined using the Breguet equation. Fuel fractions are taken from from Roskam (lightest aircraft class) [9], prop efficiency is assumed to be 80%, fuel consumption is 0.47 lbs/hp/hr, and a lift-to-drag ratio of 8 (cruise) and 9 (loiter) is used. The payload-range diagram has been constructed with a 30-minute loiter included. The fuel tank allows for 75 L (20 gallon) of fuel.

Please note that the initial ferry range requirements are 300 nm and 250 nm for the one- and two-seater respectively. However, from market analysis (Section 2.1) it follows that the range of most competitors exceeds this requirement. To compete on the market, the SALSA family can achieve the required ranges *with payload*. This results in a ferry range of 500 and 450 nm, respectively.



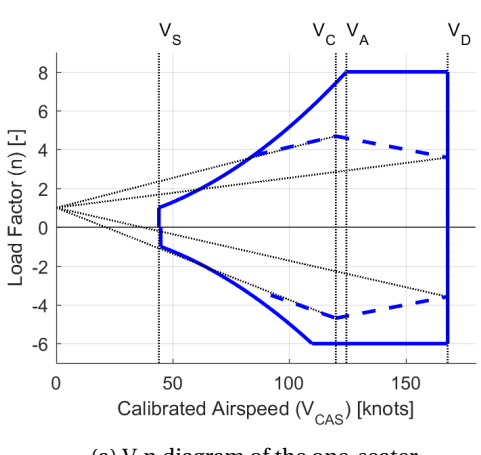


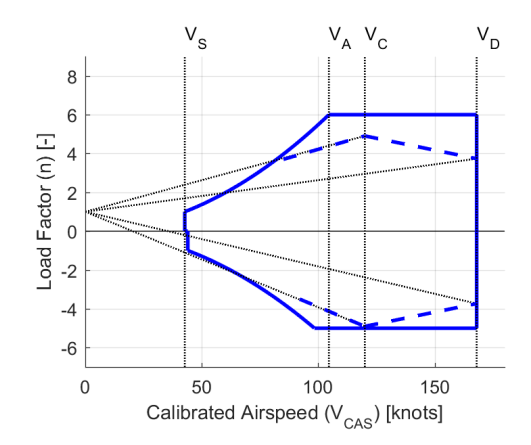
- (a) Payload-Range diagram of the one-seater.
- (b) Payload-Range diagram of the two-seater.

Figure 10.7: Payload-Range diagrams of the ALSA family.

10.2.5. V-n Diagram

Figure 10.8 shows the V-n diagrams of the aircraft family, displayed with the limit loads. The diagrams have been constructed according to the ASTM standards for LSA [2]. It appears that the gust loads are no driving factors for either design. Furtherdmore, the aircraft cannot reach its ultimate loads at cruise speed (V_C) , which has a positive effect on safety. However, the limit load of the one-seater (8 G) is a reachable target while flying at cruise speed.





(a) V-n diagram of the one-seater.

(b) V-n diagram of the two-seater.

Figure 10.8: V-n diagrams of the SALSA family.

Verification and Validation

This section includes verification and validation of the design methods. Validation is carried out for requirements, weight estimations, commonality, and aerodynamics and verification process is carried out for structural analysis, control surface design, and financial analysis.

11.1. Requirements Validation

Some aspects of which the requirements were not clear, in particular concerning visibility, stall characteristics, and inverted flight, are discussed with a pilot who flies regularly in IAC competitions. This provided much insight. Hereby we would like to thank Dr.ir. A.C. in 't Veld for his time.

11.2. Validation of Component Weights

The estimations of component weights as presented in section 6.4 are checked by comparing them to the component weights of several home-built aircraft[33][p. 136]. Figure 11.1 shows how the estimated component weights compare with the component weights of existing home-built aircraft. It is noticed that some component weight estimations are out of the ballpark. The nacelle is estimated to weigh ca. 15 kg, which is adjusted to 6 kg. The fuel system is estimated to weigh only 2.0 kg, which seemed too little when plotted against empty weight as well as when plotted against fuel weight. Therefor the fuel system weight is adjusted to 4.0 kg, which is in the ballpark. The estimated electric system weights are 11.4 and 14.6 kg for the one-seater and two-seater respectively. This appeared unreasonably heavy, so the weights are adjusted to 10 kg for both variants. The estimated weight of avionics and electronics are 12.0 and 24.0 kg for the one-seater and two-seater respectively. This appeared unreasonably heavy, so the weights are adjusted to 10 and 20 kg respectively.

11.3. Commonality Validation

One specific requirement that deserves a highlight is the commonality between the SALSA aircraft family members. The commonality is defined as the weight of the components used in both the single and two seat aircraft, divided by the total component weight of the aircraft. The components exclude the engine and propeller, as stated in the request for proposal. It is assumed that the fuselage structure is common, along with the empennage, landing gear, electronics and the aircraft parachute. It is assumed that the control system, avionics and furnishing from the single-

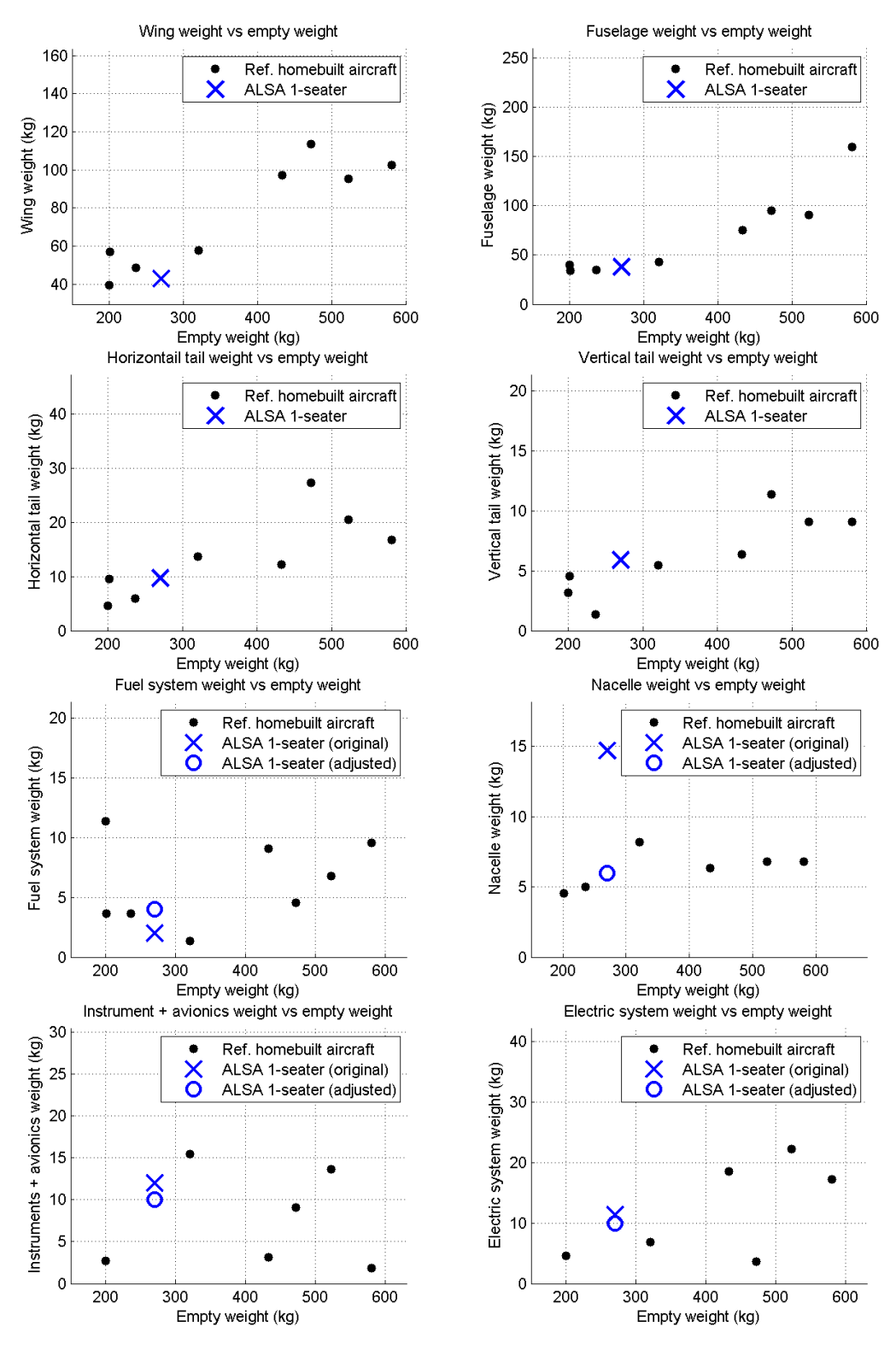


Figure 11.1: Comparison of component weight estimation with component weight data of home-built aircraft. The reference aircraft are: RV-6, BD-4, Volksplane, Long-EZ, Nemesis.

seater can be partially used in the two-seater. The wing extension is a component unique to the two-seat aircraft. The (common) components between the SALSA family aircraft and their weights are listed in Table 11.1.

Table 11.1: Component weight estimation excluding components in front of the firewall. An estimation for commonality between the two aircraft is given based on these values.

Component name	One seater weight [kg] ([lbs])	Two seater weight [kg] ([lbs])
OEW	278 (613)	316 (697)
OEW - engine - cowling - prop	176 (388)	220 (485)
Fuselage	42 (93)	42 (93)
Wing	46 (101)	70 (154)
Tail	10 (22)	10 (22)
Main landing gear	27 (60)	27 (60)
Tail gear	4 (9)	4 (9)
Control system	8 (18)	10 (22)
Avionics	6 (13)	10 (22)
Furnishing	6 (13)	14 (31)
Fuel system	4 (8.8)	4 (8.8)
Electronics	10 (22)	16 (35)
Full aircraft chute	13 (29)	13 (29)
Total common weight	176 (388)	176 (388)
Commonality %		80%

This results in at least 80 % commonality by weight among two family members. Only 20% of the two seat aircraft weight is composed of components unique to this aircraft. Thus the commonality requirement has been met at this point in the design process. In detailed design even more attention must be given to design sub-components with as many common parts as possible.

11.4. Control and Stability Verification

The control and stability derivatives as computed using Roskam have to be verified to perform a reliable simulation of the aircraft's eigenmotions. To do so, the stability derivatives as computed using the developed MATLAB tool are verified through verification of the code. Subsequently, the output (the actual stability and control derivative values) are verified against the derivatives as computed in the Advanced Aircraft Analysis program which are based on the same equations. Moreover, the stability and control derivatives are compared to reference aircraft of similar size such as those found in [21] and [23]. Finally, whenever a derivative value could not be verified through this procedure alternative computation methods were applied. For example, $C_{l_{\beta}}$ could not be verified initially but could be verified after incorporating the relevant equations as found in Raymer. In this manner the resulting eigenmotions were concluded to be reliable when all stability and control derivatives were verified. When compared to reference aircraft it can be said that the resulting eigenmotions are within the expected range of values and are therefore verified as well.

11.5. Structural Analysis Verification

The loads on the aircraft structure are obtained by integrating the aerodynamic forces acting upon it. These integrals are evaluated by hand as well as with MATLAB, and both yielded consistent results. The same approach is used to verify the loads in the wing structure.

11.6. Control Surface Design Verification

The verification of the design of the control surfaces is done by using the examples given in the reference of the used method. A program is written which incorporates the method and calculates the required output with the given input. To verify the code the input values from the examples are used. The output of the program is then compared to the output given in the example.

11.7. Performance Analysis Verification

All graphs and parameters of the aerodynamic analysis are obtained using the methods of Roskam [21], Hoerner [29], and Abbot [17] in Matlab and are verified and validated with *Advanced Aircraft Analysis* by DARcorporation. Final output parameters are compared to the reference aircraft.

The calculations used for the performance analysis are done using the methods of Roskam. [21] The calculations have been verified by carrying them out both in Matlab and Excel. The final results are compared to the performance characteristics of reference LSAs found in Section 2.1.

11.8. Financial Analysis Verification

The final cost break-down structure of the development and manufacturing phase of the aircraft is normalized and compared to the examples presented in Roskam VIII [34]. Next to this, final aircraft price has been compared to the current market, both in the U.S. and beyond. Direct Operating Cost has been compared to current comparable aircraft. ¹

 $^{^{1}} CTLS \ Flight \ Design-www.flight design.bg/files/Brochure_CTLS_small.pdf$

Realization

In this chapter all aspects concerning the realization of the SALSA programme are discussed.

12.1. Operations and Logistics

The operations and logistics of both aircraft differ due to their intended mission. Figures 12.1 and 12.2 show the typical operational profiles of the one and two-seater respectively. The mentioned pre-flight checks include refueling if necessary.

The one-seater may be stored at the residence of the owner due to its removable wing and horizontal tail surfaces, avoiding hangar costs. It may be transported by trailer to an airfield, after which it is assembled on-site. Without removable horizontal tail and wing surfaces the aircraft would not fit in a typical trailer of 102 inches. Regular flight operations are performed at the airfield, after which the horizontal surfaces are disassembled and the aircraft is mounted on the trailer for its return home.

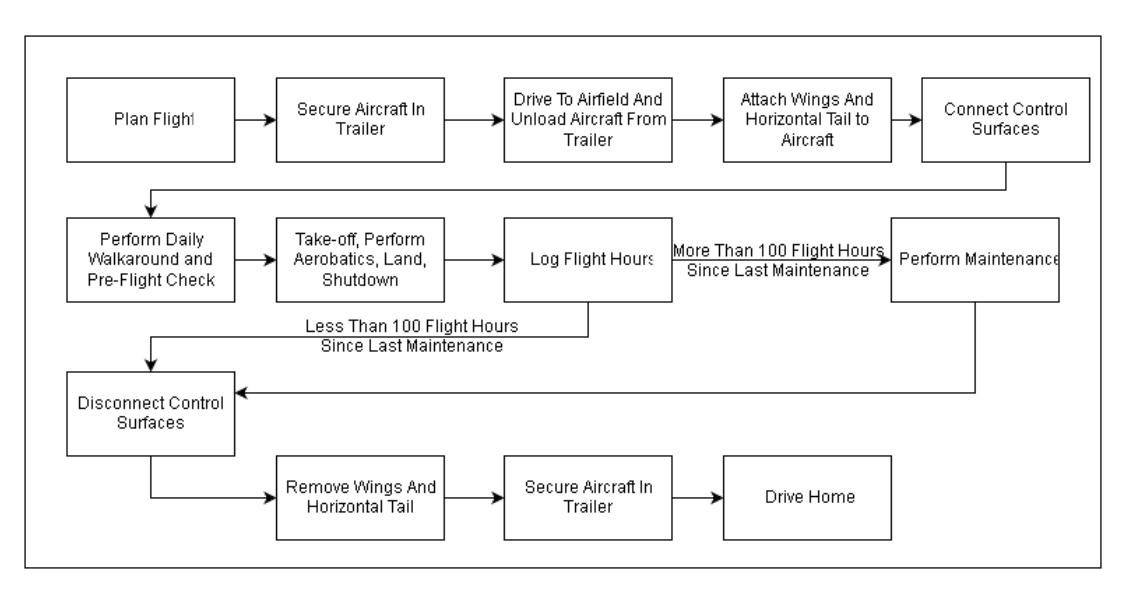


Figure 12.1: Operations profile for the one-seater, a privately owned aircraft stored at the owner's residence

The two-seater is stored at the flight school, occupying little hangar space without its horizontal surfaces. The aircraft is assembled and used to train students during the day, after which it is disassembled and stored.

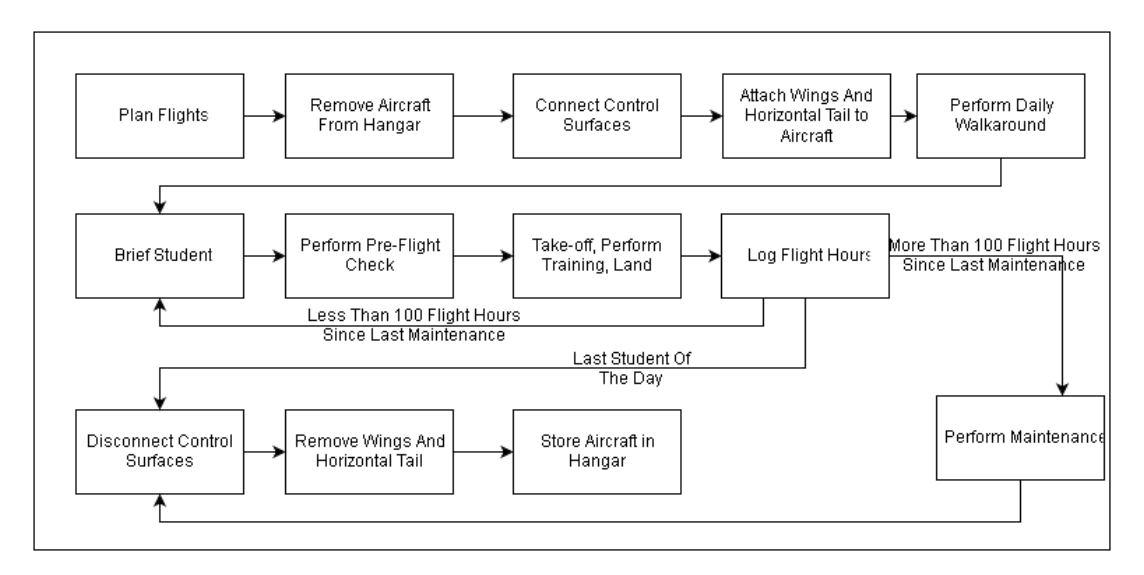


Figure 12.2: Operations profile for the two-seater, a trainer aircraft for flight schools stored at an airfield

The maintenance schedule is the same for both aircraft with 100 hour or yearly maintenance intervals, as explained in Chapter 12.3.

12.2. Production Plan

This section contains the production plan of the aircraft. The high part commonality incorporated in the design philosophy aims to minimize the production costs. An example of how this cost reduction is achieved is the fact that less moulds are needed to produce parts for the two aircraft.

12.2.1. Manufacturing of Parts

Wing The wing skin material is a glass fiber and foam composite sandwich structure. The skins will be made in two sections (a top and a bottom skin) using moulds. Starting at the bottom section, the glass fibre cloth is laid up in a mould by hand lay-up technique and is impregnated with resin. At the front and rear spar locations, spar caps made out of unidirectional carbon fibers are laid up and epoxy resin is applied such that spar caps are laminated in the wing skin. The foam layer is shaped to the right dimensions and glued to the glass with a layer of glass micro balloons. The transition of the foam to the carbon spar cap fibers should be smooth. On top of the foam layer another layer of micro balloons is applied after which a couple of layers of fiber glass are laid up to complete the skin. Vacuum bagging is used to shape the laminate. This is then cured under slightly elevated temperature.

The spar core is made separately and cured before bonding to the wing skins. The spar core consists of a foam core covered with a couple layers of carbon fiber in +-45deg direction to deal with the in plane shear. Before being bonded to the skins, the ribs are made separately as well. Ribs are made out of a glass-foam sandwich panel which will be

CNC milled into the right contour.

The spar webs and ribs are bonded onto the lower wing skin with epoxy adhesive to form the skeleton. Subsequently, an adhesive is applied to the top side of the spars, ribs and skin overlap sections. Using an overhead crane, the top mould is fitted on top of the bottom mould. Both moulds are tightly clamped, forcing excess glue out. The whole wing is cured in an oven, after which the moulds are separated. The resin overflow is trimmed and seams are sanded down until smooth. Finally, the ailerons are installed. The wing cross-section showing wing skin sandwich structure, with spar caps laminated inside wing skin can be seen in Figure 12.3.

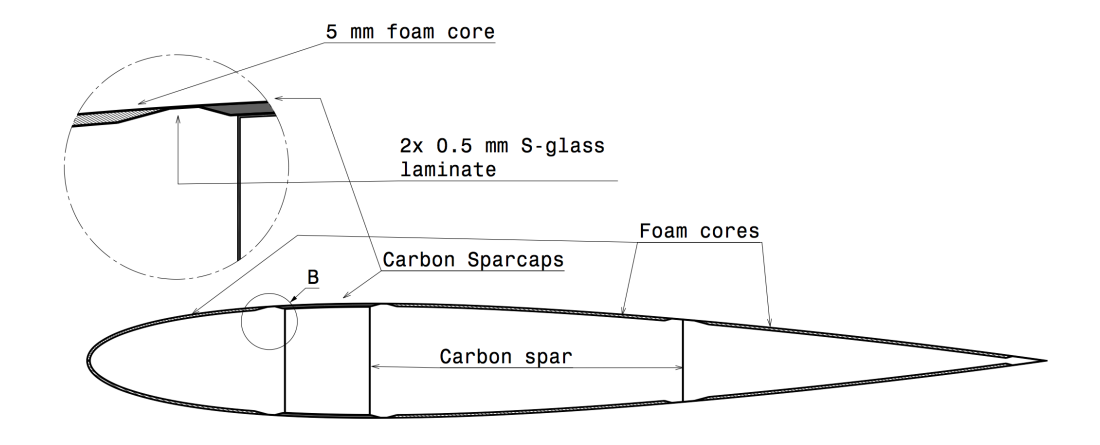


Figure 12.3: Cross-section of a wing

Since the wings are symmetric the top and bottom skins of both wings are produced with one type of mould. The root extensions for the two-seater are manufactured with the aforementioned procedures.

Fuselage The fuselage will be made out of a glass fiber composite semi-monocoque structure with fuselage frames. The fuselage is built in two pieces using a left and right mould. The fuselage skin has a sandwich structure with foam core and glass fibre cloth. It features the same production process as for the wing skins. The unidirectional longerons made out of glass fibers are laid up during the layup of the skins itself and impregnated with resin. Fuselage frames are laid up separately and cured before bonding into a side half of the fuselage skin with epoxy adhesive. Adhesive is applied to the structure and other side of the fuselage is bonded in place by clamping both moulds. The fuselage is then post-cured in an oven. Finally, trimming, sanding and polishing is done to a mirror finish.

Tail The same production methods as described for the wing apply to the production of the empennage and control surfaces.

Landing Gear The landing gear system consists of the struts, wheels and aerodynamic wheel fairings. The struts and fairings are made out of glass fiber, using a mould and hand lay-up method. Tires and wheels are bought as

off-the-shelf products.

Fuel system The fuel tank is made of aluminum and is produced using bending or rubber forming and is welded together. The fuel distribution system consists of fittings and fuel lines made of off-the-shelf aluminum tubes that are cut and bent to fit the fuel system.

Other components The engine, avionics, and control system components will be supplied by an external manufacturer, ready to be installed on the aircraft. Cockpit equipment includes seats, avionics and handles to open the canopy. The frame of the seats, avionics panel and handles can be 3D printed in-house. The canopy is made of acrylic glass that is produced by casting.

12.2.2. Assembly Process

The aircraft assembly process begins with putting the fuselage in an assembly jig, where the wing center section will be bonded to it.

Sub-assemblies are painted before the final assembly. Firstly the landing gear will be installed with bolts to the fuselage, and the rudder will be put into place. The next step is to install all operational subsystems such as fuel, electrical, control system, brake lines and antennas. After that, the fuselage interior can be installed. At this point any avionics options selected by the customer are installed.

After the fuselage is complete, the wing root extensions and relevant control system can be installed for the two-seater by means of one main bolt for each side. After that the outer wing can be installed, including the connection of the control system. The wings will be mounted by the means of the same type of main bolts. The assembly of wings can be seen in Figure 8.3 and Figure 8.2. The horizontal tailplane and its control system complete the assembly. The horizontal tailplane integration with vertical tail can be seen in Figure 8.9.

The final parts that need to be connected are the engine, propeller and cowling. All the wiring and connectors will be connected to their right counter parts. After which the cowling can be closed and a thorough inspection of all the systems can commence. An overview of the assembly line is given in Figure 12.4.

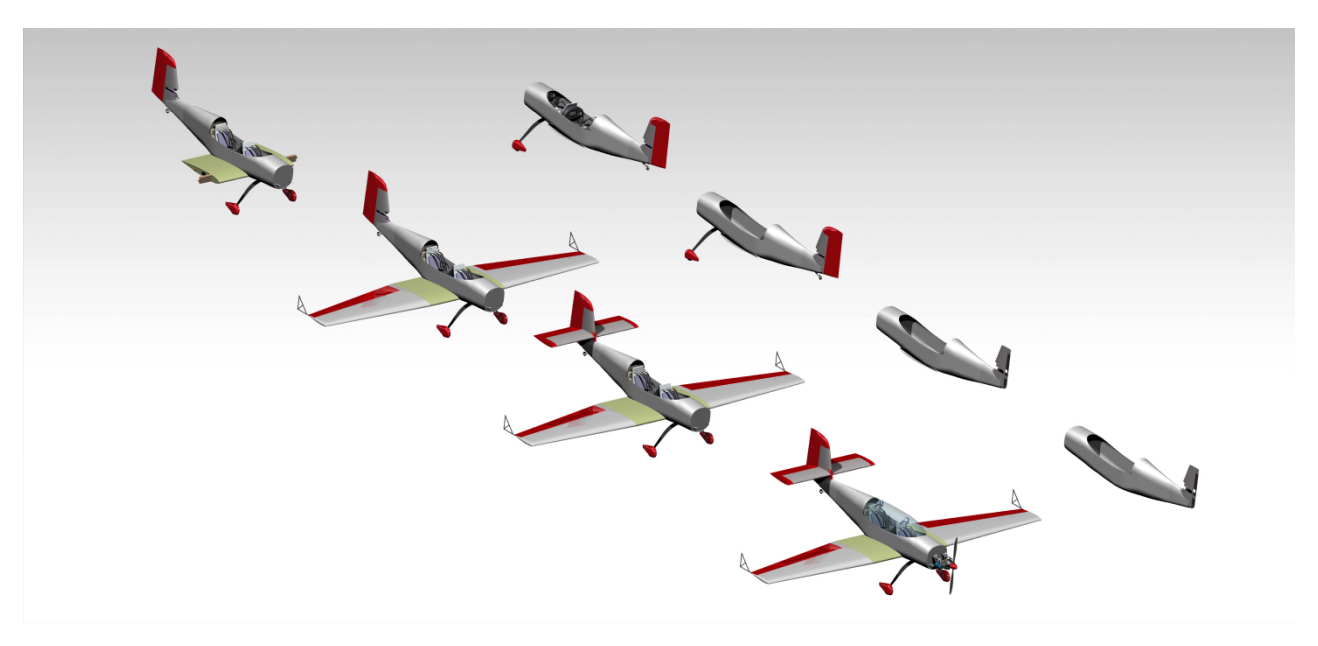


Figure 12.4: Graphical representation of the production plan showing assembly line

12.2.3. CO₂ Neutral Production Plan

The carbon footprint of the production process is a significant contributor to the total environmental impact of the SALSA over its lifespan. Possible strategies that can be implemented to make the production process Co_2 neutral are given in Table 12.1

Table 12.1: Strategies for CO_2 Neutral production

Front 1	Eliminate Waste: Reduce and Recycle all possible forms of waste, send minimum waste to landfills.
FIOIIL 1	Reduce waste due to over-production and product defects.
Front 2	Benign Emissions: Minimize and try to eliminate usage of toxic substances for production .
Front 3	Renewable Energy: Use 100 % renewable energy sources for operating facilities and machines.
Front 4	Closing waste generation Loop: use recycled and bio-based materials for production.
Front 5	Sustainable Transportation: People and products will be transported efficiently.

The assembly line will be optimized according to lean manufacturing principles. For a given workstation in the assembly line, the exact amount of parts required at the following workstation should be produced to minimize waste due to waiting. When the exact production rate of the aerobatic LSA family is known for a given time span, the exact amount of required materials can be ordered and inventory waste is minimized. Movement waste is minimized by lowering the physical distance between workstations, effectively establishing a continuous line of assembly. Overproduction is prevented using *kanban*, a method to control just-in-time processing [35]. Produced parts must always be accompanied by a kanban stating production and transportation information associated with these parts. The result is an assembly line in which there is no overproduction and the amount of transportation is minimized. Additionally, the implementation of kanban ensures that defective products are removed from the assembly line. In the case of LSA the production process is on a significantly smaller scale when compared to a large general aviation

12.3. Maintenance

manufacturer. This makes it feasible to implement the aforementioned production philosophy in a successful way.

12.3. Maintenance

This section describes how the maintenance of the SALSA family is organized.

12.3.1. Maintenance regulations

The SALSA aircraft are sold with a maintenance manual. It details how certain tasks should be performed and whether a certified mechanic should perform the maintenance activity. There are three types of people that can do maintenance on an LSA: a certified airframe and power plant (A&P) mechanic, with or without inspection authorization, a light-sport repairman with a maintenance rating for aeroplanes (LSRM-A) and certified-pilot LSA owners. Modifications to the aircraft are forbidden, unless approved by the aircraft manufacturer. If approved, a document describing the modifications becomes a permanent attachment to the airplane's operation instructions manual and maintenance manual.

A&P mechanics can service other categories of aircraft as well and they are free to do more demanding maintenance tasks on an LSA. On the other hand, the Light-sport repairman with LSRM-A rating limits the holder to S-LSA and E-LSA maintenance and inspections only.² As with Part 23 aircraft, certified-pilot owners can do limited routine maintenance on their aircraft. These more trivial tasks include routine-check, simple maintenance items such as oil changes, switching spark plugs, and fixing tires. If a particular maintenance or repair task is not addressed in the maintenance manual (MM), this task is considered critical and the manufacturer must be contacted for the proper procedure. Engine manufacturers also put limitations on certain maintenance: Rotax allows only approved Rotax Service Centers to do heavy maintenance, engine overhaul, and major repairs on its engine. The Rotax 915 engines have inspection intervals of 100 hours.

12.3.2. Maintenance tasks

Maintenance of the SALSA family starts with a daily inspection of the aircraft prior to flight. In this inspection the engine is visually checked for proper condition and the oil level is checked. Next, a thorough pre-flight inspection is performed. During this inspection, around the aircraft, the pilot checks for proper connection of the control surfaces to their respective inputs, proper rigging, visual damage or any other anomalies. Visual inspection of the wing and fuselage are quite effective, because glass fiber shows damage very well. In the cockpit all flight controls are checked for proper response, the avionics are checked for damage or incorrect readings and the condition of the safety harness is visually inspected. The aircraft is subjected to a more thorough inspection at 100 flight hour intervals or

¹https://www.aea.net/AvionicsNews/ANArchives/Jul08LSAMaintenance.pdf

²https://www.ussportaircraft.com/documents/CFI_guide_to_LSA_maintenance.pdf

12.4. Reliability 85

annually, whichever comes first. These inspections have to be performed by a LSRM-A.

Some design choices increase the aircraft's maintainability. The engine cowling is removable, providing easy access to the engine. The wings feature inspection holes in their end ribs. The structural components of the aircraft are designed with a 10,000 cycle safe life operation in mind and should not need many repairs. It is however important to keep the finish of the aircraft in good condition to prevent cracks from growing into the glass fiber.

12.3.3. Costs of maintenance

Costs are about 50 USD/flight hour, strongly dependent upon flight hours per year. When used for 100 hours annually, the aircraft will cost about 100 USD/flight hour. Commercial use may be in the order of 300 flight hours annually, resulting in costs of 70 USD/flight hour. Insurance costs are about 5000 USD annually for commercial aircraft. When flown for training purposes, insurance costs increaese significantly.³

12.4. Reliability

The SALSA family is designed to be very reliable in the LSA category. Reliability is mainly influenced by the mechanical system and weather conditions.⁴ The composite aircraft structure is designed to be safe-life. Composites are generally resistant to fatigue and highly loaded parts are designed including a safety factor of 1.5. Additionally, Rotax is seen as a very popular engine manufacturer, who have a lot of experience in engine production. Therefore, provided the aircraft is properly rigged and maintained, it will be as reliable as existing LSA.

The LSA category is not allowed to fly in IFR conditions, according to ASTM standards. In the US, FVR night-flight is allowed. Weather does limit the operation of SALSA, though these limiting conditions (such as icing) have not been established yet. It is, however, prohibited to fly an LSA in instrument meteorological conditions (IMC). In conclusion, the SALSA family can only be operated in VFR conditions which limits its reliability to perform the mission at any given time. [2]

12.5. Availability

The SALSA family is designed to operate in uncontrolled and controlled airspace, so this does not limit the availability of the aircraft. Availability is mainly limited by the amount of scheduled and unscheduled maintenance ⁴. Maintenance is further elaborated upon in Section 12.3. As mentioned in this section, the amount of maintenance required for LSA is low. The result is an aircraft family that is able to perform its mission under many circumstances.

³http://sportpilottalk.com/viewtopic.php?t=1711

⁴ https://www.conklindd.com/t-measuringreliabilityandavailability.aspx [accessed 20-1-2016]

12.6. Safety 86

12.6. Safety

In order to ensure that the SALSA adheres to safety standards a number of systems can be implemented which includes the mandatory five-point seat belt. In addition to the mandatory personal parachutes, the aircraft is equipped with a full aircraft parachute to further increase overall safety in case of an emergency. These types of parachutes are already widely implemented in a range of LSA's and have been proven to work reliably. These parachutes can be bought from an external supplier, such as BRS Aviation. The system will weigh 13.2 kg and will cost around \$5000. In order to implement this the airframe will have a few hard points to attach the lines from the parachute.⁵

Another safety feature that will be incorporated is a Pilot Attention Monitoring system. This is already implemented in the automotive industry. The system monitors the driver's face, his eyes and head movements for any sign of sleep or loss of attention. A similar system can be used to track pilots and to warn the pilot in case he/she loses consciousness during aerobatic maneuvers or regular flight. This will be coupled with an alarm in the cockpit to get the pilot's attention. It is also coupled to the deployment system of the full aircraft parachute in case the pilot cannot continue to control the aircraft.

12.7. Sustainability

Various global market analyses indicate that the aviation industry worldwide doubles every fifteen years ⁶. "Noise and emissions have been of concern since the beginning of aviation, and continuous air traffic growth and increasing public awareness have made environmental performance one of the most critical aspects of commercial aviation today" [36]. If no action is taken, emissions will continue increasing as shown in Figure 12.5.

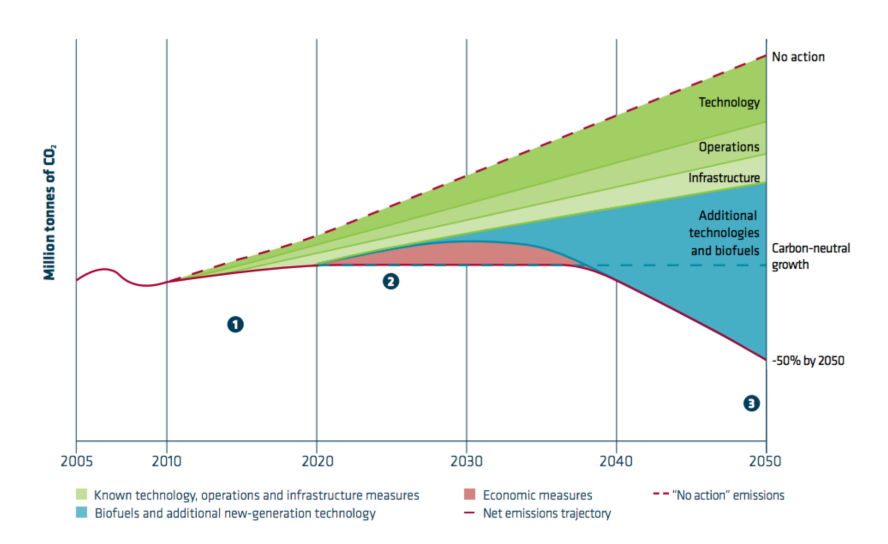


Figure 12.5: Industry commitments (source: ICAO Assembly 2013⁷)

⁵http://www.aircraftspruce.com/catalog/appages/brscanister1350SP.php

 $^{^6} Projected \ Emissions \ Growth. \ www.airbus.com/company/market/forecast/\ [cited 8 \ December 2015].$

12.8. Risk Assessment 87

Even though general aviation is only responsible for about 0.2 percent of the global green house gas emissions⁷, every sector is responsible for its share and should do everything in its power to meet international goals on noise and emissions⁸. As sustainability is increasingly prioritized in the industry, the SALSA aircraft are required to meet today's standards to reduce their environmental impact.

12.7.1. Propulsion

The Rotax 915 iSc consumes regular automotive petrol (mogas), as opposed to avgas which often contains lead additives. A blend of up to 10% ethanol (E10) may be used in the 915[37]. Ethanol is produced from corn (making it a biofuel) across the United States [38]. Recent developments have seen waste products from industrial plants recycled into usable fuels. For example, Virgin partnered with LanzaTech to create jet fuel from waste gasses from steel mills and other CO and CO_2 rich gasses 9 Microbes are used to convert the gases into alcohols, after which chemical converters convert this into hydrocarbon fuel 10 . Emerging techniques such as these should be considered by pilots when fueling their LSA.

12.7.2. Manufacturing

The U.S. Environemntal Protection Agency (EPA) concludes that the best approach to energy saving during manufacturing is efficient employee practices (turning off lights in empty rooms, closing windows/doors, etc) rather than costly technological improvements[39]. The highest energy savings were achieved by combining ISO 14001 environmental certification¹¹ and employee management programs, as reported by an EPA Energy Star partner. One factory in Born, The Netherlands reported electricity savings of 10% and natural gas savings of 2.5% in the first year of an employee energy management program, totaling almost US\$400,000 of savings and recovering the cost of the program in less than one year[39].

12.8. Risk Assessment

A risk analysis is done in order to become aware of the major risks that exist within the project. Risk is the uncertainty that is concerned with a particular event that has a negative impact on the project. The goal of this risk analysis is to determine which risk events have the largest impact, such that measures can be taken in order to increase the probability of success of the SALSA project.

⁷Aviation Emissions. www.gama.aero/files/documents/general_aviation_industry __information_on_aviation_48fe490ca1.pdf [cited 8 December 2015]

⁸Emissions Goals. www.iata.org/policy/environment/Documents/iata - factsheet - climatechange.pdf [cited 8 December 2015]

9Virgin Biofuel Initiatives. http://www.businessgreen.com/bg/news/2307887/virgin - atlantic - and - lanzatech - prepare - low - carbon - jet - fuel - for - take - off [cited 11 January 2016]

 $^{^{10} \}mbox{Biofuel Conversion Processes. } http://web.ornl.gov/adm/partnerships/events/SPARK_Dec12/Presentations/04_Catalytic%20Conversion-Bio-alcohols%20to%20Hydrocarbons-Speck.pdf [cited 11 January 2016]$

 $^{^{11}} ISO\ 14001\ Industry\ Standard.\ https://committee.iso.org/sites/tc207sc1/home/projects/published/iso-14001---environmental-manage/benefits-of-iso-14001---5000-use.html\ [cited\ 12\ January\ 2016]$

12.8. Risk Assessment 88

12.8.1. Areas of Risk

The risks can be divided into three areas based on performance, schedule, and cost[40]. A risk in one area can sometimes be reduced with resources from another area, but not always. Risks should be reduced in magnitude in order to increase the probability of successfully completing the project. There are two ways of reducing the risk of an event: by reducing the probability of occurrence (prevention) or by reducing the severity of consequence. On the other hand, plans can be made to cope with the consequences in case risk events do happen.

12.8.2. Risk List

A list of risks has been identified for the technical design, development, production, operation, maintenance and disposal aspects of the SALSA project. The first three items contain risks for the project team ("the company"), while the latter three items contain risks for the customer who operates the aircraft.

Technical design risks In Table 12.2, the most important technical design risks are given. These are very important to mitigate, because they influence the design of the aircraft. If the final product does not meet requirements, it can never enter production and all research costs are wasted.

Development risks Three risks that can be encountered during development are shown in Table 12.3. If development takes too long, or if the aircraft turns out differently than designed initially, revenue may be lost.

Production risks The production phase brings new risks. The amount of labour and costs of this phase are all estimated values. Deviations from the planned production such as mentioned in Table 12.4 cost the company a lot of money.

Operation risks During operation, the consequences of risks shift from mostly financial to potentially lethal, as shown in Table 12.5. Becoming a good aerobatic pilot requires a lot of experience. The LSA class poses a threat that too inexperienced pilots, without a proper medical, fly the SALSA family.

Maintenance risks Aircraft maintenance is a critical task to be performed and documented very accurately. If done incorrectly, it can result in potentially dangerous situations, such as those given in Table 12.6.

Disposal risks Disposal of the SALSA family is quite difficult with the selected composite materials. Therefore, material processing expenses might be higher than initially estimated. Disposal risks are mentioned in Table 12.7.

Investment risks Generally speaking, everything that reduces the number of aircraft orders to below the predicted market share could pose a large financial risk to the SALSA project. Less aircraft orders reduce the amount of aircraft

12.8. Risk Assessment

over which the fixed development costs are divided. This in turn has catastrophic effects on the profit per aircraft. A loss per aircraft could even bankrupt the company. What makes these risks all the more dangerous is the lack of countermeasures that can be taken to mitigate the problem. The only way to reduce the chance of bankruptcy is increasing profit margins, though this leads to a higher price. Table 12.8 shows the most important examples of these risks.

Table 12.2: Technical design risks of the SALSA project. These risks are for the company.

ID	Event
1	A requirement is missed in requirement analysis
2	Using out-of-date parameter values during de-
	sign
3	Initially guessed parameter values not replaced
	by properly estimated values

Table 12.4: Production risks of the SALSA project. These risks are for the company.

ID	Event
7	delay in tooling availability due to delay of tech-
	nology maturity
8	workforce costs too much
9	delay in material availability
10	chosen production method is too expensive
11	part damage during production process, result-
	ing in higher part costs
12	delay in availability of production drawings
13	delay in availability of production facilities

Table 12.6: Maintenance risks of the SALSA. These risks are for the operator.

ID	Event
22	degradation when improperly stored
23	no qualified mechanics available
24	incorrectly performed maintenance
25	degraded components not replaced in time

Table 12.3: Development risks of the SALSA project.
These risks are for the company.

ID	Event			
4	Engine not	available	before	entry-in-
	service			
5	Aircraft	heavier	thai	n de-
	signed/spec	ified		
6	Certification	ı takes too	much t	ime

Table 12.5: Operational risks of the SALSA. These risks are for the operator.

ID	Event
14	incident due to lack of pilot skill
15	human injury due to ground operation
16	in-flight failure due to improper main-
17	tenance aircraft damage due to ground han- dling
18	aircraft access denied on airport
19	material strength degradation
20	increased fuel price
21	difficult transportation

Table 12.7: Disposal risks of the SALSA. These risks are for the operator.

ID	Event
26	material re-use value decreases
27	increased expense of material recycling

Table 12.8: Investment risks of the SALSA. These are carried by the company

ID	Event
28	Less expensive or generally better competitors enter the LSA market and obtain a large market share
29	The LSA market forecast does not live up to expectations
30	The SALSA family does not get certification for other markets than the US
31	The design of the SALSA family does not accurately fit the customers needs and requirements
32	LSA category gets abolished by FAA

12.8.3. Risk map

Figure 12.6 depicts the most important above mentioned risks in a plot. The axes of the plot describe on a range of one to five how probable an occurrence of the risk event is, and how large the consequences of occurrence are.

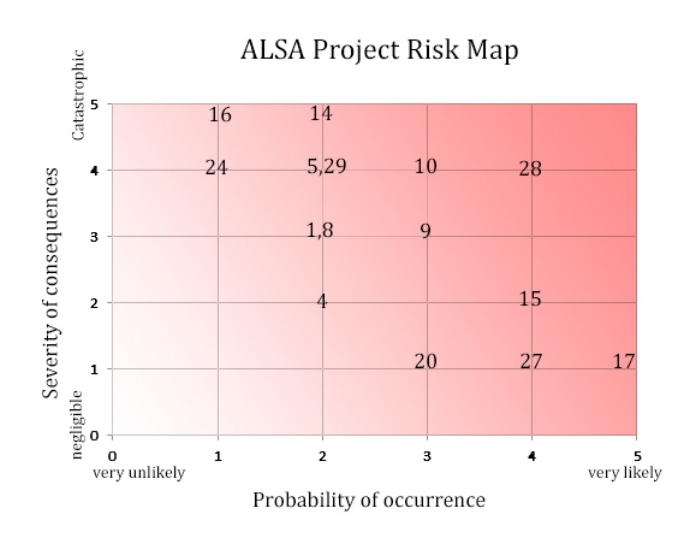


Figure 12.6: Risk map of the most important risks mentioned in subsection 12.8.2

12.8.4. Conclusion

In conclusion, continuing the SALSA project can be seen as a risky endeavour. The LSA market is not very mature and its future prospects are up to debate. With Cessna pulling their Skycatcher off the market, trust in the future success and durability of the LSA category is diminished. A new competitor on this small market is seen as the largest risk to the SALSA project. The probability that a competing aircraft enters the LSA market is quite high, while the total production period of the SALSA family is planned to be 15 years. Moreover, the event can have catastrophic consequences for the SALSA project and no adequate corrective actions can be taken to overcome this event.

12.9. Sensitivity Analysis

A sensitivity analysis is performed to obtain insight in how major cost and performance parameters vary with changing design parameters. When this is known the feasibility of the project can be assessed as well as its robustness to changes. Last but not least, the results can be interpreted as indication for optimization of the design.

12.9.1. Approach

In the sensitivity analysis, the "sensitivity" of a certain dependent parameter (Y) to a certain independent parameter (X) is investigated. This can be mathematically represented as finding the partial derivative $\frac{\partial Y}{\partial X}$. In this analysis the independent parameters are increased by 10% of their nominal value and the corresponding change of the dependent

dent parameter was determined. These changes are then transformed into a partial derivative. Table 12.9 shows the parameters that are selected for sensitivity analysis in the first and third column.

The sensitivities of the MTOW, as shown in Table 12.9, are determined using the weight estimation methods as mentioned in 6.4. The sensitivities of the performance parameters in Table 12.9 are determined with methods detailed in 10. The sensitivities of the cost parameters in Table 12.9 are determined with methods detailed in 12.10.

12.9.2. Results

Table 12.9 shows the results of the sensitivity analysis. For example, the first row shows that increasing the wing area by $1.0 \ m^2$ would cause the MTOW to increase by $1.1 \ kg$. The method used for obtaining these values is essentially a linearization. This implies that the results are reliable only close to the point of linearization, which is the nominal value in this case, shown in the second column of Table 12.9.

12.9.3. Conclusions

The partial derivative $\frac{\partial MTOW}{\partial max.loadfactor}$ is unusually small. This is probably due to the fact that in the component weight estimation methods, only for the weight estimation of the wing this load factor is taken into account. However, increasing the load factor by large amounts, like 20 %, would likely cause much larger increases in MTOW, because in that case the fuselage and tailplanes have to be reinforced as well. Furthermore, the MTOW seems to be especially sensitive to the wing aspect ratio.

Table 12.9: Sensitivity analysis results for the one-seater

Dependent parameter	Nominal value	Independent parameter	Nominal value	Partial derivative	Partial derivative
	X		Y	$\frac{\Delta Y}{\Delta X}$	$\frac{\Delta Y/Y}{\Delta X/X}$
MTOW	425 kg	Wing area	$10.2 \ m^2$	$1.1 \frac{kg}{m^2}$	0.026
MTOW	425 kg	Fuselage length	5.7 m	$3.2 \frac{kg}{m}$	0.042
MTOW	425 kg	Wing aspect ratio	6.0	9.5 $\frac{kg}{-}$	0.13
MTOW	425 kg	Max. load factor	12.0	1.0 kg	0.028
Stall speed	22.9 m/s	Max. lift coefficient	1.3	$-8.5 \frac{m/s}{-}$	-0.48
Climb rate	15.3 m/s	Propeller efficiency	80 %	0.25 <u>m/s</u>	1.3
Climb rate	15.3 m/s	Max. engine power	135 hp	$0.12 \frac{m}{hp}$	1.1
Take-off field length	221 m	Propeller disk loading	$4.0 \frac{hp}{f t^2}$	$23 \frac{m}{hp/ft^2}$	0.41
Take-off field length	221 m	Max. engine power	135 hp	$-1.8 \frac{m}{hp}$	-1.1
Non-recurring devel. cost	2.31e6\$	Empty weight	270 kg	$10000 \frac{\$}{kg}$	1.2
Fly-away cost	1.35e5\$	Empty weight	270 kg	480 \$\frac{\$}{kg}\$	0.96
Price for profit	1.53e5\$	Empty weight	270 kg	$520 \frac{\$}{kg}$	0.92

12.10. Financial Analysis

In this chapter a financial analysis of SALSA is made using the cost estimation methods from Roskam Part VIII [34]. From market analysis, it follows that 1200 aircraft will be produced for the global market over 15 years, with an average production of 6.6 aircraft per month. These values are used as input for the given cost breakdowns. Since the aircraft family-members are very similar, they are considered as one aircraft during the development phase. The considered costs in this chapter are shown in a Cost Breakdown Structure in Figure 12.7. It reflects the cost from the PD&D logic of Section 12.13.

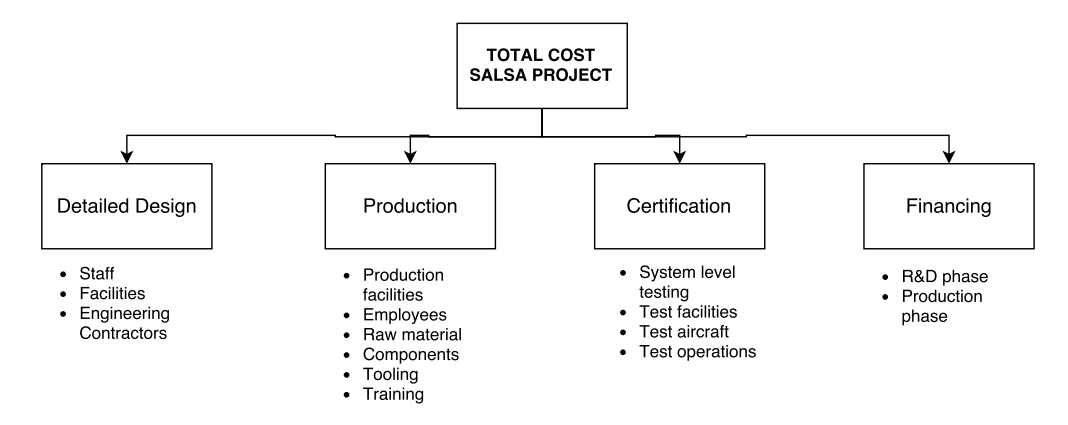


Figure 12.7: Cost Breakdown Structure of the SALSA Project

12.10.1. Development and Production Cost

The total non-recurring Research, Development, Testing and Evaluation (RDTE) cost for the project is 2.8 Million (M) USD. This consists of the elements shown in Figure 12.8a. For a total production volume of 1200 aircraft, the result is an average of \$2,400 USD of development costs per aircraft. The important assumptions are listed below:

- Four static and four dynamic test aircraft are manufactured.
- Difficulty of design is moderately high due to high part commonality. (1.5 out of 2)
- The material usage and manufacturing efficiency has been assumed to be respectively 20% and 30% more efficient than a regularly designed aircraft, due to the large amount of uniform parts.
- 10% of all RDTE costs are due to financing.
- Labor rates: engineering [\$120 USD], tooling [\$90 USD], and manufacturing [\$55 USD].
- 5% of all RDTE cost is reserved for non-standard test facilities.
- Off-the-shelf parts: the engine (\$23,000), the propeller (\$1,760), and the avionics (\$8,000 / \$10,000).
- 13% of all manufacturing labor hours are reserved for quality control.

12.10. Financial Analysis 93

These values were all obtained from Roskam [34] and corrected with a Cost Escalation Factor (CEF) of 6 where necessary. ¹² Detail design of certain subsystems (e.g. the ailerons) could be subcontracted to a specialized engineering firm, increasing development efficiency and thus decreasing cost (Section 12.13).

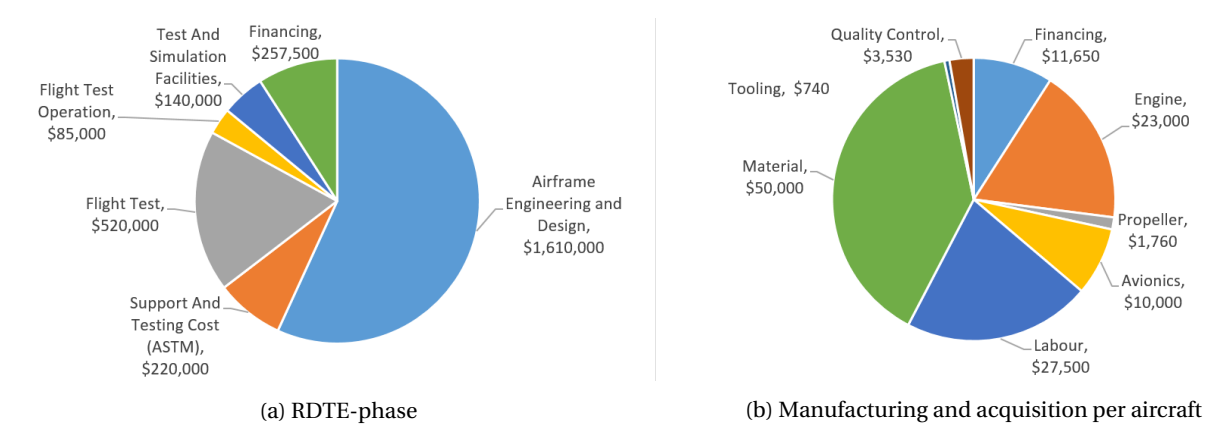


Figure 12.8: Cost breakdowns of the development and manufacturing phases for the two-seater.

The total costs of the production phase of the two-seater are shown in Figure 12.8b. The largest cost difference between the one and two-seater consists of avionics and the added weight due to the root extensions. This results in a fly-away cost of \$119,000 USD and \$128,000 USD respectively. When the non-recurring development costs and a 10% profit margin are included, this results in an aircraft unit price of \$135,000 USD and \$145,000 USD for the one and two-seater respectively. This is considered as a bottom-market price when compared to participants in the Intermediate IAC category.

12.10.2. Direct and Indirect Operating Cost

The Direct Operating Cost (DOC) consists of maintenance (\$2000 USD/yr, including replacement of brakes and tires), insurance (\$1,000 USD/yr)¹³, and consumption of fuel and oil (\$24 USD/FH / \$34 USD/FH). Assuming 240 flight hours per year for a flight school, the DOC is calculated to be \$35 USD/FH for the one-seater and \$45 USD/FH for the two-seater due to higher fuel consumption. For LSA, Indirect Operating Cost (IOC) consists largely of airport servicing and is not included in this analysis due to the great cost variation per airport. However, it should be noted that storage/hanger costs are considerably lower due to the detachable wings of the aircraft.

Considering the two-seater, current hourly rates for renting small aircraft are range around \$70 USD/FH dry¹⁴, which means that, after deduction of DOC without fuel, \$50 USD/FH is available for company expenditures, airport servicing, and aircraft depreciation, given a 10% profit margin. With \$30 USD/FH depreciation and an average of 8 flying hours per week, **the two-seater can be depreciated within 12 years**. Return on investment is heavily dependent on

¹² westegg.com/inflation/

¹³ben.com/flying/costown.html

 $^{^{14}} http://www.premierflightacademy.com/premier-fleet.htm \\$

12.11. Resource Allocation 94

cost-breakdown and profitability of the flight school and irrelevant for private aircraft holders.

12.10.3. Break-Even Point of Manufacturing

Regarding the manufacturer's point of view, in the first few years the obtained profit will be required to pay-off all loans of the RDTE phase. Equation 12.1 shows the Break-Even Point (BEP), the amount of years after which expenses are equal to revenue. $C_{\rm RDTE}$ represents total RDTE cost (2.8 mln USD), $f_{\rm profit}$ is a 10% profit margin (slightly higher for the one-seater), AEP the aircraft unit price (\$145,000 USD), $tx_{\rm rev}$ is US income taxes (20%), and $N_{\rm m,annual}$ the amount of aircraft to be sold yearly (40, corrected for a 50% lower production in the first years, i.e. the learning curve effect [34]). The BEP is computed to be 6 years after first aircraft roll-out.

$$BEP = \frac{C_{\text{RDTE}}}{f_{\text{profit}} \cdot AEP(1 - tx_{\text{rev}})N_{\text{m,annual}}}$$
(12.1)

12.11. Resource Allocation

This section describes the allocation of resources and constraints during the design of the aircraft. A design team of ten members designed the SALSA family of two aircraft within the span of ten weeks. In the final stage of the project, people were divided into teams working on a specific area of expertise. This resulted in easy communication and a smooth integration of systems while people from different areas of expertise could work on one aircraft component at once.

Next to time, weight is the first critical resource to budget in the SALSA design. The maximum limit of 600 kg (1320 lbs) MTOW is imposed by LSA regulations. The one seat aircraft is estimated to have a MTOW of 450kg (990lbs) and the two seat aircraft has an estimated MTOW of 595 kg (1310 lbs). Special attention must be given during the detailed design that the weight of the final two seat aircraft does not increase beyond what is legally allowed by LSA regulations.

Money is another critical resource to budget for the SALSA project. Entering a market with any new aircraft carries substantial financial risk since large development costs are made and it takes a long time to earn these back. To offer a financially attractive aircraft in the LSA market, the maximum retail price was determined to be 85,000 USD. The one seat SALSA has an estimated retail price of 135,000 USD and the two-seater SALSA's retail price is estimated to be 145,000 USD, with a total production number of 1200 aircraft. Therefore the target price is not reached at this point. In hindsight, the 85,000 USD target price is very low when compared to competitors in the aerobatics competition. Based on these aircraft, 150,000 USD is a much more feasible price per unit target.

12.12. Business Plan 95

12.12. Business Plan

The two members of the SALSA family introduced and it is decided that the two-seater aircraft will have its EIS in 2020. With this entry strategy, potential customers for the one-seater are able to first follow a training program on the two-seater. This also provides the opportunity to review the test process of the two-seater, from which lessons can be learned for the more demanding requirements of the one-seater. One year after the two-seater, in 2021, the one-seater will enter the market.

The SALSA family will be released initially in the USA. As became clear from Section 2.1 there are many manufacturers active on the LSA market in the US, a market where five manufacturers combined share almost half of the market. Nonetheless, because of the limited number of options of aerobatic LSAs, a high 10% market share is estimated for the US market. With this market share maintained for fifteen years this would result in a total of 189 aircraft sold, only one per month. Therefore the aircraft will also be sold in the countries selected in Section 2.1.2. The EIS for these additional markets is late 2021, after the EIS of the one-seater in the USA. The expected market share in each of these countries is shown in Table 2.1. In Europe the market share is estimated to be 10% as well, due to the fact that many LSA manufacturers are located in Europe. For the other countries a market share of 15% is estimated, as on those emerging markets less manufacturers are active. In every market except Europe and Canada, 30% of the SALSA family units sold will be a one-seater model. As current regulations in Europe and Canada do not allow aerobatics, it is estimated that 20% of all sales there will be one-seaters. [41, 42]

One of the strengths of the LSA category is the relative ease with which aspiring pilots can obtain the sport pilot certificate. The following activities are carried out to further lower the entry barrier of the ownership of a and attain the predicted market share:

- Fractional ownership programs.
- Sell the aircraft with an optional pilot training program.
- $\bullet\,$ Maintenance plans for the aircraft in cooperation with local repair stations.
- Collaborate with flight schools to promote the aircraft. Use two-seaters to introduce people to, and instruct people on, the SALSA two-seater (similar to the Cessna Pilot Center program).

12.13. Project Design & Development

In this section a planning for the realization of this design is presented. Figure 12.9 shows a flowchart of the tasks to be completed. The flowchart implies that the activities are completed sequentially. However, Figure 12.10 clearly shows the length of these activities, as well as which are completed in parallel. Both figures breakdown the completion of

the design phase, the beginning of the marketing phase, the setting up of the manufacturing, and the 'established business' phase. In this final phase additional aircraft family members are put into production, the performance of the aircraft in the IAC is reviewed, and the aircraft is certified for other large international markets.

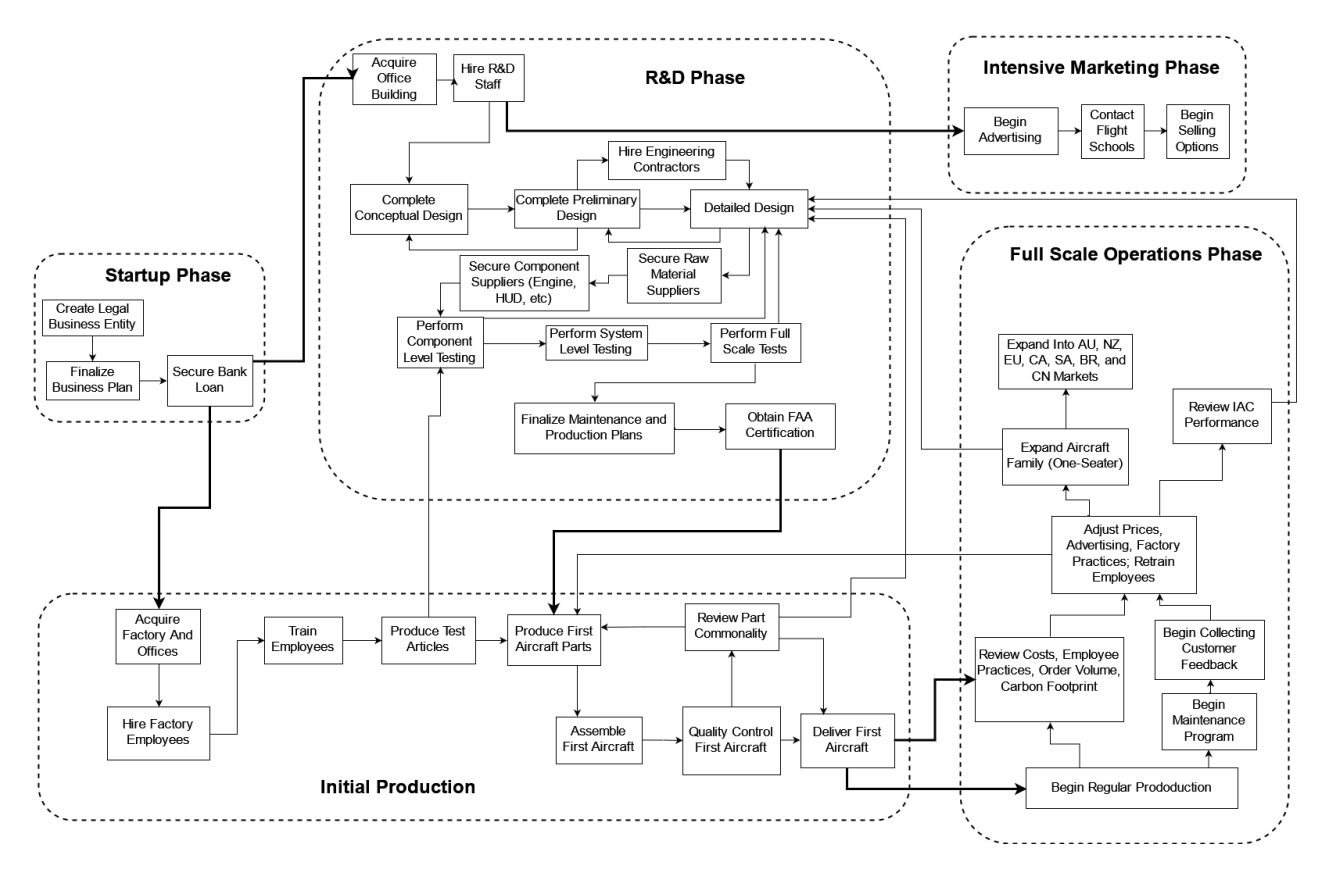


Figure 12.9: Flowchart showing the realization of the design.

12.14. Requirement Compliance

It has been checked which requirements have been complied with in order to determine in how much the mission of this project has been fulfilled. Figure 12.11 and 12.11 present this in matrix form. All requirements have been complied with, except for ALSA-CON-COS.1-TS: The two-seat variant shall be priced competitively in the LSA market, at at most \$85,000. However, the actual unit price of \$135,000 is such that the aircraft is one of the cheapest on the market, so it actually is competitively priced.

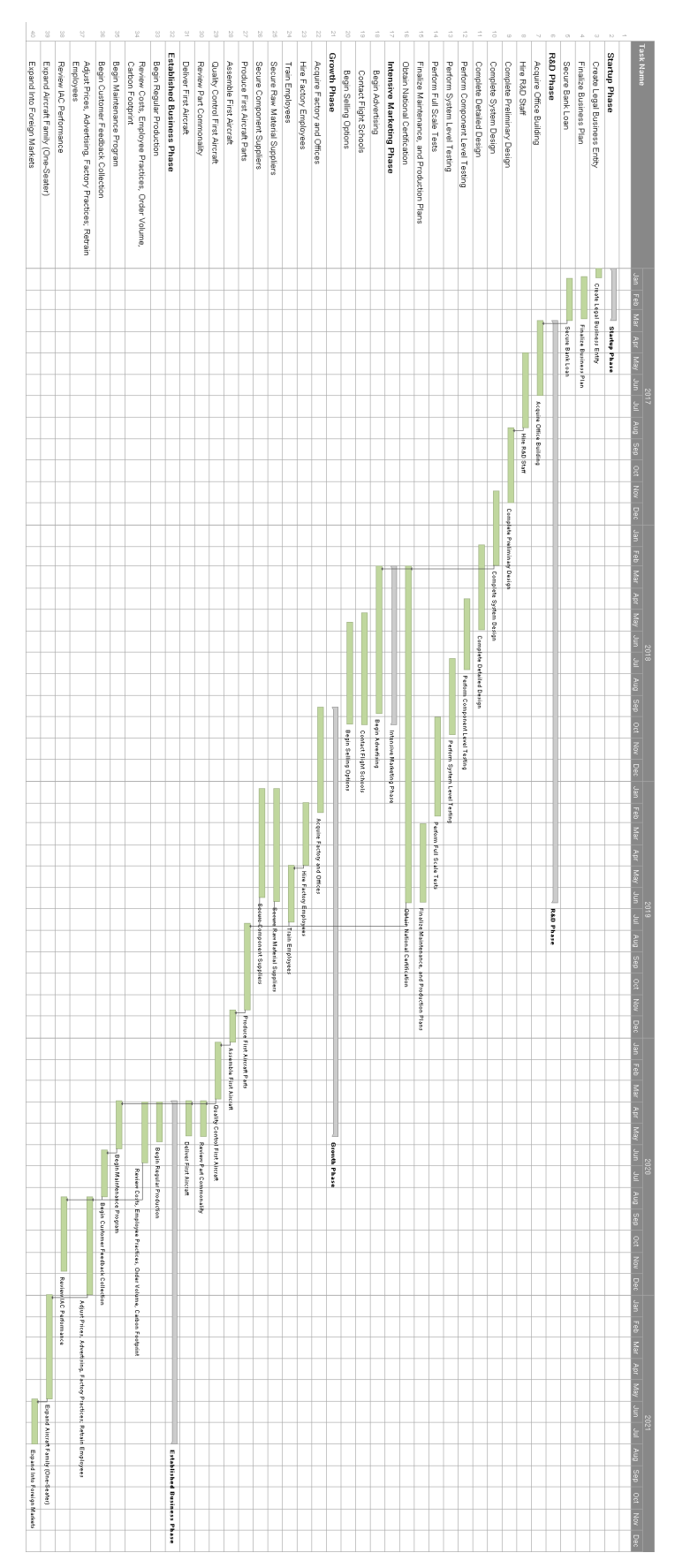


Figure 12.10: Gantt chart showing the realization of the design.

Identifier	Requirement	Complied with	Achieved	Report
ALSA-TEC-FLY.1	The engine shall be able to provide continuous and adjustable power, part of which can be converted into electrical power.	Yes		5.1
ALSA-TEC-FLY.2	It shall be possible to store the fuel, distribute it to the engine and continuously consume the fuel by the engine.	Yes		9.4
ALSA-TEC-FP.1	The aircraft shall be able to fly in trimmed condition as required for all relevant flight conditions as specified in the flight envelope.	Yes		7.2
ALSA-TEC-FP.2	The aircraft shall have control feedback characteristics that are characterized as level 1 handling qualities.	Yes		7.3
ALSA-TEC-FP.3-OS	The aircraft shall be able to perform the manoeuvres that are flown in the IAC intermediate category.	Yes		9.4, 10.2
ALSA-CON-OPS.1	The speed in level flight shall be at most 120 knots calibrated airspeed (CAS) at sea	Yes		
ALSA-CON-OPS.2	The aircraft shall be able to operate in controlled airspace.	Yes		9.8
ALSA-CON-OPS.3	The aircraft shall be able to operate in uncontrolled airspace.	Yes		8.6
ALSA-CON-OPS.4	The aircraft shall be able to take off at 5000 ft Mean Sea Level (MSL) at ISA + 10±C	Yes		
ALSA-CON-OPS.5	The aircraft shall be able to land at 5000 ft MSL, at ISA + 10±C.	Yes		10.2
ALSA-CON-OPS.6	The aircraft shall be able to take off from a grass field at sea level, at ISA + $0\pm C$.	Yes		10.2
ALSA-CON-OPS.7	The aircraft shall be able to land at a grass field at sea level, at ISA + 0±C.	Yes		10.2
ALSA-CON-DES.1	The gross take-off weight shall be at most 1320 lbs.	Yes	1016 / 1305 lbs	6.4
ALSA-CON-DES.2	The cabin shall have at most two seats.	Yes		4.3
ALSA-CON-DES.3	The cabin shall be unpressurized.	Yes		4.3
ALSA-CON-DES.4	The aircraft shall accommodate 95 percentile human pilots in terms of size.	Yes	99 percentile	4.3
ALSA-CON-DES.5	The type of landing gear shall be a fixed landing gear.	Yes		9.3
ALSA-CON-DES.6	The aircraft shall have at most one engine.	Yes		5.1
ALSA-CON-DES.7	The type of propeller shall be either fixed pitch or ground adjustable.	Yes		5.2
ALSA-CON-DES.8	The stall speed shall be at most 45 knots CAS in clean configuration.	Yes	44.4 kts	4.1
ALSA-CON-DES.9-OS	The climb rate of the one-seat variant shall be at least 1500 fpm at sea level, at ISA + $10\pm C$.	Yes	2180 fpm	8.2
ALSA-CON-DES.9-TS	The climb rate of the two-seat variant shall be at least 800 fpm at sea level, at ISA + $10\pm\mathrm{C}$.	Yes	1660 fpm	8.2
ALSA-CON-DES.10-OS	The negative limit load of the one-seat variant shall be at most -5G, with a 230 lbs pilot, 15 lbs parachute and 1.5 hours of fuel.	Yes		10.2
ALSA-CON-DES.10-TS	The negative limit load of the two-seat variant shall be at most -3G, with two 200 lbs pilots, two 15 lbs parachutes and 1.5 hours of fuel.	Yes		10.2
ALSA-CON-DES.11-0S	The positive limit load of the one-seat variant shall be at least	Yes		10.2

Figure 12.11: Requirement compliance matrix, page 1

	6G with a 230 lbs milet 15 lbs narachite and 1 5 bolins of final			
ALSA-CON-DES.11-TS	The positive limit load of the two-seat variant shall be at least 66, with two 200 lbs pilots, two 15 lbs parachutes and 1.5 hours of fuel.	Yes		10.2
ALSA-CON-DES.12-OS	The ferry range of the one-seat variant shall be at least 300 nm, with a 30 minute fuel reserve.	Yes	500 nm	10.2
ALSA-CON-DES.12-TS	The ferry range of the two-seat variant shall be at least 250 nm, with a 30 minute fuel reserve.	Yes	450 nm	10.2
ALSA-CON-DES.13-OS	The takeoff field length of the one-seat variant shall be at most 1200 ft, over a 50 ft obstacle to runway with dry pavement at sea level, at ISA + $10\pm$ C.	Yes	610 ft	10.2
ALSA-CON-DES.13-TS	The takeoff field length of the two-seat variant shall be at most 1500 ft, over a 50 ft obstacle to runway with dry pavement at sea level, at ISA + 10±C.	Yes	900 ft	10.2
ALSA-CON-DES.14-OS	The landing field length of the one-seat variant shall be at most 1200 ft, over a 50 ft obstacle to runway with dry pavement at sea level, at ISA + $10\pm$ C.	Yes	1110 ft	10.2
ALSA-CON-DES.14-TS	The landing field length of the two-seat variant shall be at most 1500 ft, over a 50 ft obstacle to runway with dry pavement at sea level, at ISA + 10±C.	Yes	1120 ft	10.2
ALSA-CON-DES.15-0S	The roll rate of the one-seat variant shall be at least 180 degrees per second at the maximum cruise speed or 120 knots CAS, whichever of the two is lowest.	Yes	360 deg/s	7.2
ALSA-CON-DES.16	The aircraft shall be capable of flying inverted for at least five minutes.	Yes	unlimited	9.4
ALSA-CON-DES.17-OS	The aircraft shall provide space for 30 pounds and 4 cubic feet of baggage for ferry missions.	Yes	30 lbs, 6 ft³	4.3
ALSA-CON-DES.17-TS	The aircraft shall provide space for 30 pounds and 6 cubic feet of baggage for ferry missions.	Yes	30 lbs, 6 ft³	4.3
ALSA-CON-REG.1	The aircraft design shall meet ASTM standards by entry in service.	Yes		
ALSA-CON-REG.2	The engine shall meet ASTM standards by entry in service.	Yes		
ALSA-CON-REG.3	The avionics shall meet ASTM standards by entry in service.	Yes		
ALSA-CON-REG.4	The aircraft shall comply with noise regulations as stated in International Civil Aviation Organization (ICAO) Annex 16/Volume 1/Chapter 10.	Yes	63 / 68 dB	5.3
ALSA-CON-DEV.1-OS	The entry in service (EIS) shall be no later than 2020 for the one-seat variant.	Yes		
ALSA-CON-DEV.1-TS	The EIS shall be no later than 2021 for the two-seat variant	Yes		
ALSA-CON-COS.1-TS	The two-seat variant shall be priced competitively in the LSA market, at at most \$85,000.	No	\$145,000 / \$135,000	12.11
ALSA-CON-COS.2	The aircraft shall be sold at a price such that at least a 10 % profit is generated.	Yes	10 %	12.11

Figure 12.12: Requirement compliance matrix, page 2 $\,$

73 Conclusion

The purpose of this report is to present the final conceptual design of the swift aerobatic light sport aircraft family (SALSA). The design process began with the mission and requirement analysis for fixing configuration for the conceptual design phase. Two independent conceptual designs of the two variants were generated based on the configuration proposed in the baseline report. The trade-off was conducted to choose the concept that meets the requirements and on top of that is competitive in the market regarding performance and cost. It was concluded that the mono-plane concept outperforms bi-plane and thus was chosen as a final configuration.

The design approach included minimizing manufacturing and development cost by maximizing the re-use of major airframe components for both the one-seat and two-seat variants. This was achieved by keeping identical fuselage, empennage, landing gear, fuel system. The wings of the one-seat variant are used as outer wing section of the two-seat variant with root extensions. The proposed SALSA family achieves 80% commonality by weight. Additionally, in designing the structural components of the aircraft, it was attempted to produce the aircraft using as many straight components as possible. Their simplified production will lower production costs even further.

The maneuverability of the aircraft is another major design objective. The designed one-seat variant is capable of performing all maneuvers in the IAC Intermediate category. The roll rate that can be achieved with SALSA is slightly above the roll rate that are generally found in aircraft competing in the IAC intermediate category. Extensive analysis of the stability and control characteristics show that all level 1 handling qualities are satisfied. The flight controls meet ASTM standards. The aircraft can be trimmed in any flight condition and the spin stability conditions are met as well.

The performance of the aircraft is an important design driving factor. The wing features sharp stall characteristics which are favorable for aerobatics The wings stall completely within a small angle-of-attack range and reattaches readily. The take-off and landing requirements in the most critical condition, at MTOW, are satisfied. For performing aerobatic maneuvers, the climbing performance of the SALSA has paramount importance and both aircraft meet the minimum requirements.

A design philosophy of minimizing costs hand-in-hand with maximizing performance and maneuverability, makes SALSA at \$135,000 USD for one-seat and \$145,000 USD for two-seat variant feasible and competitive in the market.

Recommendations

It is recommended that the structural analysis is done into more detail since this is required for a more detailed weight estimation. The obtained information can then be used to iterate upon the concept as is. The structure can first be optimized using hand calculations, followed by detailed finite elements methods.

The aerodynamic analysis should also be taken to the next level, using computational fluid dynamics software. The results form these detailed design methods will undoubtedly reveal flaws in the design as is, which have to be fixed before a preliminary design is obtained.

Additionally, the control system, including weight balance and aerodynamic balance of the control surfaces, should be further investigated. More detailed methods for control system design should give sizes and weights for horn balances, balance weights and aileron spades. This enables detailed sizing of the control system.

Finally, the moments of inertia parameters that have been computed are empirically seen to be incorrect. Adequate computations of these parameters have been performed but in reality these will be slightly different. A recommended way to determine the exact moments of inertia is to measure them after production of a prototype of the SALSA.

Bibliography

- [1] Federal Aviation Administration. Light-Sport Aircraft Airworthiness Certification. FAA, 2013.
- [2] American Society of the International Association for Testing and Materials. *Standard Specification for Design and Performance of a Light Sport Airplane*. ASTM, 2015.
- [3] Federal Aviation Administration. *Airworthiness Certification of Products and Articles, Order 8130.2H.* ASTM, 2015.
- [4] General Aviation Manufacturers Association. General aviation statistical databook & 2015 industry outlook. Published 2014.
- [5] The American Institute of Aeronautics and Astronautics. Aerobatic light sport aircraft family (lsa) request for proposal.
- [6] P. v. Pelt A. in 't Veld R. Boerma, J. Mussini. Interview with aerobatic pilot dr.ir. alexander in 't veld (tu delft), 15-12-2015. (unpublished).
- [7] John D. Anderson. Aircraft performance and design. McGraw-Hill, 1999.
- [8] Daniel P. Raymer. Aircraft Design: A Conceptual Approach. AIAA, 1992.
- [9] J. Roskam. Airplane Design Part I: Preliminary Sizing of Airplanes. DARcorporation, 1985.
- [10] Inc. International Aerobatic Club. Official contest rules 2012.
- [11] J. Roskam. Airplane Design Part V: Component Weight Estimation. DARcorporation, 1985.
- [12] E. Torenbeek. Synthesis of Subsonic Airplane Design, volume 9th print. Kluwer Academic Publishers, 1982.
- [13] D. Stinton. *The design of the aeroplane*. BSP Professional books, 1983.
- [14] J. Roskam. Airplane Design Part II: Preliminary Configuration Design and Integration of the Propulsion System. DARcorporation, 1985.
- [15] J. Roskam. Airplane Design Part III: Layout Design of Cockpit, Fuselage, Wing and Empennage: Cutaways and Inboard Profiles. DARcorporation, 1986.
- [16] J. Roskam. Airplane Design Part IV: Layout of Landing Gear and Systems. DARcorporation, 1986.
- [17] A.E von Doenhoff I.H. Abbot. *Theory of Wing Sections Including a symmary of airfoil data*. Dover Publications, Inc., New York, 1959.
- [18] C. Edward Lan J. Roskam. Airplane Aerodynamics and Performance. DARcorporation, 1997.
- [19] G. La Rocca. Systems engineering and aerospace design lecture 5 design for longitudinal stability. Lecture slides.
- [20] G. La Rocca. Systems engineering and aerospace design lecture 5 design for longitudinal control. Lecture slides
- [21] J. Roskam. Airplane Design Part VI: Preliminary calculation of aerodynamic thrust and power characteristics. DARcorporation, 1987.
- [22] Mohammad H. Sadraey. Aircraft Design: A Systems Engineering Approach. Wiley, 2013.
- [23] J.C. van der Vaart E. de Weerdt C.C. de Visser A.C. in 't Veld E. Mooij J.A. Mulder, W.H.J.J. van Staveren. *Flight Dynamics*, volume First Edition. Delft University of Technology, Faculty of Aerospace Engineering, Control and Simulation division, 2013.

Bibliography 103

- [24] D.H.Middleton. Composite Materials in Aircraft Structures. Longman, 1990.
- [25] BRP-Powertrain GmbH & Co. KG. Operators manual for rotax[©] engine type 912 i series. Rotax Aircraft Engines. Accessed 20-11-2015.
- [26] Federal Aviation Administration. *Aviation Maintenance Technician Handbook Airframe*. U.S. Department of Transportation, 2012.
- [27] National Transportation Safety Board. Safety study: Introduction of glass cockpit avionics into light aircraft. http://www.ntsb.gov/safety/safety-studies/Documents/SS1001.pdf. Updated March 9, 2010,.
- [28] Airman Testing Standards Branch. *Pilot's Handbook of Aeronautical Knowledge*, volume I. United States Department of Transportation, Federal Aviation Administration, 2008.
- [29] S.F. Hoerner. Fluid-Dynamic Drag. Hoerner Fluid Dynamics, Vancouver, 1965.
- [30] John V. Becker. Boundary layer transition on the n.a.c.a 0012 and the 23012 airfoils in the 8-feet high-speed wind tunnel. National Advisory Committee for Aeronautics.
- [31] J. Roskam. Airplane Design Part VII: Determination of Stability, Control and Performance Characteristics: FAR and Military requirements. DARcorporation, 1986.
- [32] BRP-Powertrain GmbH & Co. KG. Rotax 915 is/isc. Rotax Aircraft Engines. Retrieved December 2015.
- [33] Daniel P. Raymer. Simplified Aircraft Design for Homebuilders. Design Dimension Press, Los Angeles, CA, USA, 2003.
- [34] J. Roskam. Airplane Design Part VIII: Airplane Cost Estimation: Design, Development, Manufacturing and Operating. DARcorporation, 1990.
- [35] Taiichi Ōno. Toyota production system: beyond large-scale production. Productivity press, 1988.
- [36] Nicolas E. Antoine and Ilan M. Kroo. *Aircraft Optimization for Minimal Environmental Impact*, volume Vol. 41, No. 4, July–August 2004. Journal of Aircraft.
- [37] BRP-Powertrain GmbH & Co. KG. Rotax service instructions. Rotax Aircraft Engines. Published April 2009.
- [38] Jeffrey; Adrian Goettemoeller Goettemoeller. Sustainable Ethanol: Biofuels, Biorefineries, Cellulosic Biomass, Flex-Fuel Vehicles, and Sustainable Farming for Energy Independence. Prairie Oak Publishing, Maryville, Missouri
- [39] E. Worrell C. Galitsky. Energy efficiency improvement and cost saving opportunities for the vehicle assembly industry. University of California.
- [40] W. Verhagen R. Curran. Ae3221-i systems engineering & aerospace design risk management and reliability. PowerPoint slides.
- [41] European Aviation Safety Agency. Certification Specifications for Light Sport Aeroplanes. EASA, 2011.
- [42] Light Aircraft Manufacturers Association of Canada. *Design Standards for Advanced Ultra-Light Aeroplanes*. LAMAC, 2001.